Studies on the Mechanisms of Cardiac Arrhythmias
Role of stress, mapping atrial fibrillation and prediction of ventricular tachycardia origin

Child, Nicholas James Alexander

Awarding institution:
King's College London

Studies on the Mechanisms of Cardiac Arrhythmias:

Role of stress, mapping atrial fibrillation and prediction of ventricular tachycardia origin

A Thesis Submitted to King's College London University

For the Degree of

Doctor of Medicine (MD)

By

Dr Nicholas James Alexander Child, BM MRCP

Department of Cardiovascular Imaging
and Biomedical Sciences
King's College London
London SE1 7EH

Department of Cardiology
Guy's and St Thomas' Hospital
Westminster Bridge Road
London SE1 7EH

Kings College London

2018

Abstract

Background

Despite rapid advances in the treatment of complex cardiac arrhythmias major flaws remain in our understanding of the mechanisms underlying common arrhythmias. The incidence of life-threatening cardiac arrhythmias, primarily ventricular tachycardia, is significantly greater during times of psychological stress, but the underlying mechanism for this association is unclear. Sudden cardiac death remains a common cause of death in the developed world and our methods of risk stratification methods are sub-optimal. The underlying mechanism in persistent atrial fibrillation, the most common cardiac rhythm disorder, is very complex and remains controversial.

Methods and Results

1. In subjects with structurally normal hearts undergoing invasive electrophysiology studies (n=19) unipolar electrograms were recorded from the right and left ventricle whilst watching an emotionally charged film, and repeated during a respiration control period. Activation recovery interval (ARI) decreased during the stress component (RV 193.8±14ms vs 198.0±13ms, LV 199.8±16ms vs 201.6±15ms, p=0.004).

2. In subjects with diseased hearts ARI was measured non-invasively from permanent epicardial left ventricular pacing leads during photographic and film-stimuli stress (n=16). ARI decreased during the stress periods (by 2.3 to 3.6ms for different sequences, p=0.02, 0.05).In addition ARI was observed to oscillate

at the respiration frequency in 52% of recordings, and at the sympathetic 0.1Hz frequency in 55% of recordings.

3. An algorithm was developed that tested recent experimental work that identified the time interval between repolarization proximal to a line of functional block and the activation at the adjacent distal side, as a critical determinant of re-entry, termed the re-entry vulnerability index (RVI). This algorithm sampled all points on a multielectrode grid and calculated RVI between all pairs of electrodes within a given radius. Using data from an established Langendorff pig heart model the algorithm successfully identified the spatial region with increased susceptibility to re-entry. The feasibility of RVI mapping was evaluated during a clinical procedure by co-registering with the anatomy and physiology in a patient undergoing a VT ablation.

4. In patients undergoing ablation for persistent atrial fibrillation high density contact mapping was performed using bi-atrial 64 electrode mapping catheters (n=14). Phase singularities (PS) were located in both atria but we observed more PS in the left atrium (LA 779 ± 302, RA 552 ± 235, p=0.015). There was no significant difference in the mean dominant frequency (DF) in the LA compared to the right atrium. However, although some PS of duration sufficient to complete >1 rotation were detected, the maximum PS duration was only 1150ms, and the vast majority (97%) of PS persisted for too short a period to complete a full rotation. Whilst in selected patients there was evidence of PS local clustering, overall we found that PS were distributed globally throughout both chambers with no clear anatomical predisposition.

Conclusions

Our results document for the first time direct recordings of the effect of a mental challenge protocol on ventricular action potential duration in conscious humans. The effect of mental challenge on ARI was not secondary to emotionally-induced altered respiration or heart rate. The RVI algorithm accurately identified the region of re-entry in animal models of functional re-entry. The possibility of clinical application was demonstrated in a patient with VT. In the AF study no sustained rotors or localized drivers were detected, and instead the mechanism of arrhythmia maintenance was consistent with the multiple wavelet hypothesis, with passive activation of short-lived rotational activity.

Dedication

This thesis is dedicated to my colleagues and friends who I have worked with over a number of years during this research, all of whom have been inspirational and have voluntarily given their precious time teaching and supporting me during my work.

In addition I would like to dedicate this thesis to my beloved wife, Navara, my parents and all my friends who have endured the long hours and missed social engagements associated with this research. For their patience I am eternally grateful.

List of Abbreviations

AF – atrial fibrillation

ANS – autonomic nervous system

AP – action potential

APD – action potential duration

AS – aortic stenosis

AV – atrioventricular

β – beta

CAD – coronary artery disease

CFAE – complex fractionated atrial electrograms

CHD – congenital heart disease

CHED - Carbon^{11}-hydroxyephedrine

CMR – cardiac magnetic resonance imaging

CCF – congestive cardiac failure

DADs - delayed after depolarisations

DF – dominant frequency

DI – diastolic interval

EADs - early after depolarisations

ECG – electrocardiogram

FF – Fibrillation Factor

IAPS - International Affective Picture System

ICD – internal cardioverter defibrillator

LVEF – left ventricular ejection fraction

LVSD – left ventricular systolic dysfunction

MAP – monophasic action potential

MIBG - meta-iodobenzylguanidine

NE - norepinephrine

PNS – parasympathetic nervous system

PET - Positron emission tomography

PsAF – persistent atrial fibrillation

PKA – protein kinase A

RPD – Rate of arterial pressure development

RVI – Re-entry Vulnerability Index

SA – sinus node

SNS – sympathetic nervous system

SCD – sudden cardiac death

UEG – unipolar electrogram

VA – ventricular arrhythmia

VF – ventricular Fibrillation

Contents

Page

Chapter 1: Introduction and Literature Review

Page

List of Tables

List of Figures

Chapter 3: Results: The effect of psychological stress on APD in normal hearts undergoing invasive electrophysiology studies

Chapter 4: Results - The effect of psychological stress on APD in diseased hearts during ambulatory non-invasive studies

Chapter 5 – Results: Activation-repolarization time metric algorithm to predict the site of a clinical re-entry tachycardia

Chapter 6 – Results: High-density contact mapping during PsAF

Chapter 7 - Discussion and Limitations

Declaration

The work related to this thesis was carried out under the supervision of Professor Jaswinder Gill and Professor Reza Razavi. Some of these studies included collaborations with a number of scientists and computer engineers which contributed techniques and skills to this research that would not have otherwise been possible, and are described in the following passage. Professor Peter Taggart helped devise the hypothesis for studies 1-3. I collected the initial data in study 1 (invasive mental stress study), the APD measurements were performed using automated custom software by Dr Ben Hanson, and subsequent analysis was performed collectively. In study 2 (non-invasive mental stress study), I carried out the studies, the APD was again calculated off-line using the same automated custom algorithms in study 1, and I also measured APD manually to verify the accuracy of the automated process. I performed the initial time-frequency analysis included in the results section, but the highly complex statistical coupling of the variables described in the conclusion section were mainly performed by Dr Ben Hanson. The contents of study 3 (RVI) and study 4 (mapping in PsAF) involve complex international collaborations. My role in study 3 was in the helping to develop the hypothesis and setting up, designing the clinical protocol and performing the clinical case and then interpreting the results. Colleagues performed the animal models, computer simulations and algorithm development, which are described accordingly in the thesis. In study 4 my role was in setting up the local clinical study, performing the research protocols and extracting and collating the data. Some of the clinical studies were performed elsewhere as described in the

chapter and the complex phase analysis was performed mainly by Professor Clayton, with my continued clinical direction. Analysis was performed collectively with the majority of the statistics being performed by myself.

Ethical considerations

All studies which contribute to this thesis were performed in accordance to the correct Caldicott principles and all studies were agreed by local ethics committees. In the studies involving invasive measurements these were performed at the time of clinically indicated invasive studies, and there were no complications secondary to the research component.

Publication List

This contents of this thesis is based on the following publications:

1. **Child N**, Hanson B, Bishop M, Rinaldi CA, Bostock J, Western D, Cooklin M, O'Neil M, Wright M, Razavi R, Gill J, Taggart P. Effect of mental challenge induced by movie clips on action potential duration in normal human subjects independent of heart rate. Circ Arrhythm Electrophysiol. 2014 Jun;7(3):518-23. PMID: 24833641

2. Hanson B, **Child N**, Van Duijvenboden S, Orini M, Chen Z, Coronel R, Rinaldi CA, Gill JS, Gill JS, Taggart P. Oscillatory behavior of ventricular action potential duration in heart failure patients at respiratory rate and low frequency. Frontiers Physiology. 2014 Oct 28;5:414. PMID: 25389408

3. **Child N**, Bishop MJ, Hanson B, Coronel R, Opthof T, Boukens BJ, Walton RD, Efimov IR, Bostock J, Hill Y, Rinaldi CA, Razavi R, Gill J, Taggart P. An activation-repolarization time metric to predict localized regions of high susceptibility to re-entry. Heart Rhythm. 2015 Jul;12(7):1644-53. PMID: 25863160

4. Van Duijvenboden S, Hanson B, **Child N**, Orini M, Rinaldi CA, Gill JS, Taggart P. Effect of autonomic blocking agents on the respiratory-related oscillations of ventricular action potential duration in humans. Am J Physiol Heart Circ Physiol. 2015 Dec 15;309(12):H2108-17. PMID: 26475587

5. Hill YR, **Child N**, Hanson B, Wallman M, Coronel R, Plank G, Rinaldi CA, Gill J, Smith NP, Taggart P, Bishop MJ. Investigating a Novel Activation-Repolarisation Time Metric to Predict Localised Vulnerability to Reentry Using Computational Modelling. PLoS One. 2016 Mar 2;11(3). PMID: 26934736

6. Laughner J, Shome S, **Child N**, Shuros A, Neuzil P, J Gill, Wright M. Practical Considerations of Mapping Persistent Atrial Fibrillation With Whole-Chamber Basket Catheters. JACC: Clinical Electrophysiology. 2016 Feb 2:1:55-65

7. **Child N**, Clayton RH, Roney C, Laughner J, Shuros A, Neuzil P, Petru J, Jackson T, Porter B, Bostock J, Niederer SA, Razavi RS, Rinaldi CS, Taggart P, Wright MJ, Gill J. Unravelling the Underlying Arrhythmia Mechanism in Persistent Atrial Fibrillation: Results from the STARLIGHT Study. Circ Arrhythm Electrophysiol. 2018 Jun;11(6). PMID: 29858382

Following my 2014 publication, “Effect of mental challenge induced by movie clips on action potential duration in normal human subjects independent of heart rate” this was reported in a number of press reviews, including the following URLs;

1. http://www.bbc.co.uk/news/health-27425469
2. http://www.express.co.uk/news/health/476216/Warning-Blockbuster-action-films-can-be-too-thrilling-for-our-health
3. http://www.scotsman.com/what-s-on/film/scary-films-can-be-risky-for-the-faint-hearted-1-3413047
4. http://www.financialexpress.com/news/beware-watching-stressful-movies-changes-hearts-beating-pattern/1251504

Chapter 1 – Introduction and Literature Review

1.1 Introduction

Clinical cardiac electrophysiology is a rapidly progressing branch of cardiology translating our scientific understanding of the mechanism of arrhythmias into increasingly successful patient treatments. Whilst the last 100 years have seen a rapid scientific development there remains significant gaps in our current understanding of even the most common cardiac arrhythmias. An improved understanding of the basic mechanisms of these common arrhythmias is likely to lead to more successful treatments and improved survival.

This content of this thesis aims to add to the current understanding of a number of key elements accounting for common arrhythmias;

1. The effect of psychological stress on intracardiac repolarization
2. Whether local repolarization could aid in predicting the origin of ventricular tachycardia
3. Identify the arrhythmia mechanism responsible for the maintenance of persistent AF

1.2 The mechanical structure and function of the heart and the electrical regulation of normal cardiac function

The normal heartbeat involves the co-ordinated contraction of millions of cardiac myocytes resulting in an efficient pump mechanism, requiring both a series of highly specialized cardiac tissues and a complex electrical system to regulate and synchronise the cardiac cycle. In order to understand the mechanisms of arrhythmia a detailed understanding of normal cardiac structure and function is required.

1.2.1 Structure of the normal human heart and the cardiac cycle

The primary role of the heart is to act as a pump to push blood, containing oxygen and metabolic substrates, around the body's circulatory system. The human heart is effectively composed of 2 separate pumps; the right and the left side. The right, which is at low pressure, pumps deoxygenated blood through the pulmonary system where it becomes oxygenated. The left, which is at higher pressure, propels the oxygenated blood around the body where the oxygen is removed from the blood, and then deoxygenated blood returns to the right side of the heart. The continual uninterrupted repeating of this cycle is a basic requirement of life.

This is obviously a very simplistic synopsis of cardiac function, which in fact is a very complex system that has undergone marked anatomical and functional changes during evolution in order to achieve the cardiac output and durability

required for human existence (Jensen, 2013). The human heart is composed of 4 chambers, with both a left and a right atrium and ventricle and its basic anatomical structure is depicted in Figure 1A. A series of one-way valves are essential to ensure blood flows through the heart in the right direction, which open and closed based on the pressure difference across each valve. The mitral valve sits between the left atrium and left ventricle and the tricuspid valve between the right atrium and right ventricle and both are also known as the atrioventricular (AV) valves. The aortic valve connects the left ventricle to the aorta and the pulmonary valve connects the right ventricle and pulmonary artery and these are also known as the semilunar valves.

Figure 1: Basic anatomical structure of the heart, cardiac cycle and cardiac electrical system

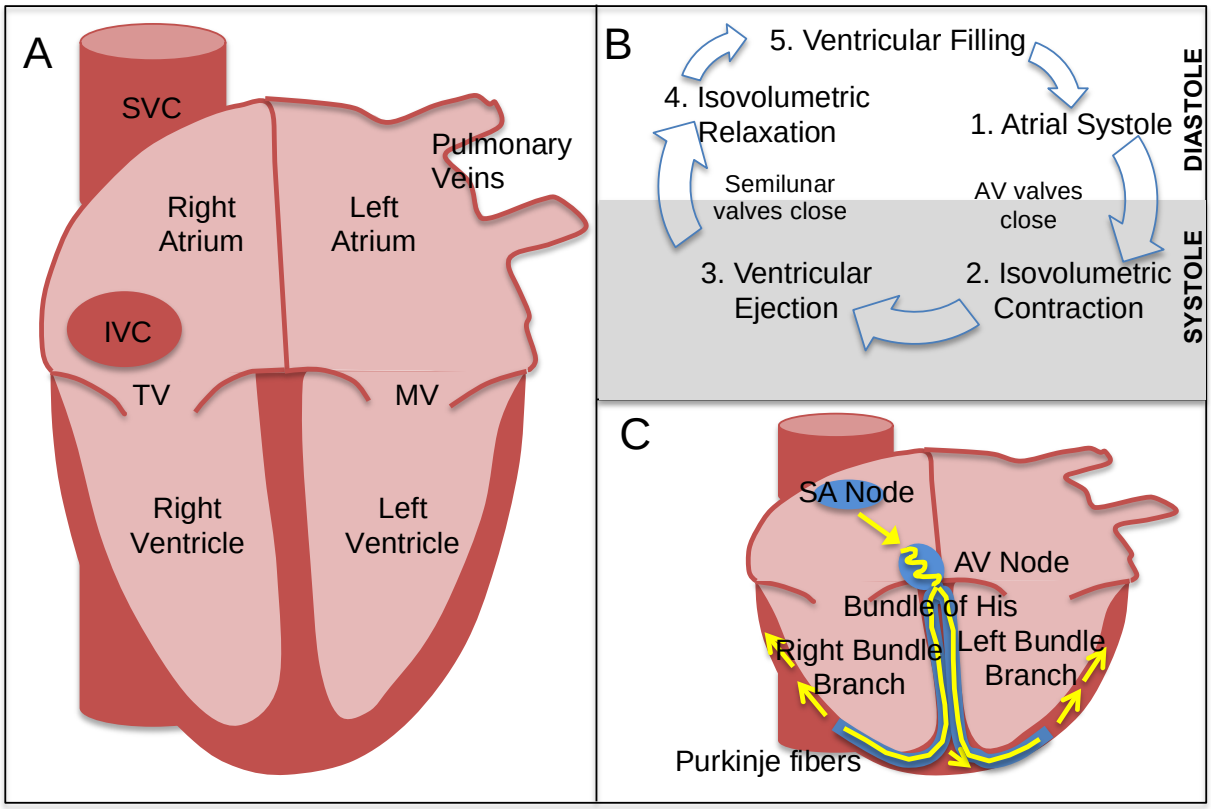

Figure 1. 1A – Basic anatomical structure of the heart. Blood is ejected from the ventricles via the aortic and pulmonary valves (also known as semilunar valves) to the aorta and pulmonary artery respectively (not shown on the figure). Figure 1B – Stages of the cardiac cycle. 1C – Basic illustration of the main components of the cardiac electrical conduction system. TV – tricuspid valve, MV – mitral valve (TV and MV are also known as AV valves), SVC – superior vena cava, IVC – inferior vena cava, SA node – sinoatrial node, AV node – atrioventricular node.

1.2.2 The cardiac cycle

The cardiac cycle describes the series of mechanical and electrical events that makes up each heartbeat, and is composed of a diastolic phase during which the ventricles are filled with blood, and a systolic phase during which this blood is propelled (Figure 1B). The basic cardiac cycle is described below;

1. Systole starts when the mitral valve closes and ends when the aortic valve closes. During the first part of systole the ventricles begin to contract against closed semilunar valves, and the volume of the chamber remains unchanged as the intraventricular pressure increases (isovolumetric contraction phase).

2. When the intraventricular pressure exceeds the pressure in the aorta and pulmonary artery respectively, these valves then open and blood is ejected from the ventricle (ventricular ejection phase).

3. As the ventricles then begin to relax and the pressure within the chamber becomes less than the pressure in the aorta and pulmonary artery, these semilunar valves then close again, marking the start of diastole.

4. As the ventricles relax with both the semilunar and AV valves closed the pressure within the chamber falls further (isovolumetric relaxation) until the pressure within the ventricles is less than the atria and the AV

valves open and the ventricle is filled passively from the atrium (ventricular filling).

5. The final stage of diastole involves blood being actively pumped from the atria into an already partially filled ventricle (atrial systole). As pressure in the ventricle then exceeds that of the atrium the AV valves close marking the start of systole.

The atria have a mechanical role in receiving blood and passively funnelling it to the ventricles (ventricular filling), and also an active role in providing the final amount of filling during diastole (atrial systole). However, whilst atrial active mechanical contribution to overall cardiac output is considered relatively modest (10%) (Nowak, 1995), this increases to 30% due to atrially mediated chronotropic increases (Kruse, 1982).

In order to achieve this carefully coordinated contraction of different cardiac chambers at the exact appropriate time within the cardiac cycle, involving millions of individual myocytes contracting in unison, there is a need for a complex communication system throughout the heart. This is achieved through specialist cardiac conduction tissues, first through the production of an electrical impulse (action potential - AP), and then through the conduction of the AP through specialized conduction tissue to the cardiomyocytes.

1.2.3 The electrical system of the heart

Electrical activity in the heart is a very complex system involving multiple electrical and mechanical feedback loops that will be discussed in detail later during this chapter, but in order to understand the coordination of the normal cardiac cycle a brief simplistic understanding of normal electrical initiation and propagation in the electrical activation of the heart is required.

Approximately 1% of all cardiac cells consist of specialized electrical cells. These have the potential both to generate electrical impulses (autorhythmicity) and the ability to conduct electrical activation quickly. In the normal cardiac cycle the heartbeat impulse is generated from the sinoatrial node (SA node), consisting of specialized pacemaker myocytes, situated at the junction of the right atrium and superior vena cava (Van Weerd, 2016). The impulse then spreads through the atrium to the atrio-ventricular node (AV node). There is a delay as the impulse passes through the AV node, which allows time for the atria to fully contract to complete ventricular filling. Apart from impulses travelling through the AV node and connected conductive tissue, the atria and ventricles are normally completely electrically isolated from each other by a layer of fibrotic connective tissue, which includes the AV valves. When the impulse has passed through the AV node it is then passes rapidly down specialized conduction tissue, first the Bundle of His and then right and left bundles before travelling in smaller Purkinje fibres before the wave of activation arrives at the designated myocyte causing local depolarization and subsequent contraction (Figure 1C).

1.2.4 Cardiac impulse formation and the role of ion currents

The cardiac impulse is the result of changes in intracellular electrical currents caused by transmembrane ion channels, ion exchangers and ion pumps. Myocytes maintain an electrical gradient across their cell membranes by a continual process of transfer of electrically charged ions both in and out of the cell, such that there is an overall loss of positively charged ions within the cell, and a resting -80 to -85 mV gradient exists across the cell membrane (Liu, 2016). In response to depolarization of an individual cardiac myocyte a sequential chain of changes to ion currents occur that results in the influx and efflux of a number of key ions, and subsequent effect on the transmembrane electrical potential, and is called the monophasic action potential (MAP) (Yang, 2010). The shape and timing of the MAP shows significant heterogeneity between different regions of the heart (Liu, 2016).

The MAP is traditionally considered to consist of 5 phases, including phase 0 (Figure 2), and described below:

Phase 0 – Depolarization. When the membrane potential reaches the threshold voltage-gated fast sodium channels open resulting in an inflow of sodium ions along the electrochemical gradient producing a rapid depolarization. Under normal conditions, the initiation of phase 0, and subsequent influx of positively charged I_{Na} is triggered by myocyte depolarization from electrotonic coupling between adjacent myocytes by gap junctions (Liu, 2016). Mutations in genes encoding sodium channels resulting in abnormal function during this phase are

well recognised in ventricular arrhythmia (VA) and sudden cardiac death (SCD). Mutations in the SCN5A gene, which encodes for alpha-subunit of the cardiac sodium channel is a common mutation found in Brugada syndrome and Long QT syndrome 3 (Priori, 2013).

Phase 1 – Potassium channels open allowing the exodus of potassium out of the cell, at the same time as sodium channels close. In addition to this there is activation of depolarizing calcium currents and the sodium-calcium exchanger and calcium activated chloride ions. The outward currents during phase 1 are termed transient and this is a relatively short phase

Phase 2 – Voltage gated slow calcium channels (L-Type) open in the sarcolemma and sarcoplasmic reticulum, as well as cell membrane, and calcium enters the cytosol. During this stage the voltage change caused by the outward migration of potassium ions and release of calcium is equal and is termed the plateau phase of the MAP. As described previously there is significant electrical heterogeneity in the MAP between different regions of the heart and in the atria phase 2 is relatively short (approx. 100ms) compared to the ventricles (approx. 180 – 200ms) (Liu, 2016). During high heart rates this phase shortens in part due to the effect of beta-adrenergic receptor activation of the slow potassium channel via protein kinase A. The effect of the sympathetic nervous system on the MAP is described in more detail later. Mutations in genes encoding for calcium channels have been identified as causes of VA and SCD, including the ryanodine receptor, which is associated with catecholaminergic polymorphic ventricular tachycardia (Priori, 2013).

Phase 3 – Repolarization. Voltage gated potassium channels open, and further potassium diffuses out of the cell at the same time as the calcium channels are closing. The membrane potential returns towards baseline until the resting membrane potential is restored. Mutations encoding for potassium channels are well recognised as causes of VA and SCD, including mutations in KCNQ1 and KCNH2, found in long QT syndromes type 1 and 2 (Priori, 2013).

Phase 4 – Recovery. The membrane potential remains negative (approximately -80 mV) due to due to voltage-regulated inward rectifier potassium channels. This phase is also called the diastolic phase. Within the working myocardium of the ventricles and atria this phase continues until depolarization occurs as a result of an electrotonic coupling from an adjacent myocyte, which has just been depolarized. Pacemaker cells (SA, AV node and purkinje fibres) demonstrate a slow depolarization of the resting potential due to ionic leak during phase 4 allowing them to spontaneously generate their own MAP (Liu, 2016).

Figure 2: The 5 phases of the monophasic action potential

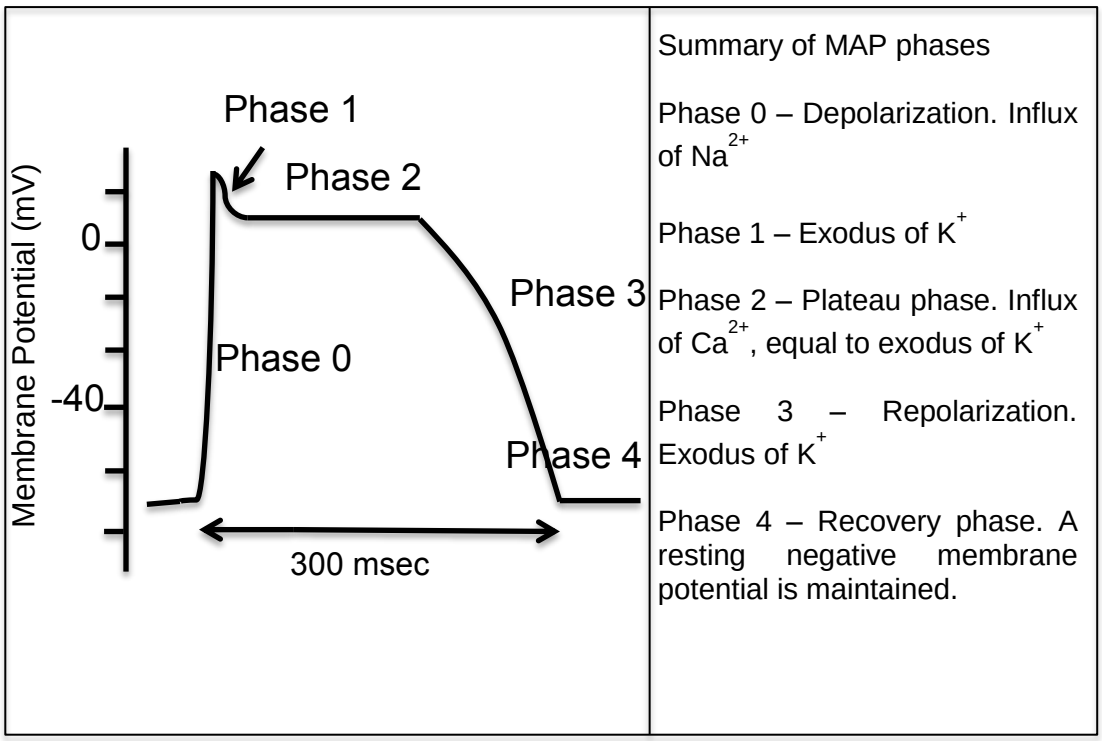

Figure 2. Left – The monophasic action potential shows the transmembrane electrical potential change over time due to the effect of ion currents in response to depolarization. Right – summary of the main component of each phase. MAP – monophasic action potential, Na^{2+} - Sodium ions, K^{+} - Potassium ions, Ca^{2+} - calcium ions.

1.2.5 Refractory Period

The refractory period is the timespan during which an individual cell is still repolarizing and is unable to initiate another repolarization. The refractory period can be divided into the absolute refractory period when a cell will not re-depolarise irrespective of activation amplitude and the relative refractory period during which some of the fast sodium channels have returned to their excitable state and the cell could depolarize under the right conditions. The refractory period is of significant interest in understanding and predicting arrhythmias

because longer refractory periods prevent arrhythmias, and regional variation in refractoriness produce functional block, which is an important component of re-entry tachycardia. Studying refractory properties of local tissues is time consuming, as it requires separate pacing protocols for each position being tested.

1.2.6 Measuring the MAP: the Activation Potential Duration and the Activation Recovery Interval

The activation potential duration (APD) measures the time from the start to the end of the MAP and is a critical component of studies examining arrhythmias. Local repolarization can be accurately assessed using intracellular micro-electrodes to calculate exact trans-membrane action potentials. However, this is not practical in most research studies or in clinical electrophysiology, as it requires open access to the heart (Haws 1990). The surface electrocardiogram (ECG) an essential part of everyday clinical practice, but because it represents the summation of all of the atrial and ventricular MAPs it cannot identify local changes in activation and repolarization which are responsible for arrhythmia initiation and maintenance. The unipolar electrogram (UEG) measures local depolarization and repolarization at the exploring electrode tip of a catheter inserted into the heart, and can be used to calculate the activation-recovery interval (ARI), which is a validated surrogate for APD (Hanson, 2009; Wyatt, 1981; Millar, 1985). Hence ARI can easily be measured during in vivo studies, either with standard intracardiac electrophysiological catheters, or potentially from established permanent pacing leads where manufacturers allow unipolar

recordings. As such, whilst the ECG provides useful clinical measurements of the global averaged electrical activity within the heart, the UEG (and subsequently ARI) provides a more precise measure of the electrical activity at the local myocyte level. In addition the ARI is closely correlated with local refractoriness and allows estimates of temporal and spatial variation of refractory properties from multiple simultaneous exploring electrodes in clinical and experimental studies (Millar, 1985). Hence, measurement of the ARI provides a valid method of examining the refractory periods of multiple electrode positions at once.

The UEG looks very different from a standard MAP recording (Figure 3), instead resembling the deflections seen in a standard surface ECG, and the different components of the UEG are often referred to with the same lettering system as for the ECG. During phase 0 of the MAP, Na^{2+} ions flow into the cell causing an increase in intracellular voltage, and a subsequent decrease in the electrical potential outside the cell. The corresponding local UEG taken from an electrode tip, which is positioned outside of the cell, displays a substantial negative deflection. The time of local depolarization on the UEG, is termed Vmin, and is taken as the point in the activation wave with the greatest downward slope and this approach is widely accepted (Wyatt, 1981; Chen, 1991; Millar, 1985).

Figure 3: Measurement of cardiac electrical activity

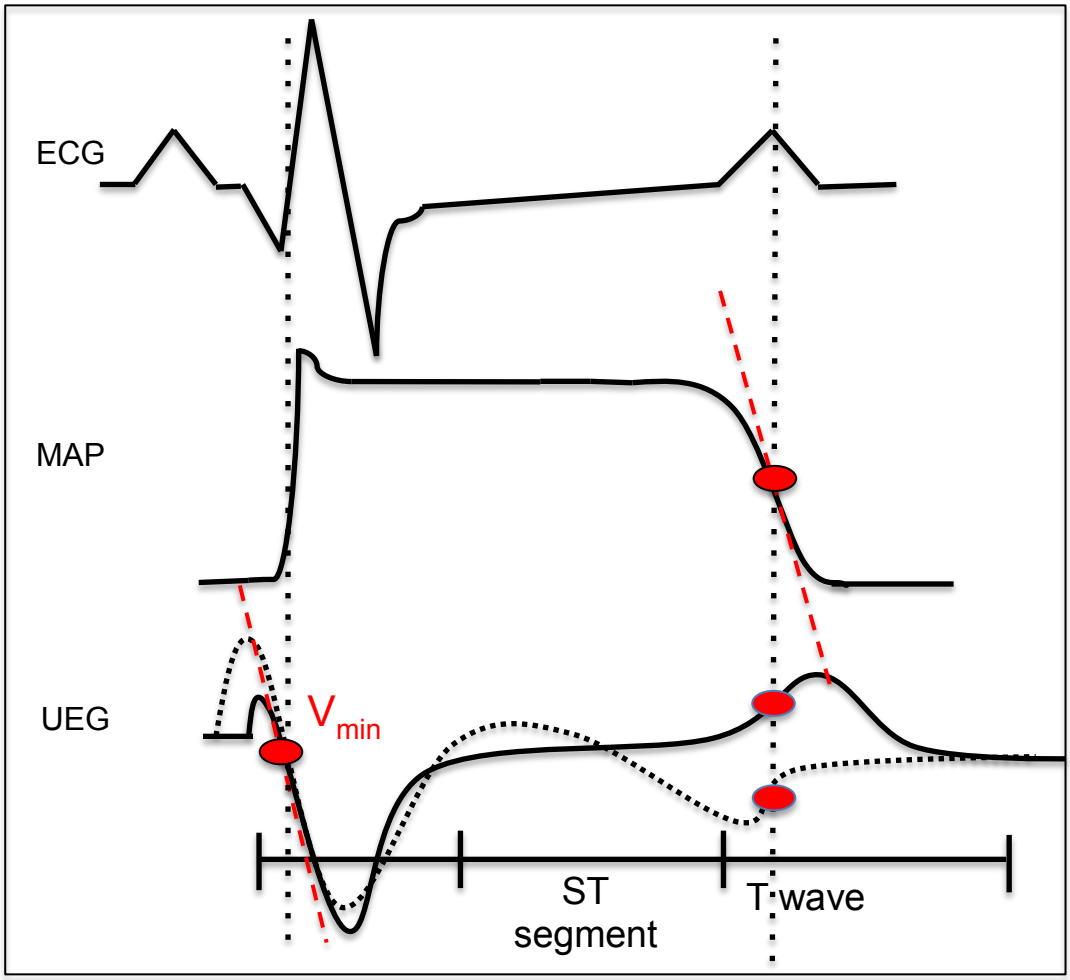

Figure 3. Top – The ECG is a summation and average of all the cardiac electrical activity as measured from the skin surface. The p wave is the result of atrial depolarization and repolarization, the QRS ventricular depolarization and the ST segment and T wave is caused by ventricular repolarization. Middle – the MAP has a very different shape to the ECG and represents local depolarization and repolarization. Bottom - the UEG has a similar appearance to the ECG. The action potential duration (APD) can be calculated by measuring the time interval between V_{min} and T_{up} (Wyatt, 1981). V_{min} local activation with the maximal rate of change, T_{up} – maximal upward slope in the T wave.

Potassium leaving the cell in phase 3 of the MAP results in a reduction of intracellular voltage, and an increase in extracellular voltage, which corresponds on the unipolar electrogram to the T wave repolarization. There is

however some controversy regarding the optimal position in the T wave to be measured and 2 different methods exist; the Wyatt method (Wyatt, 1981) and the alternative method (Chen, 1991). The Wyatt method identifies the local repolarization time as T_{up}, the point in which the T wave has the maximum upward slope. T_{up} has been correlated strongly with the maximum downward slope of the MAP phase 3 (Haws, 1990), and 50% repolarisation of the MAP, and is the most widely used method. In the alternative method the ARI should be measured differently for positive T waves compared to negative T waves (See Figure 3 for more details) (Western, 2015). Measurements using T_{up} have been strongly associated with the absolute refractory period in clinical studies (Haws, 1990; Millar, 1985).

1.2.7 Excitation-contraction coupling

The MAP leads to a mechanical response (contraction) after a short lag time, a term known as excitation-contraction coupling. As the voltage gated calcium channels (phase 2) open, calcium enters the cytosol and binds to specialized calcium-sensitive calcium release channels called ryanodine receptors. This causes a much larger release of calcium from the sarcomplasmic reticulum and causes the overall concentration of calcium in the cytosol to increase, which binds to troponin C in the myofilaments to initiate contraction (Greenstein, 2011).

1.2.8 Restitution

There are different speeds of ion channel opening and closing within the thousands of ion channels that make up a cardiac APD. The result of this is that each APD is dependent upon the diastolic interval (DI) of the preceding APD, termed APD restitution. APD increases as the DI increases and this can be assessed during an electrophysiological study using different diastolic intervals. The slope of the APD restitution curve, composed of APD plotted against DI gives important insight into arrhythmia risk as a gradient greater than 1 is associated with the risk of APD alternans (a long-short-long-short alternating pattern of APD) (Zipes, 2004). Isoprenaline, a sympathetic agonist, and adrenaline have both been shown to steepen this curve, which may relate to the known effects of adrenergic stimulation increasing ventricular fibrillation (VF) (Taggart, 2003).

1.3 Mechanisms of arrhythmia - automaticity, triggered activity and re-entry mechanisms

There are 3 main mechanisms that contribute to the initiation of arrhythmia (Zipes, 2004):

1. *Automaticity* – the ability of cardiac cells to undergo spontaneous diastolic depolarization and initiate an electrical impulse in the absence of an external

electrical stimulation. This is the origin of the normal heartbeat but can also be pathological.

2. *Triggered Activity* – abnormal impulse initiation that is dependent on oscillations in membrane potential that follow the upstroke of an action potential. If this oscillation raises the membrane potential to the threshold for a further activation then a cardiac impulse is started, termed an after-depolarization. These are subdivided into delayed after depolarisations (DADs) and early after depolarisations (EADs):

- DADs are caused by oscillations that occur after repolarization of an action potential. DADs occur in situations where there is increased calcium in the sarcoplasmic reticulum. Catecholamines are recognized as a cause of these by causing increased cellular calcium uptake.
- EADs occur during repolarization (phase 2 or 3) and are caused by a shift in the voltage relationship so that the outward current approaches 0, or even becomes inwards.

3. *Re-entry and Unidirectional block* - the majority of ventricular tachycardia episodes are based on re-entry mechanisms involving interaction between electrical activation and repolarization wavefronts. Requirements for re-entry are an area of inexcitable tissue (unidirectional block) around which the wavefront propagates, and the maintenance of excitable tissue ahead of the wavefront. These required criteria are facilitated either by slowing of conduction, shortening of the refractory period, or both. The unidirectional block

may be either functional (refractory normal myocardium) or anatomical (such as scar).

1.4 Ventricular arrhythmia and sudden cardiac death

In recent decades overall cardiovascular mortality has decreased in developed countries as a result of preventative measures to decrease the incidence of ischemic heart disease and heart failure (Niemeijer, 2015). However cardiovascular disease remains a major cause of death in the developed world, accounting for 17 million deaths per year, 25% of which are the result of SCD (Priori, 2015). The cause of SCD is different in older and younger patients. In younger patients the most common causes are channelopathies, cardiomyopathies and myocarditis, whilst in older patients, who form the bulk of SCD patients, the majority is the result of ischemic heart disease (Figure 4) (Priori, 2015). SCD remains a major cause of death worldwide, accounting for in excess of 350,000 deaths a year in the USA and 60,000 in the UK. The majority of these deaths are due to a sudden alteration in heart rhythm, most commonly ventricular tachycardia and its rapid degeneration into ventricular fibrillation (Rubart, 2005). Despite the development of over 100 antiarrhythmic medications, efforts at prevention of serious and fatal ventricular arrhythmias have proved disappointing and the most reliable strategy is the implantation of an internal cardioverter-defibrillator (ICD) (Ezekowitz, 2007). Current practice is to target therapy towards subjects who have had prior arrhythmias or have poor left ventricular ejection fraction (LVEF). Unfortunately a patient's first presentation of arrhythmia may be sudden death, most patients with sudden

cardiac death do not have poor LV function (Figure 4) and the majority of patients with ICDs never use them (Moss 2002a). There is therefore urgent need to improve our identification of subjects at high risk. In addition, the treatment of ventricular tachycardia by radiofrequency ablation has disappointing success rates (50-90% with 20-40% late recurrence) (Aliot, 2009) and does not negate the need for an ICD. Research that improves our understanding of the pathophysiology and mechanism of these arrhythmias will be of great benefit in treatment and risk stratification.

Figure 4: Causes of sudden cardiac death and the presence of impaired ejection fraction in SCD

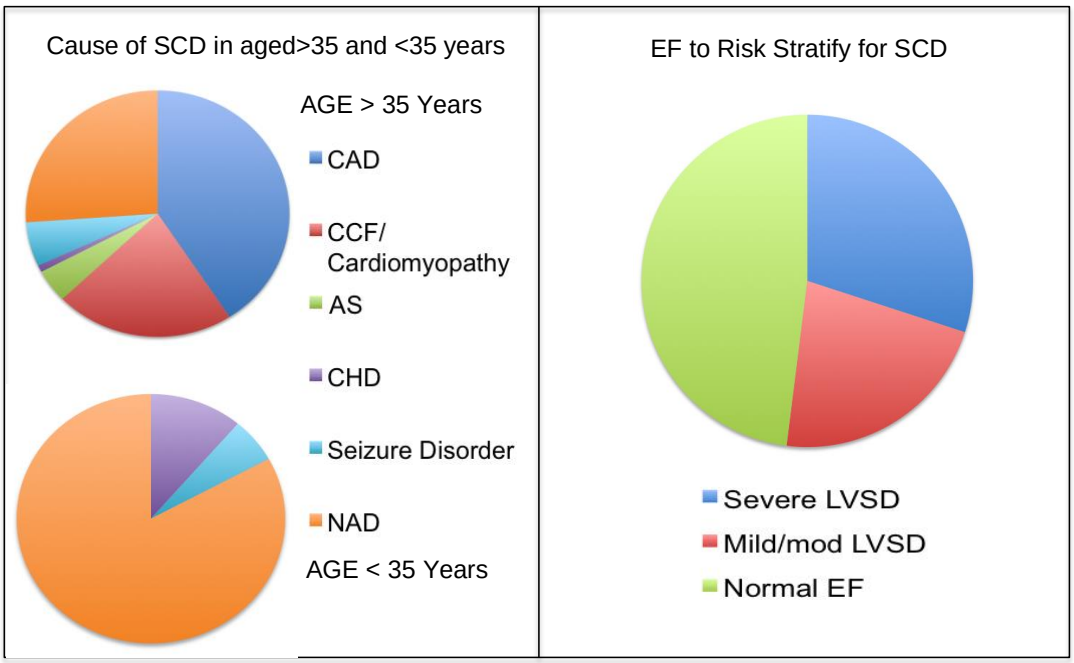

Figure 4. Left – The causes of SCD vary between different age groups. In the older patients the majority of causes of SCD are either directly related to CAD or CCF/cardiomyopthy, whilst in younger patients there were most commonly no associated conditions (Adapted from Chugh, 2004). Right – The presence of severe left ventricular systolic dysfunction is found in under 1 third of cases of sudden cardiac death. (Adapted from Chugh, 2008). SCD – sudden cardiac death, CAD – coronary artery disease, CCF – congestive cardiac failure, AS – aortic stenosis, CHD – congenital heart disease, NAD - no abnormality discovered, EF – ejection fraction. LVSD – left ventricular systolic function – severe <35%, mild/ moderate 35-55%.

Methods of predicting arrhythmia

As our understanding of the mechanisms that cause cardiac arrhythmias has developed there has understandably been significant research into predicting which patients are at risk of significant arrhythmia, in order to better target treatments and improve outcomes. The vast majority of SCD occurs due to arrhythmias originating from the ventricles rather than the atria, and hence the bulk of research relates to ventricular arrhythmias.

1.5 Predicting risk of SCD in supraventricular arrhythmia

In patients with ventricular pre-excitation there is a small increased risk of SCD (estimated 0.25% per year) (Obeyesekere, 2012), thought to be secondary to the risk of developing rapidly conducted atrial fibrillation during which the accessory pathway is able to conduct rapidly resulting in VF. An invasive electrophysiology study to test the conduction properties of the accessory pathway has been shown to accurately risk-stratify pathways. A “high-risk” pathway is thought to be present when the shortest pre-excited R-R interval is less than or equal to 250ms, and these will then usually be ablated even in the absence of symptoms on prognostic grounds (De Ponti ,2015; Al-Khatib, 2016).

1.6 Predicting risk of SCD in ventricular arrhythmia

This is an area of intense scientific research and has the potential to both identify more patients at risk and hence prevent SCD, and also better target expensive and invasive treatments to patients most likely to benefit. However,

risk prediction is a very complex area, especially when the underlying mechanism of ventricular arrhythmia is incompletely understood. An arrhythmic event is likely the combination of a vulnerable substrate (e.g. scar in IHD) or predisposition (e.g. inherited cardiomyopathy) and multiple transient factors that acts as triggers. A summary of key research into ventricular risk prediction is detailed below:

1.6.1 Non-invasive risk stratification

Genetic Testing

Family screening, sometimes including gene testing, of first degree relatives of patients with SCD in whom a possible inherited cardiomyopathy or inherited channelopathy is indicated to identify family members with the condition in whom treatment might be indicated. Aside from aiding diagnosis, in certain diseases such as LQTS and lamin dilated cardiomyopathy genetic information can be used as an additional level of risk stratification in order to target appropriate ICD implantation (Priori, 2013).

The ECG

The standard ECG is ubiquitous and inexpensive and provides significant clinical information both about the presence of underlying structural heart disease (e.g. Q waves post MI, changes consistent with ARVC or HCM) as well as a global overview of a variety of depolarization and repolarization

parameters (e.g. long QT syndrome), which would make it an ideal means to improve risk stratification. The main ECG criteria examined for SCD risk stratification are;

- **QT interval.** This represents the duration of global ventricular depolarization and repolarization. Genetic abnormalities can result in both a pathologically short QT or long QT, all of which are associated with increased risk of arrhythmia. Long QT syndrome can also be secondary to drugs (Abdelghani, 2016). Studies of QT prolongation in predicting arrhythmic risk in ischemic heart disease have mixed results {Pohjola-Sintonen, 1986; Zareba, 1994) and is not used routinely.

- **QRS duration.** This represents the time taken for ventricular depolarization. Whilst prolonged QRS duration is associated with increased mortality it is unclear how much this is to do with an increased predisposition to arrhythmia, as opposed to being a surrogate indicator of myocardial damage and hence future pump failure. In the Multi-centre UnSustained Tachycardia Trial (MUSTT) there was no significant association seen with inducibilty of VT and the QRS duration (Zimetbaum, 2004).

- **Fragmented QRS complexes.** This finding is thought to represent conduction disarray caused by ventricular scarring and an ECG can be given an overall score for fragmentation. Whilst there are reports of the degree of fragmentation being associated with the incidence of

ventricular arrhythmia, including a substudy of 797 patients from the Sudden Cardiac Death in Heart Failure Trial (SCD-HeFT) (Abdelghani, 2016), it is unlikely to be a powerful addition to independently risk stratify.

- **Holter Monitoring**. Ambulatory monitoring of 2 or 3 lead ECGs over a sustained period of time, typically 24 or 48 hours, can reveal significant findings not present on a resting ECG. Non-sustained VT on a Holter monitor is associated with both arrhythmias and mortality (Abdelghani, 2016; Makikallio, 2005).

- **Heart Rate Variability.** This is derived from a period of ambulatory monitoring, such as a Holter monitor. Reduced heart rate variability has been associated with ventricular arrhythmia and mortality, but is also dependent on a number of confounding factors, such as age, gender and medications so is difficult to compare between populations. Various components of the heart rate variability have been examined and these may give a higher association with mortality (Abdelghani, 2016).

- **Signal-Averaged Electrocardiogram**. This requires an amplified and processed ECG that can detect microvolt-level late potentials during the terminal portion of the QRS complex that are not visible on a standard ECG. This type of ECG is quite technically challenging as the signals are very low frequency and take considerably longer than a standard ECG to perform. A number of studies have identified the presence of these late potentials are associated with both an increased inducibility

{Hammill, 1992), and SCD (Gomes, 2001) but others have failed to show any significant association (Bigger, 1997; Abdelghani, 2016). It remains a minor diagnostic criteria for ARVC (Priori, 2013).

- **T wave alternans.** This refers to the beat-to-beat fluctuation in the amplitude of the T wave, which is a normal response in tachycardia but is an abnormal finding at slower heart rates. It represents increased dispersion of repolarization of the left ventricle but using it to predict SCD has again mixed results (Abdelghani, 2016).

- **T peak to T end.** This is the interval from the peak of the T wave to the end and is a measure of dispersion of repolarization. This is a relatively new predictive marker and has shown promising results in a variety of populations, but further work is required to further validate (Abdelghani, 2016).

Cardiac Imaging

- **Echocardiography.** This is the most common method of identifying structural heart disease that might predict ventricular arrhythmias, as well as providing an accurate assessment of left ventricular ejection fraction. As previously discussed ejection fraction is the main tool used for risk stratification, both in ischemic and non-ischemic cardiomyopathy and forms the basis for international guidelines on ICD treatment (Moss, 2002; Moss, 1996), despite its relatively low sensitivity and specificity. Despite these failings it remains the strongest predictor of SCD

(Solomon, 2005) and the main source of EF estimation in initial studies was by echocardiography.

- **Cardiac magnetic resonance Imaging (CMR).** CMR is now considered the gold standard for measuring ventricular volumes and ejection fraction, and is potentially more reproducible than echocardiography (Karamitsos, 2009). CMR has the potential to image both replacement scar (by late gadolinium enhancement (LGE)) and diffuse scar (by T1 imaging). Both the infarct size by LGE and the peri-infarct zone in ischemic cardiomyopathy has been shown to predict arrhythmia risk (Klem, 2012; Chen, 2015; Kuruvilla, 2014). There is increasing evidence that diffuse fibrosis measured by T1 may be a potential risk stratification tool and diffuse fibrosis has been associated with arrhythmias in both ICM and NICM (Chen, 2015).

- **Cardiac CT.** Provides quantification of LV volumes and EF as well as detailed imaging of the coronary arteries.

- **Nuclear cardiac imaging.** Myocardial perfusion single-photon emission CT has traditionally been used to provide information about EF and ischemia. SPECT with iodine-123 meta-iodobenzylguanidine (MIBG), can be used to identify sympathetic over-activity in heart failure, which partly predicts prognosis (Jacobson, 2010). Positron emission tomography (PET) using radio-labelled tracers that are either specific for pre-synaptic innervation (Matsunari, 2010; Caldwell, 2008) or post-

synaptic innervation (Tsukamoto, 2007) displays regional denervation with superior spatial resolution. Carbon^{11}-hydroxyephedrine (CHED) is the best validated of these tracers (Rosenspire, 1990; Sasano, 2008; Luisi, 2005; Law, 2010; John, 2007) The volume of denervated myocardium on CHED PET has been identified as an independent risk marker for arrhythmia and mortality in a large prospective study (Fallavollita, 2014).

1.6.2 Invasive risk stratification

- **Coronary angiography.** Angiography is used to identify significant coronary artery disease, the extent of which has prognostic value.

- **Electrophysiology study (EPS) and VT stimulation.** The basic premise of an EP study is to identify the presence of an electrical substrate for re-entrant tachycardia and was first performed in 1968 as a means of identifying patients at high risk of sudden cardiac death (Wellens, 1972). There are a number of variables that determine the accuracy of a VT stimulation test, including type and severity of the underlying heart disease, the presence or absence of spontaneous VT, concomitant drug therapy, the stimulation protocol chosen and the site of stimulation. Most centres use 8 ventricular stimuli at drive cycle lengths between 600ms and 400ms at the RV apex, at twice the diastolic threshold and pulse duration of 0.5-2ms, delivering 1-3 ventricular extrastimuli. Some centres then repeat this at an alternative location (eg

apex and outflow tract). The test may be repeated during isoprenaline infusion. The main criteria for a positive test is induction of sustained monomorphic VT, whilst other induced arrhythmias including polymorphic fast VT and VF can be of clinical significance depending on the clinical situation (Kossaify, 2013).

VT stimulation protocols were previously used routinely to identify patients thought to be at high-risk of recurrent ventricular arrhythmias and was previously considered the “gold standard” method for SCD risk stratification in ischemic heart disease. A number of older studies demonstrated that patients who had inducible VT during EPS had a higher rate of SCD (Bourke, 1991; Nogami, 1991). However, more recent larger studies including the MUSTT-II EPS substudy (n=593), have failed to show any significant difference between patients in whom the EPS is positive or negative in patients with an ejection fraction <40% (Daubert, 2006). In the MADIT-II study (in which patients had an EF<30%) whilst ICD implantation clearly resulted in improved survival, the absence of inducibility did not predict prognosis (Moss, 2002b). The current role for EPS for risk stratification in ICM is now less clear, and current guidelines recommend its use in a much smaller subset of patients, including those with NSVT and moderate systolic function and patients presenting with either syncope or sustained palpitations with evidence of previous myocardial scar (Pedersen, 2014).

In patients with NICM EPS is generally not considered useful in risk stratification (Al-Khatib, 2007). VT stimulation studies are of limited value in causes of non-reentry VT, such as papillary muscle VT and outflow tract VT (Kossaify, 2013). Results of EPS in Brugada syndrome are inconclusive (Priori, 2012; Priori, 2013) and a metaanalysis from 2007 appears to confirm that it does not predict arrhythmia (Paul, 2007). In ARVC VT stimulation may be useful and is indicated in the european society of cardiology guidelines (Priori, 2015) and an electrophysiology study with voltage mapping can be used to identify regions of fibro-fatty replacement and to guide catheter ablation (Bai, 2011; Philips, 2012) VT stimulation has been shown not to influence the high rate of death in patients with syncope who have significant structural heart disease (Middlekauff, 1993). It may have some use in adult congenital heart disease, such as in patients with repaired Tetralogy of Fallot who have additional risk factors (LVSD, QRS duration >180ms, extensive RV scarring) (Khairy, 2014).

The need for improved risk stratification

As described in the previous section decades of research have been dedicated to improving our understanding of common arrhythmias and improving our ability to identify patients most at risk. In the current era, with the widespread availability of the ICD, which has been shown to significantly reduce mortality (Moss 2002a), identifying the patients who will benefit is essential. Despite the plethora of potential arhythmogenic markers available, ejection fraction remains

the only risk stratification robust enough to be routinely used in primary prevention ICD selection for the majority of acquired heart disease. This however has significant flaws though as evidence suggests that if all patients who had an EF<35% were implanted the majority would not experience an arrhythmic event requiring device intervention over many years follow up (Banna, 2011), and the majority of patients who suffer a cardiac arrest do not have a severely impaired ejection fraction (Moss, 2002a). Whilst ICDs are effective they remain very expensive (£16,250 estimated cost per ICD, NICE 2006) and an improved selection method could result in major savings. In 2010 over 4500 ICDs were implanted in the UK (UK national clinical audit 2010). This is in addition to more general costs associated with lost productivity and long-term care.

Despite current guidelines recommending ICD implantation for patients with NICM and an EF of <35% (Priori 2015), a recent large randomized controlled trial (Defibrillator Implantation in Patients with Nonischemic Systolic Heart Failure (DANISH)) in this patient group (n=1116) failed to show any reduction in mortality (Kober, 2016). This highlights current flaws in our current ability to risk stratify and is likely to change future guideline recommendations. Clearly a better understanding of the underlying mechanisms of arrhythmia and improved or additional arrhythmogenic markers has the potential to improve our risk stratification. The following sections of this review will assess some of our current limitations in understanding arrhythmia mechanisms, which have been studied in the following chapters.

1.7 Stress and its role in arrhythmia

The human heart is put under a number of significant stresses on a daily basis, including both physical and psychological stress. The association between physical stress and sudden cardiac death has been well studied. The mechanistic effect of psychological stress on cardiac arrhythmia remains incompletely understood. Whilst the incidence of life-threatening cardiac arrhythmias, primarily ventricular tachycardia, is significantly greater during times of psychological stress, the underlying mechanism for this association is not clear. The stimulation of the sympathetic nervous system (SNS), which occurs during psychological stress, has been studied in relation to the effect on global cardiac function (heart rate, inotropy etc), but its effect on the intra-cardiac electrophysiological properties is unknown.

1.7.1 The link between psychological stress and cardiac arrhythmia

Psychological stress is known to be associated with SNS activation, and there are large population studies showing an increased incidence of SCD at times of sustained psychological stress, such as during wars and natural disasters, with only a small proportion occurring due to increased physical workload at these times (Taggart, 2011; Aoki, 2012). This increase could be explained by either an increase in primarily arrhythmic events, or alternatively stress is recognised to cause an increase in ischemic events through it's effect on platelet activation and vasoconstriction (Lampert, 2016), as well as increased workload (Kop 2001). Studies have also shown a link between more chronic

forms of psychological stress, such as job insecurity (Ferrie, 2013), bereavement (Mostofsky, 2012) and marital stress (Orth-Gomer, 2000) with sudden cardiac death.

Studies in humans have shown that anger emotion may affect arrhythmia induction and termination (Taggart, 2011). The mechanism for this is unclear but probably involves a combination of central processing at the cortical and brainstem level, autonomic innervations and the electrophysiology of the myocardium. Studies in animals show strong emotions like anger are a potent cause of VF (Skinner, 1981). Several studies have shown that emotion may influence ECG measures of repolarization, known to be important in arrhythmias (Taggart, 2005; Toivonen, 199; Kop, 2004; Lampert, 2009). However, there are few studies looking at the intracardiac electrophysiological properties of human myocardium during psychological stress, which would show more localized changes in repolarization parameters.

Heterogeneity of the SNS input and cardiac receptor heterogeneity are thought to be factors in arrhythmia generation, although the exact mechanisms remain unknown.

1.7.2 Psychological stress and the autonomic nervous system

Stimuli triggered by emotional or psychological stimuli (e.g. sight or emotional stressor) are processed via the brains cortex, amygdala and brainstem and results in activation of the dorsomedial hypothalamus followed by the medulla and then activation of sympathetic activity (Dampney, 2016). The autonomic response to emotion was first reported in 1915, although aside from stimulation of the SNS and PNS respectively, the neurophysiology that underpins this relationship is still incompletely understood (Kreibig, 2010). Some researchers argue that specific emotions result in specific autonomic responses that are unique for that emotion (for example fear might produce a very different autonomic pattern than disgust). Whether this specific emotion profile might result in differing changes in APD is unknown.

1.8 The Autonomic Nervous System

The autonomic nervous system (ANS) is responsible for regulating and modifying the activity of most internal organs and glands. The ANS usually functions without conscious control in response to a number of different afferent signals, however it is also regulated by areas within the brain, mainly in the hypothalamus and brainstem that receive input from the limbic system and other regions of the cerebrum. It is this relationship that underpins the connection between emotional stress and changes in the sympathetic nervous system.

1.8.1 Actions of the sympathetic nervous system

Activation of the SNS and release of adrenergic hormones by the adrenal medullae set into motion a series of physiological responses collectively called the “fight or flight” response which include the following effects: pupil dilatation, heart rate and blood pressure increases, redirection of blood-flow towards skeletal and cardiac muscle, airway dilatation and the breakdown of glycogen to glucose (glycogenolysis) by the liver. Due to heterogeneous innervation and receptor densities activation of the SNS results in different degrees of response in each ventricle, with a mainly chronotropic response in the right ventricle compared to an inotropic response in the left ventricle (Miyano 1998). Whilst effects such as increasing heart rate and blood pressure are easy to measure and widely accepted it is thought that stimulation of the SNS has many more subtle cardiac effects that may play important roles in arrhythmia initiation and maintenance, although the details remain unproven and much debated.

At the cardiomyocyte level, norepinephrine (NE), acts as the post-synaptic neurotransmitter, which is released when the SNS is activated. NE binds to the myocardial Beta (β**)** receptors, which are linked intracellularly to the enzyme adenyl cyclase by the stimulating guanine nucleotide binding protein Gs. Stimulation of adenyl cyclase increases intracellular levels of second messenger cyclic AMP, which activates protein kinase A (PKA). PKA causes phosphorylation of the L-type calcium channels, leading to influx of calcium from the sarcomplasmic reticulum, further increasing amounts of calcium

available for activation of myocardial contractions through the ryanodine receptor. These responses at the cell level are depicted in Figure 5.

Figure 5: The intracellular effects of SNS stimulation

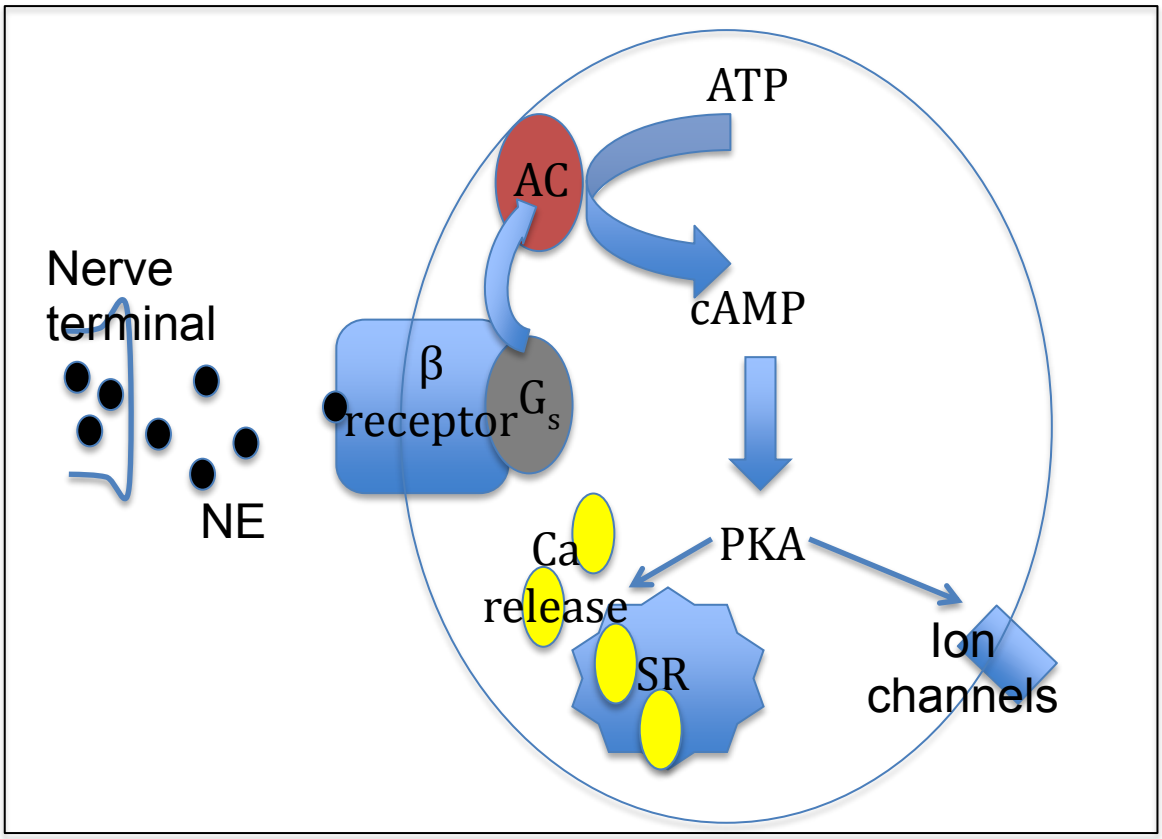

Figure 5. Schematic representation of cardiac β receptor activation. β receptor activation by norepinephrine (NE) activates, via the G protein, Adenylate Cyclase (AC). AC catalyzes the conversion of ATP to cAMP, which subsequently activates PKA. PKA has a number of effects including ion channel function and Ca^{2}+ release from the sarcoplasmic reticulum (SR) (Adapted from Taggart, 2011).

Stimulation of the SNS will also result in release of adrenaline and noradrenaline from the adrenal medullae. These 2 circulating hormones further enhance the more local effects of the SNS.

1.8.2 Different forms of psychological stress employed in clinical studies

In order to activate a stress response in humans a number of physical (environmental and physiological) or psychological/mental stressors (cognitive and emotional) are commonly studied. Common environmental stressors include cold and hot temperatures, physical workload and hypoxia and physiological stressors include illness, muscular fatigue and dehydration. A commonly used environmental stress test is the cold pressor test, where the subject's hands are immersed in ice-cold water. Whilst physical stressors trigger activation of the ANS and hypothalamus-pituitary axis through mechanisms involving the brainstem and hypothalamus, mental stressors elicit their response through the frontal lobes and limbic systems that connect to the hypothalamus (see 1.7.2) (Bali, 2015).

During this research we have focussed on the effects of psychological stress in arrhythmia, which remains poorly understood. The psychological and mental stressors primarily have a central effect in the brain, without directly affecting the rest of the body. These can be either cognitive (affecting thought processes) or emotional (affecting feeling responses, including anger, fear and disgust) (Bali, 2015).

Clinical methods of eliciting cognitive stressors include anger re-call, where a subject is asked to recall and describe a stressful event, and mental arithmetic

challenges (including serial 7's where a subject is asked to repeatedly subtract 7 from a large number).

Typical methods of eliciting emotional stressors include the displaying of emotional pictures of movie clips. There are a number of standardised collections of positively and negatively emotionally evocative photographs used routinely in neuro-behavioural studies, such as the International Affective Picture System (IAPS), which have been widely studied (Lang P, 1999). Tools like the IAPS have been validated using functional MRI as eliciting specific neural responses (such as the amygdala being mainly involved in the processing of negative emotions) (Aldhafeeri, 2012). Movie clips have been shown to be amongst the most powerful tools available in clinical studies for eliciting emotional responses (Westermann, 1996; Schaefer, 2010).

1.8.3 Measuring and quantifying levels of psychological stress during clinical studies

Psychological stress is associated with changes in specific circulating hormones as a result of activation of the hypothalamus-pituitary system or the sympathetic nervous system, and the following biochemical markers and tests have all been used to quantify response to stress (Bali, 2015):

- cortisol (in blood, urine or saliva)

- cortisol awakening response (deviations from the usual 50% increase in circulating cortisol that occur 20-30 minutes after awakening are associated with a number of chronic stress conditions)
- dexamethasone suppression test
- salivary α-amylase
- plasma/urinary norepinephrine
- norepinephrine spill-over rate
- interleukins (representing an acute response of the immune system to psychological stress).

Whilst some of these biomarkers can be sampled relatively non-invasively (as in the case of urine and sputum samples) and others can be used to identify acute changes in stress response (such as plasma norepinephrine) they all have technical considerations and add complexity and cost to designing clinical studies. The measurement of certain physiological parameter changes in response to acute stress has the potential benefits of reflecting direct increases in stress and occur instantaneously and can often be measured non-invasively. However they can also be more difficult to quantify than the biochemical parameters, and there is frequently a wide degree of inter-subject variability in response.

Examples of commonly used physiological parameters include:

- Heart rate
- Systolic, diastolic and mean arterial blood pressure
- Rate of pressure change in systolic pressure (dp/dt)

- Heart rate variability
- Pupil size

Blood pressure responses to measure SNS activation

Sympathetic activation due to physiological stressors, such as isometric hand grip, incremental and steady state exercise and cold exposure, results in an increase in systolic and diastolic blood pressure (Van Herwaarden, 1979; Morrison, 1982). These physiological responses are thought to be mainly neurogenic (noradrenaline mediated) and results in vasoconstriction, and are similar to what is seen during a noradrenaline infusion (caused by α-receptor mediated vasoconstriction) (Kumana, 1986).

The adrenergic response is more complicated and intravenous infusions of adrenaline in healthy control subjects have been shown to lead to reduced diastolic pressure (due to β_2-receptor mediated vasodilatation), but increased systolic pressure (β -receptor mediated and reflex actions). During prolonged catecholamine infusions (<1 hour) there is evidence of feedback between the β (facilitatory) and α (inhibitory) components (Kumana, 1986; Barcroft, 1951). β-blocking drugs are established treatment for hypertension, because of their blood pressure lowering effects, since the first β –blocker study published in 1985 (MRC study looking at propranolol in mild hypertension) (Larochelle, 2014). Psychological stress has been shown to cause an increase in blood pressure, both in the chronic state (Gasperin, 2009) and the direct result of provoked acute stress (Carroll, 1995).

The rate of pressure increase (dp/dt) within the left ventricle is an alternative haemodynamic measurement. It is usually measured with a pressure-sensing catheter within the left ventricle and is calculated from the maximal increase in left ventricular pressure during systole divided by time. Dp/dt has been shown to be a good surrogate for sympathetic activity (as sympathetic activation increases the forcefulness of contraction) and has been validated against norepinephrine spill-over (Azevedo, 1999). Studies have shown that arterial dp/dt measured from central arterial pressure can be used as an accurate surrogate for direct left ventricular pressure measurement (Morimont, 2012).

Galvanic skin response (GSR)

GSR can be used as an indirect measure of stress-induced activation of the SNS in clinical studies. As a result of SNS activation there is an increase in sudomotor activity, resulting in an increase in skin conductance. This test commonly involves measuring the conductance between 2 electrodes placed on different fingers.

Microneurography

It is possible to measure sympathetic activation directly by microneurography which allows measurement of peripheral sympathetic traffic (Parati, 2012). However, this technique requires very complex recording devices and has a number of practical limitations in clinical emotional stress studies.

Studies frequently use a self-reported scale of stress/anxiety to rate the stressfulness of the protocol. Whilst this is very quick and easy to perform it is clearly very subjective and comparison between patients is very difficult.

1.8.4 Brain-heart laterality hypothesis

The human brain is composed of a right and left hemisphere and current evidence suggests that different sides are responsible for processing different emotions and modulating different components of the ANS (negative emotion and the SNS by the right hemisphere, positive emotions and the PNS by the left hemisphere).

Autonomic nerve traffic between the heart and brain is mainly ipsilateral, and although there is considerable cross-communication within the plexus prior to the myocardial innervation, there remains some same-side predominance (e.g left sided hemisphere traffic directly affect innervation of the left side of the heart more than the right). There is a trend for left sided innervation to favour the postero-inferior aspect of the left ventricle, and right-sided innervation to favour the anterior aspect and right ventricle, albeit with considerable overlap. As a result different parts of the heart may be receiving heterogenous degrees of activation. This theory is termed the “brain-heart laterality hypothesis” (Taggart, 2011). Activation of the ANS will also result in the release of systemic catecholamines, which bind to receptors on both sides of the heart.

1.9 The effects of the SNS on arrhythmia initiation and maintenance

In general, in the ventricles, increased sympathetic tone is considered to be pro-arrhythmic, whilst activation of the PNS is protective (Schwartz, 1984; Zipes, 2004; Myers, 1974). Notable exceptions include long QT type 3 and Brugada syndrome. The pro-arrhythmic potential of the SNS has been established in a wide range of models, including isolated heart preparations with an intact SNS (Ng, 2007a) and selective stimulation of the SNS in vivo (Myers, 1974), and has been shown to reduce the ventricular fibrillation threshold (Zipes, 2004).

Drugs that block the actions of the SNS, particularly beta blockers have been shown to significantly improve prognosis in heart failure (Packer, 1996) and IHD (Pokorny, 2011). A more comprehensive understanding of the SNS, both in healthy and diseased hearts, may improve our ability to risk stratify and direct further drug research.

Prior experimental research has identified a number of different effects which activation of the SNS has on cardiac tissue. These can be divided into effects seen within normal healthy myocardium, and abnormal diseased myocardium where the effects are often more complex.

1.9.1 The effect of SNS stimulation on the APD duration

Adrenergic stimulation has experimentally been shown to have a number of different effects upon ion channels, most importantly the L-type calcium current and potassium channels. SNS stimulation has been shown to stimulate the L-type calcium current which would theoretically extend the plateau phase of the MAP and promote after-depolarizations (Workman, 2010), but also stimulate a number of the potassium channels which would have the opposite effect on the APD by quickening repolarisation (Zipes, 2004; Taggart, 2011).

In animal models SNS pharmacological stimulation has generally been shown to decrease APD (Vaseghi, 2012a; Volders, 2003), however the overall effect in humans remain less clear. In studies where diseased tissue was explanted NE infusion appears to increase APD (Lampert, 2002; Mitchell, 1986; Koumi, 1995), whereas in vivo pharmacological sympathetic stimulation seems to shorten APD (Vaseghi, 2012b). The use of nitroprusside (resulting in hypotension and SNS via the baroreflex) also results in APD shortening (Vaseghi, 2012b). All of these studies have used pharmacological stimulation of the SNS and there is no evidence of the effects of psychological stress on APD duration, which will be investigated in this thesis.

1.9.2 Activation of the SNS within a diseased ventricle

Coronary artery disease, with or without prior myocardial infarction is the most common cause of VT in the developed world. There has been a lot of experimental work investigating sympathetic denervation as a result of ischaemic heart disease. This can be assessed both in areas of infarction, ischemia, hibernation and heart failure and multiple different adaptive processes (see later) may apply which makes determination of the effect of psychological stress on intracardiac electrophysiological in diseased hearts much more complex that in normal hearts. The effect of psychological stress on ARI in diseased hearts has not previously been investigated and will be studied as part of this thesis.

Myocardial Infarction

Infarction causes sympathetic denervation through Wallerian degeneration (Chen, 2001; Vaseghi, 2008; Vracko, 1991). Sympathetic denervation exceeds the area of infarction, and encompasses more apical viable tissue, presumably by disruption to the sympathetic nerves that transverse the infarcted region (Barber, 1983; Fallavollita, 2010). In non-transmural infarction the sub-epicardial viability may preserve some of the SNS fibres, and limit apical denervation (Fallavollita, 2010) but the area of denervation is still likely to be substantially bigger than the area of infarct (Figure 6A). Viable tissue that is deprived of its nerve supply may respond in an exaggerated fashion to catecholamines, a phenomenon known as super-sensitivity (Figure 6B) (Kammerling, 1987; Inoue, 1987). In a canine model this effect has been

demonstrated as a failure to decrease ARI with direct sympathetic nerve stimulation, but a supersensitive response to noradrenaline and isoprenaline infusions. These areas of super-sensitivity, found in viable but denervated myocardium, were more prone to fibrillation on electrical stimulation (Inoue, 1987). Over a period of many weeks (8-17 in canine models) there is re-innervation of these areas, but the super-sensitivity remains (Zipes, 1990).

Nerve sprouting is the growth of new neurons in response to nerve injury and death and occurs many weeks post infarction. Excessive regeneration can lead to hyper-innervation and this phenomenon has been observed within myocardial scar (Vracko, 1991) and the presence of a regional increase in sympathetic nerves is associated with ventricular arrhythmia and is particularly apparent within the scar border-zone (Cao, 2000). Nerve sprouting has been demonstrated following autopsy (Cao, 2000) and in vivo from nuclear imaging (Hartikainen, 1996). Nerve sprouting may increase risk of SCD by maximising regional heterogeneity in sympathetic function (Fallavollita, 2010).

Beta agonists, such as isoprenaline, increase heterogeneity of repolarisation by reducing ARI more in viable tissue than in scar or borderzone (presumably due to reduced innervation). However, if nitroprusside is used the ARI was seen to be shortest within the borderzone, and ARI actually increased in most other areas (Figure 6C) (Vaseghi, 2012b). This may result in an increased dispersion of repolarization as the usual mechanism of coupling between activation and repolarization is lost (such that the usual relationship between APD shortening further from the area of impulse generation is no longer the case).

Figure 6: Abnormal SNS activity in areas of myocardial damage

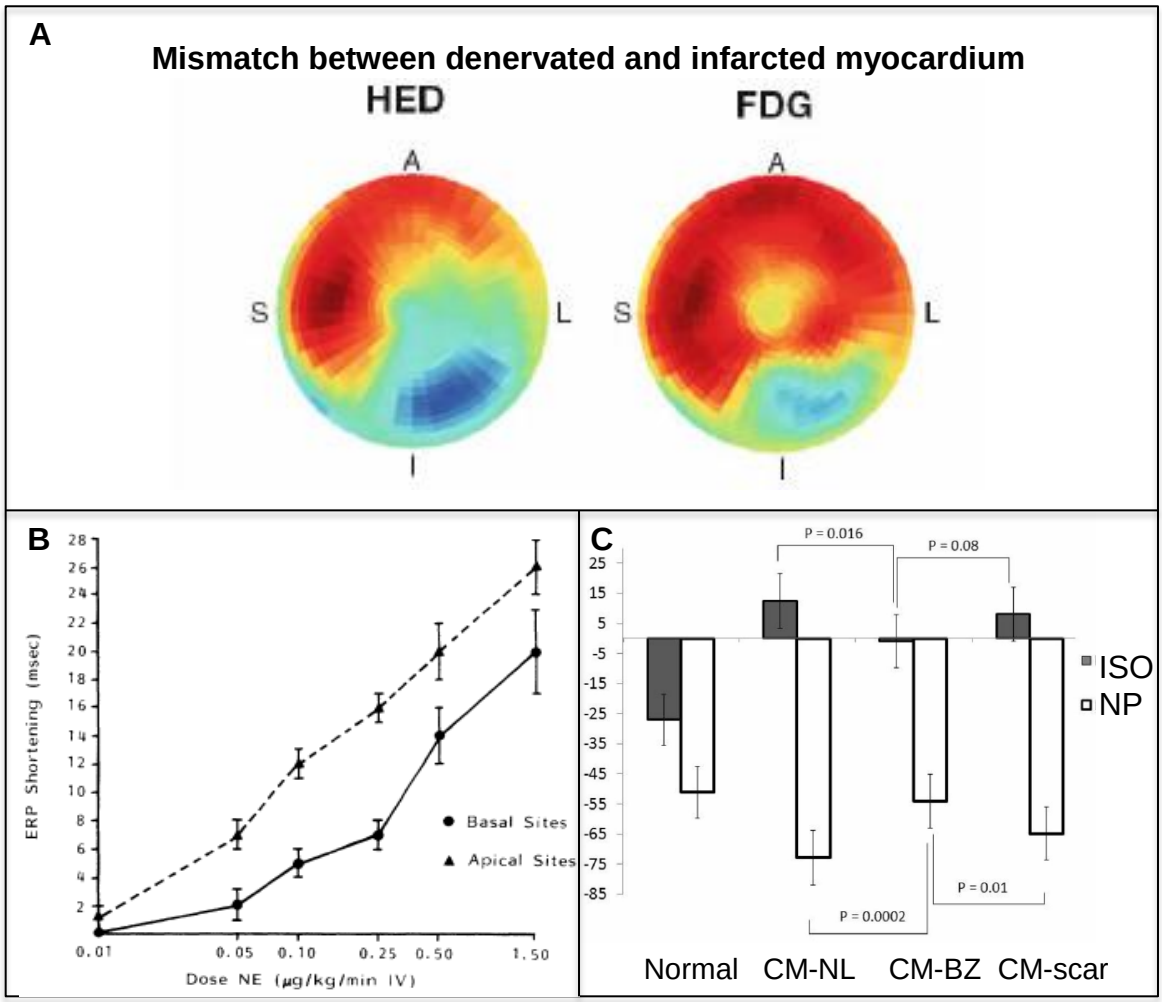

Figure 6. A– PET studies demonstrating viable but denervated myocardium after myocardial infarction using the sympathetic nerve tracer 11C-meta-hydroxyxephedrine (CHED left) and the viability tracer 18F-2-deoxyglucose (FDG right). Adapted from Fallavollita, 2010. B – In this study in infarcted dogs there was an exaggerated super-sensitivity response to norepinephrine infusion in non-infarcted apical regions compared to the areas proximal to the infarction. Adapted from Kammerling, 1987. C - Increase in dispersion of ARI response to direct and reflex sympathetic stimulation in diseased compared to normal hearts. CM – ischemic cardiomyopathy, NL – viable regions, BZ - borderzone. Adapted from Vaseghi, 2012b.

Ischaemia

Ischaemia is more likely to cause transient reversible SNS dysfunction as opposed to denervation (Fallavollita, 2010). This pathological effect is less well established than the models of SNS dysfunction following infarction. In a dog model ischaemia caused an increase in intrinsic heart rate (SNS activation) and the ventricular threshold decreased and 4/8 dogs developed spontaneous VF. However after SNS denervation there was no increase in intrinsic heart rate and only 1/8 dogs developed VF. Timely administration of B-blockers prevented VF (Pokorny, 2011).

Hibernating Myocardium

Hibernating myocardium is a result of chronic repetitive ischemia, which results in contractile dysfunction. Chronic ischemia resulting in myocardial hibernation is also associated with regional changes in SNS function and impaired sympathetic tracer uptake (Luisi, 2005) possibly caused by impairment of the Norepinephrine uptake-1 mechanism, which is normally responsible for the reuptake of NE from the synaptic cleft (Luisi, 2002).

Heart Failure

Even in the absence of CAD there are important changes in the SNS seen in heart failure. The SNS is chronically stimulated in heart failure in an attempt to maintain cardiac output. Increased circulating catecholamines and local NE spill-over from the synaptic clefts can both be demonstrated. Whilst this compensatory SNS stimulation may initially help to preserve cardiac output, chronically it results in increased myocardial oxygen consumption, promotes adverse cardiac remodelling, promotes activation of the Renin-angiotensin system and increases risk of arrhythmia (Kaye, 1995; Brunner-La Rocca, 2001). The use of B-blockers is well established as a chronic treatment for heart failure and has been shown in large randomized-controlled trials to reduce mortality (Packer, 1996).

Figure 7: The prognostic implications of SNS activity

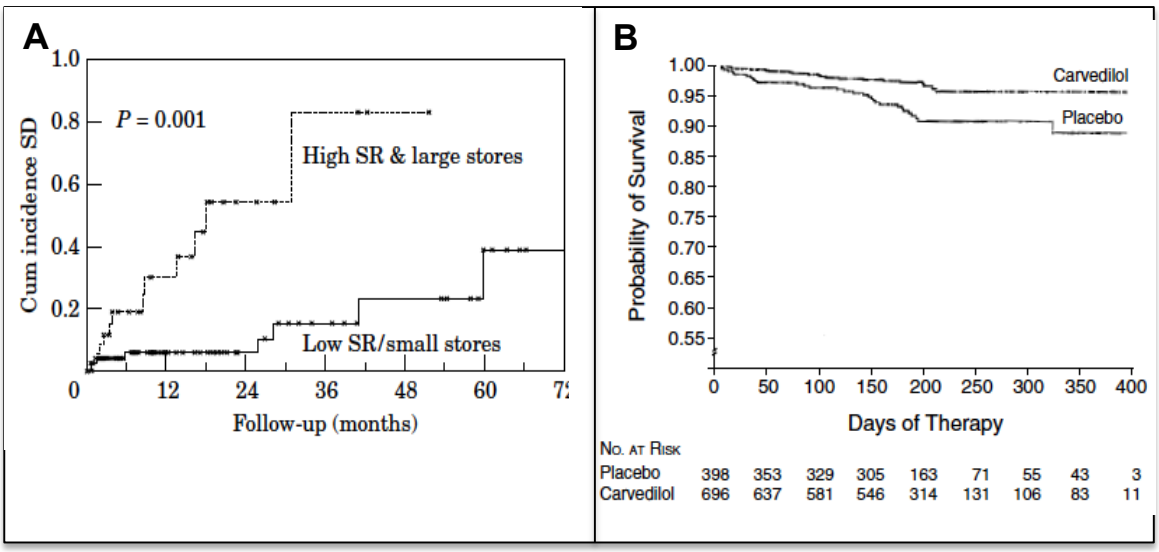

Figure 7. A - Cumulative incidence of sudden death in patients with high levels of noradrenaline spill-over and stores (representing chronically stimulated sympathetic system) compared to low levels. Patients with a chronically activated SNS were at increased risk of SCD. Adapted from Brunner-La Rocca, 2001. B – Carvedilol (a beta blocker) was associated with increased survival in chronic heart failure in the US Carvedilol Heart Failure Study Group. Adapted from Packer, 1996.

1.10 The effect of the parasympathetic nervous system (PNS) on cardiac rhythm

The heart rate decreases in response to PNS stimulation because of slowing of the SA node and AV node conduction velocities. Ventricular contractility is not affected by PNS activity when background SNS activity is low, but in the presence of enhanced SNS activity an increase in PNS is associated with a further increase in contractility. Unlike the SNS, the PNS does not affect APD and transmural dispersion in the ventricle (Vaseghi, 2008). The postsynaptic receptor for the PNS is the M2 muscarinic ventricle, which in the ventricle

activates cAMP but in the atria activates another G protein. This G protein has an effect on the potassium channel of the cell membrane, which is important for normal repolarization and results in a reduction in APD (Chen, 2014). There is a high density of vagal innervation in the atria and it is thought to be important in the mechanism of AF for some patients. Stimulation of the vagal nerve has been shown to initiate AF during animal studies (Chen, 2014).

1.11 The cardiac ganglia

There is an additional level of complexity in the cardiac ANS with cardiac ganglia positioned all around the heart in which both sympathetic and parasympathetic nerves meet and significant processing occurs, and information is relayed to the heart, the brain, and onwards to other cardiac ganglia. These ganglia also form part of a complex feedback mechanism to modulate the amount of SNS and PNS input to the heart (Vaseghi, 2008).

1.12 Studies looking at psychological stress and cardiac arrhythmia

Stimulation of the ANS by emotional stimuli is very complex and it seems likely that different emotions have varying strength of effect on SNS activation. In a study of 43 ICD patients it was found that the feeling of anger occurred at a significantly greater frequency immediately pre-shock, which was not the case for other emotions (anxiety, worry, sadness, happiness).

It is not clear whether this heterogeneity in arrhythmic response relates to stimulating different aspects of the ANS, or is simply a reflection of the magnitude of overall ANS stimulation. The concept of different aspects of the ANS (or relationship between the degree of SNS and PNS activation and their interplay) is supported by a number of studies that have recorded patterns of ANS stimulation specific for anger and other emotions in response to a number of stimuli; including emotional facial expressions (Ekman, 1983; Levenson), film clips (Christie, 2004) and recall of previous emotional experiences (Rainville, 2006). An example of this phenomenon is a study by Taggart et al, in which patients watching violence on movies demonstrated periods of heart rate slowing (PNS activation) despite evidence of raised circulating catecholamines (Taggart, 2003). These suggest a complex interplay between SNS and PNS in response to different emotions.

1.13 Cardiorespiratory feedback

Changes in respiration impact directly on cardiac activity via a number of mechanisms. During inspiration the increase in intra-abdominal pressure

activates the baroreceptor reflex resulting in an increase in heart rate via the PNS. This feedback loop is known as respiratory sinus arrhythmia, and is seen in normal physiology as a change in the R-R interval with respiration (Rainville, 2006). The interaction between respiration and the ANS is not linear and at low levels of stimulation (either high arterial pressure and sympathetic stimulation or low arterial pressure and vagal activity) respiration is thought to have more of a significant effect on autonomic traffic than at higher levels of stimulation.

Different states of arousal and emotion may be associated with varying respiratory patterns, which indirectly may influence cardiac electrophysiology via their respiratory mechanism (Rainville, 2006), as opposed to directly via the ANS. The effect of respiration on ventricular repolarization has recently been reported by our research group, demonstrating oscillations of ARI at the respiratory frequency (Hanson, 2012). Studies as part of this thesis will endeavour to further explore this relationship.

1.14 The baroreceptor reflex

The baroreceptor mechanism is the principle homeostatic feedback control maintaining arterial pressure. The baroreceptors are stretch receptors located in the walls of the carotid sinus and aortic arch. A decrease in arterial pressure results in a reduction of efferent nerve traffic from these stretch receptors, which feedbacks to the brainstem and spinal cord to cause an increase in sympathetic activity to increase vascular resistance, heart rate and contractility to maintain cardiac output (Dampney, 2016).

1.15 Oscillations in autonomic and respiration frequencies

Physiological measurements of most, if not all, biological systems demonstrate fluctuations over time, which are repeated in a predictable fashion and occur at specific frequencies. The frequency of these fluctuations, or oscillations, occurs as a result of other physiological processes. Arterial pressure fluctuations occurring at the same frequency as the respiratory rate is a classic example of this inter-relationship between different physiological processes. Whilst some of this change could be accounted for by changes in intra-thoracic pressure these changes in arterial pressure far outweigh this and therefore are not simply mechanical (Eckberg, 2000). Studies in dogs have shown a similar oscillation in heart rate intervals, which track the frequency of vagal-cardiac nerve activity (Katona, 1970). Low frequency oscillations (0.1 Hz) are thought to reflect the frequency of sympathetic nerve firing which has been recorded at this frequency.

The mechanisms responsible for the coupling between respiration and autonomic neural activity is thought to be a central sympathetic nerve activity 'gate' that is open to differing degrees during different phases of respiration which modulates sympathetic and parasympathetic traffic. Whilst respiration can gate low levels of ANS traffic, at higher levels it appears that respiration has less of a gating effect (Eckberg, 2000). Whilst the effect of respiration frequency on blood pressure has been well studied its effect on APD is unknown.

Time frequency analysis is performed either using fast Fourier transformation or power spectral analysis and are both widely used methods for investigating autonomic regulation. These techniques can identify subtle abnormal mechanisms that can act as useful prognostic markers, but would have otherwise not been appreciated using standard time domain methods. For example in the use of heart rate variability a low frequency component of the signal identifies sympathetic tone, whilst the high frequency components identify parasympathetic tone and the relationship between both these frequencies corresponds to the sympathetic-vagal balance.

1.16 Activation and Repolarization Times as key determinants for Re-entry tachycardia

As discussed in section 1.13 requirements for re-entry tachycardia, such as the most common form of ventricular tachycardia, are an area of inexcitable tissue (such as scar) around which an activation wavefront is able to propagate without extinguishing itself by meeting myocardium that is still refractory from the previous wavefront. Based on this statement it is clear that the activation properties of a tissue, as well as the refractory properties determine the required combination of conditions required to permit a re-entry tachycardia. Studies of local refractoriness are time consuming and are not used routinely in the diagnosis or risk stratification of re-entry tachycardia. However, as discussed in section 1.2.6 the repolarization time taken from the UEG can act as a surrogate for the local refractory properties. Repolarization times can be recorded quickly from multiple exploring electrodes simultaneously so may potentially be a useful tool in studying these arrhythmias. Clinical electrophysiology studies aimed at locating the re-entry pathway for ablation, routinely measure only conduction and not repolarization, relying largely on identifying local areas of abnormal slow conduction. Ventricular tachycardia is the most common cause of SCD so if the combination of local activation and repolarization properties could enable the identification of ventricular regions of high susceptibility to unidirectional block would have important clinical applications.

Unidirectional block is usually functional due to the presence of a region of late repolarization and hence prolonged refractoriness. A premature activation wavefront encountering a region of refractoriness is unable to conduct through the region and is blocked, but travels round the region and approaches the line of block from the distal side. If sufficiently delayed by slowed conduction, such that the proximal region has had time to regain excitability, the returning wavefront may re-excite proximally and form a re-entrant circuit which self perpetuates (this principle is described further below and illustrated in figure 8).

1.17 Fibrillation Factor

Basic research investigations previously published by our research group have highlighted a fundamental link between a novel metric related to activation times and repolarisation times between two neighbouring sites and the susceptibility of the region spanned by these points for sustaining a re-entrant circuit (Coronel, 2009; Coronel, 2010), These studies were performed in infarct Langendorff porcine model, where activation timings could be carefully manipulated by the regional infusion of pinacidil to shorten APD, sotalol to prolong APD and flecanide to slow activation. This was termed the fibrillation factor (FF) and is illustrated below.

Figure 8: Fibrillation Factor

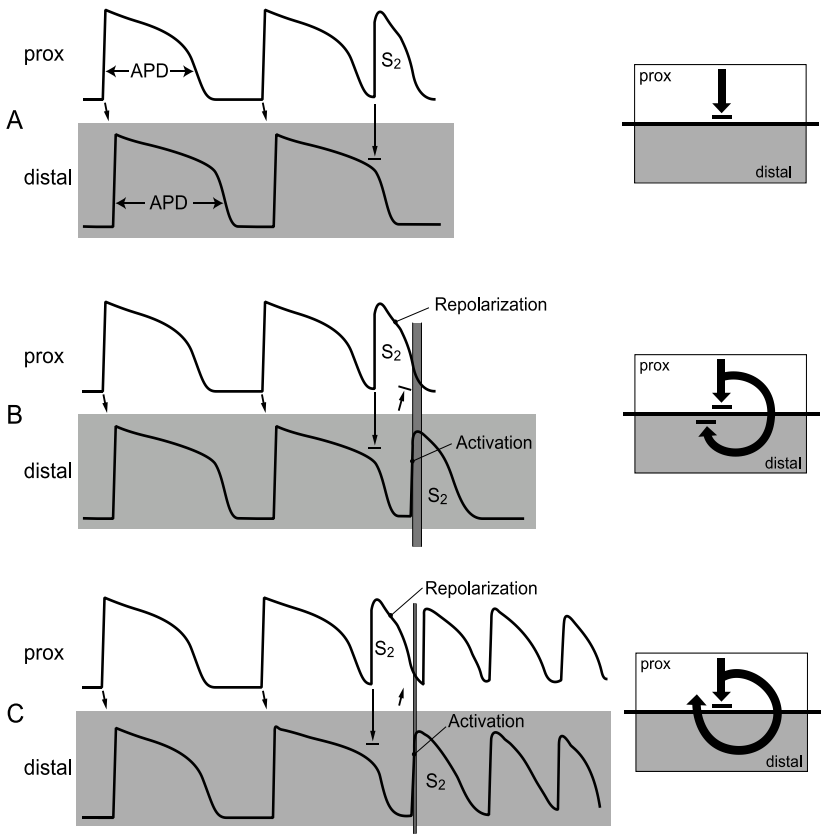

Figure 8. Illustration of FF in cases of re-entry and block. APDs are shown for the last 2 beats of a steady state train (S1) followed by a premature beat (S2). Activation conducts from proximal sites (upper rows) to distal sites (lower rows) as indicated by arrows. The interval between the time of arrival of the premature S2 beat at the distal site and repolarization of the premature S2 beat proximally (represented in panel B and C by varying thickness of the vertical grey bars) is a critical determinant of whether re-entry will occur and is referred to as the Fibrillation Factor. Adapted from Coronel et al, 2010.

According to this principle a short FF is found where there is conduction block, and hence re-entry can occur, where as a long FF is found where there is a line of bidirectional block so re-entry is not possible. In this animal study the pigs

with the short FF developed re-entry, which then deteriorated to ventricular fibrillation, whilst those with a long FF did not (Coronel, 2010).

There are no published studies looking at whether such an algorithm could successfully predict the site and probability of re-entry through the principles of FF based on the spatial relationship between tissues with different activation and repolarization properties during sinus rhythm. Part of this thesis will endeavour to explore this possibility.

1.18 Persistent AF

Atrial Fibrillation (AF) is the most common cardiac arrhythmia, affecting over 30 million individuals worldwide (Chugh, 2014). In addition, the overall worldwide incidence, prevalence and AF associated mortality is increasing, a trend that has been demonstrated in the UK (Martinez, 2015) and USA (Colilla, 2013). Whilst incidence is highest in the elderly, the burden of AF is found throughout the entire adult population and results in major morbidity (Benjamin, 1998), mortality, and healthcare costs (Sheikh, 2015). Despite the clear global impact of AF, our current understanding of the underlying disease process and mechanism of the arrhythmia remains substantially less than other common cardiac arrhythmias.

Atrial fibrillation is traditionally considered a spectrum of disease ranging from occasional short bursts of AF interrupting long periods of sinus rhythm (paroxysmal AF) up to continuous longstanding AF. Persistent AF (PsAF) is defined as continuous AF for longer than 7 days (January, 2014). AF occurs when structural (including atrial dilatation and fibrosis) and electrophysiological remodelling (including shortening APD, slowing conduction velocities and abnormalities in intracellular calcium handling) occur which alter the atrial tissue characteristics which allow the initiation and maintenance of AF. Electrophysiologically it is characterized by extremely rapid, temporally irregular and spatially disorganized electrical activity.

1.19 The underlying mechanism in persistent AF

Despite substantial cellular, animal and human studies in PsAF the underlying mechanism responsible for initiation and perpetuating the condition remains non-defined and controversial. The importance of triggers originating from the pulmonary veins are well recognised, and underlie the basis for pulmonary vein isolation in PAF (Haissaguerre, 1998). Whilst not curing all cases of PAF this approach has been shown to prevent further AF in 60-70% of PAF patients under long-term follow up (Ganesan, 2013a).

However, in PsAF the atria myocardium is thought to play an important role providing the required substrate for perpetuation of the arrhythmia, although the exact mechanism is not clear, and long-term success following ablation is significantly worse than in PAF (Ganesan, 2013a). It is hoped that a better understanding of the underlying disease mechanism will improve our ability to successfully treat PsAF. There are 3 main schools of thought as to the underlying mechanism in PsAF:

- **Multiple random propagating wavelets** – this was the dominant mechanism until the 1980s. AF results from the presence of multiple independent wavelets occurring simultaneously and propagating randomly throughout both atria. This model suggests that the number of wavelets at any one point in time depends upon the atrial conduction velocity, refractory period, and excitable mass. Perpetuation requires a minimum number of coexisting wavelets and is favoured by slow

conduction, shortened refractory periods, and increased atrial mass. Enhanced spatial dispersion of refractoriness promotes perpetuation of AF by heterogenous conduction and block. Early success with surgical ablation (the MAZE procedure) was designed on this principle, that AF needs a critical excitable mass and number of circulating wavelets (Moe, 1964).

- **Focal Triggers** – This followed the observation that in some patients AF could be cured by ablation of focal triggers (Haissaguerre, 1994). Whilst these focal triggers can occur anywhere in either atria it was found that the majority were located in and around the pulmonary veins which led to the development of the pulmonary vein isolation ablation procedure as a successful treatment for PAF. It is now well established that the pulmonary veins act as a key source of triggers that initiate AF, however in PsAF isolating the veins is frequently insufficient to cure AF.

- **Localized sources and re-entrant activity (rotors) –** In this hypothesis PsAF is maintained by a combination of focal sources and rapidly activating atrial re-entrant circuits (rotors). A substantial body of evidence is emerging substantiating this hypothesis using a variety of methodological techniques (Narayan, 2012a; Ganesan, 2013b; Lee, 2012; Skanes, 1998; Kalifa, 2006; Haissaguerre, 2014). In the CONventional ablation for atrial fibrillation with or without Focal Impulse and Rotor Modulation (CONFIRM) study rotors and localised focal sources were present in almost all AF patients (98%, mean 2.3 +/- 1.1

concurrent rotors and focal sources) and targeting these local areas with ablation terminated the arrhythmia and led to improved clinical outcomes (Narayan, 2012b), which was durable at 3 years post ablation (Narayan, 2014).

Yet despite these results by the CONFIRM group, a number of other researchers have failed to collaborate the prevalence of rotors (De Groot, 2010; Lee, 2014; Konings, 1994; Lin, 2013), or their stable nature (Cuculich, 2010). In a recent study by Benharash et al, 24 cases from the CONFIRM study were reanalysed using alternative techniques (dominant frequency and Shannon entropy) by a different research group and failed to show rotors contrary to the FIRM assessment (Benharash, 2015), and in another recent long-term study of FIRM ablation patients outcomes were poor (Buch, 2016). Other concerns regarding the FIRM data includes a high number of electrograms that were actually uninterruptable due to a low signal-noise ratio and that only approximately half or each atria were mapped on each occasion (Buch, 2016).

The development of a unifying arrhythmia mechanism that can be used to target specific individual therapies in PsAF remains elusive in cardiac electrophysiology. It is possible that understanding the underlying mechanism will lead to more successful ablation strategies in PsAF and this will be explored in this thesis.

1.20 Technical considerations in mapping PsAF

3-dimensional electroanatomical mapping has become a standard tool for electrophysiologists and there are a number of commercially available systems that are available and widely employed for both research studies and everyday clinical practice. However traditional mapping of AF is technically limited by multiple factors, including changing electrogram morphologies and variable cycle lengths, meaning that standard mapping techniques are ineffective.

Alternative strategies for mapping AF are described below:

1.20.1 Complex Fractionated Atrial Electrograms (CFAEs)

Direct contact mapping of atrial electrograms using standard mapping techniques during AF reveal some electrograms consist of multiple complex deflections, and studies have shown that this is likely to reflect distinct local electrophysiological properties at this site, such as slow conduction, functional conduction block and pivot points (Konings, 1994). An ablation strategy that includes ablation of CFAEs has previously been successful in small human studies (Nademanee, 2004), but it adds significantly to procedural complexity and time, fluoroscopy time and ablation application time, and more recent larger studies have shown less favourable results (Oral, 2007; Oral, 2009). In a large international multicentre randomized control trial (Substrate and Trigger Ablation for Reduction of Atrial Fibrillation Trial Part II – STAR AF2) there was

no improvement in outcomes with CFAE ablation in addition to pulmonary vein isolation (Verma, 2015) and CFAE ablation is now infrequently performed.

1.20.2 Dominant Frequency (DF)

DF is a tool to measure the rate and regularity of AF electrograms, and is based on the concept mathematically that if a rotor is present it will be at the location of highest frequency (effectively “driving” surrounding areas), and as such this DF would be stable in time and location. DF can be calculated from electrograms taken during direct endocardial mapping but then requires some relatively straight forward post processing analysis, which includes filtering usually followed by fast Fourier transformation to obtain a power spectrum of the electrogram at each recording site. The largest peak frequency is identified as the DF. The power of the DF and it’s harmonic peaks compared to the total power ratio is termed the harmonic index which is an additional measure used to represent the organization and local temporal regularity of the AF. Similarity index is a measure of the beat-to-beat similarity in the local activation wavefront (Lin, 2013).

DF has previously been used to guide catheter ablation of AF by identifying areas thought to represent focal sources and rotors (Sanders, 2005). However, in other studies locations thought to represent rotors using other mapping methods DF did not accurately predict rotor sites (Benharash, 2015) however this could be due to failings in either of the mapping techniques. Most studies show that the DF in AF is within a range of 4-9 Hz (240-250 cycles/minute) with

a narrow band width, suggesting AF is not completely chaotic (Ng, 2007). Whilst this is a robust technique for analysing spatial frequencies it is not useful for spatiotemporal relationships.

1.20.3 Phase

In order to perform more complicated analysis of the spatiotemporal activation in AF the electrograms need to be converted into phase. Phase analysis is used to track the progression of a defined region of myocardium through the action potential and has been validated as an effective tool to analyse the spatiotemporal changes during AF (Umapathy, 2010). Phase was first used in the study of cardiac fibrillation in the 1980's using a time-encoding technique reliant on activation periods being constant over the mapped surface (Umapathy, 2010). However, it was only later that the state-space encoding concept derived from nonlinear dynamics was employed to manage the varying activation periods (Gray, 1998).

In analysing spatiotemporal maps during AF (or VF), points at which the phase progresses through a complete cycle (from $-\pi$ to $+\pi$) are of particular interest and are termed phase singularities (PS). At these PS the activation front hinges to this point, and displays rotor properties with the activation front rotating around this PS (see Figure 9 for an example of a fixed rota in VF). Phase can be applied either to signals from electrical or optical mapping.

Figure 9: Example of a long-lived rotor during VF in a human heart from an epicardial 256 electrode sock

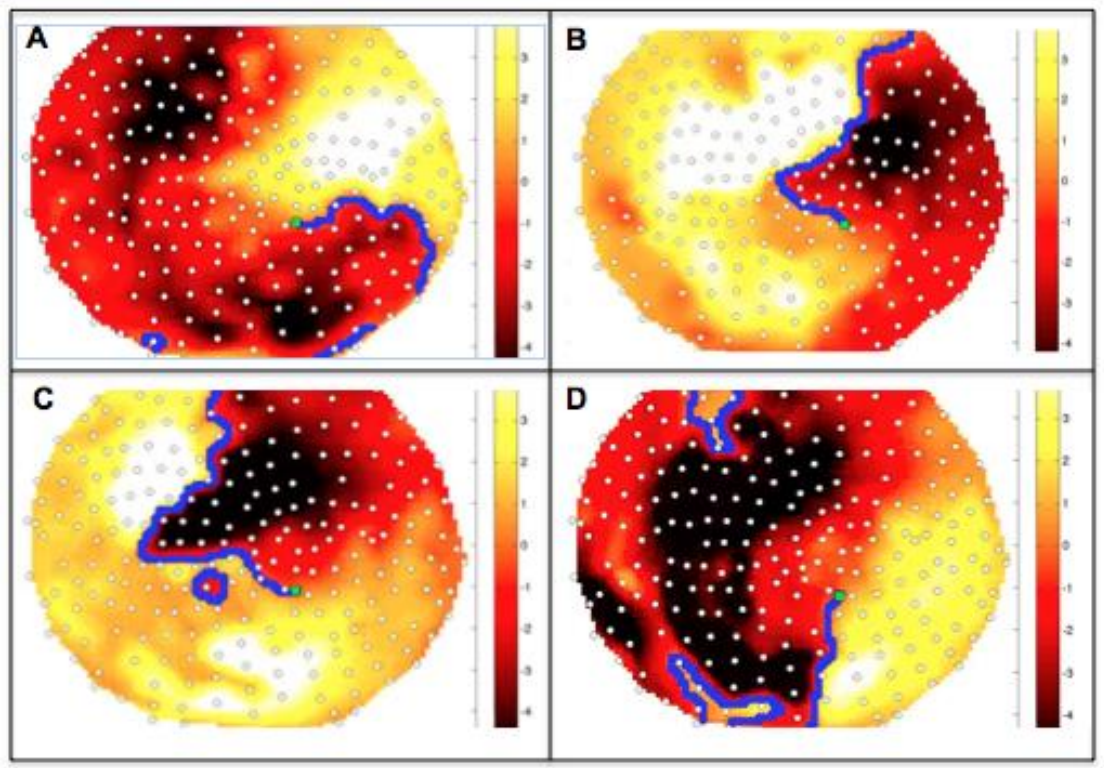

Figure 9. The phase singularity (illustrated by the green square) is relatively fixed as the activation front spirals around the fixed PS hinged point. A-D shows its progression through an entire rotation. Unpublished figure but adapted from same data as Nash et al, 2006.

Phase analysis involves a number of methodological steps in order to convert electrograms (or optical mapping data) into phase, which are briefly described below:

- Interpolation – even high-density mapping with current generation multipolar electrode catheters have insufficient spatial resolution. Additional interpolated electrograms are inserted into the surface area between electrode locations. If this is done for every instant of time then

a spatiotemporal map is obtained. In addition DF maps can be constructed from this data.

- Phase space plots – the temporal organization of a signal can be analysed using phase-space plots where the signal is plotted against its time delayed version, and if there is a consistent relationship between past electrograms at the current site and future electrograms (as would be the case with rotor activity) then the plotted trajectory will form a loop around a central point, called an attractor. An important component of this calculation relies on a derivative calculated from the cycle length of the fibrillation, which is difficult to assess in AF. A solution to this problem is in the use of the Hilbert transformation, which allows generation of a phase-shifted signal from the original signal, without the need to estimate an ever-changing cycle length. There are empiric difficulties with analysing AF as phase may not orbit the origin (attractor), in which case PS detection will be poor. Unlike VF, in which the electrogram has a sinusoidal morphology (no isoelectric line in signal), AF is characterized by smaller volume electrograms (caused by less muscle depolarization) and long isoelectric lines which is a problem for phase.

- Spatial organization – The phase of all the electrograms are then able to be studied at every point in time over the entire surface of electrode recordings, and a moving map of this phase can then be constructed. During organized activity distinct patterns of phase will be identified, such as a PS as previously described. This can be presented on a 2D

map, or then reconstructed from anatomical electrode locations to present phase as 3D. A rotor is identified if a PS persists long enough for the phase pattern to cycle at least twice around the PS (Umapathy, 2010).

Examples of these processes are illustrated below in Figure 10

Figure 10: Processes involved in performing phase analysis

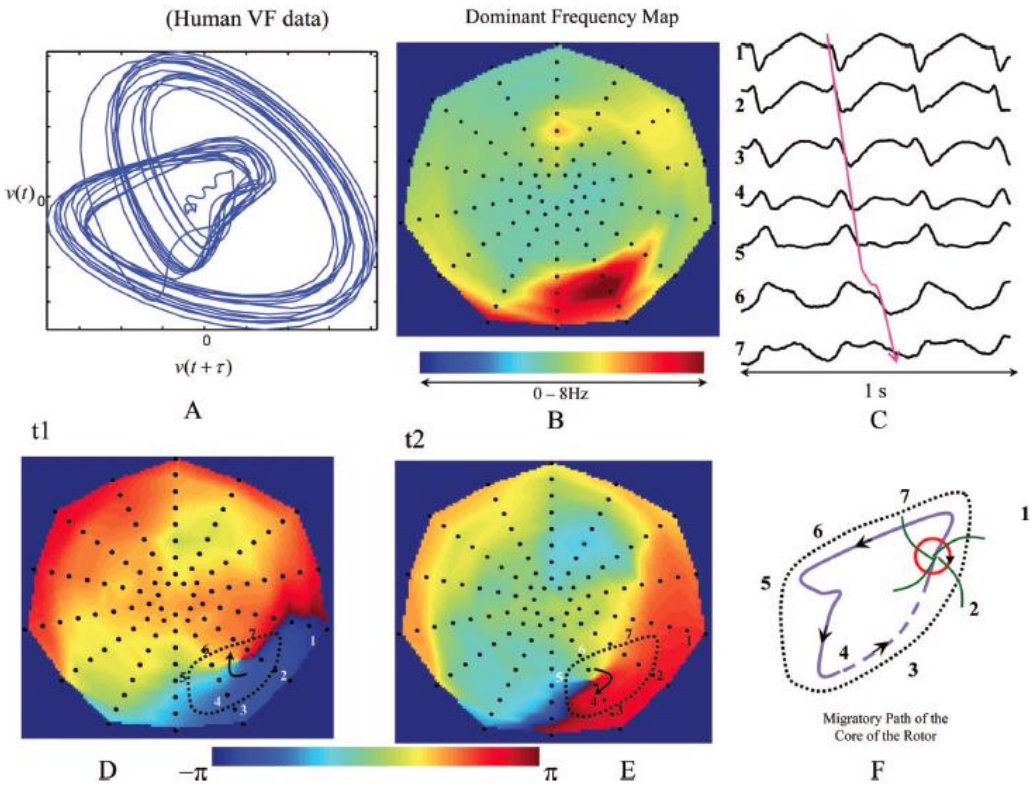

Figure 10. Phase analysis of VF data in humans using epicardial sock. A – phase-space plot. B-DF map. C – electrograms following a rotor pattern. D & E – 2 instances from the phase maps showing a PS. Curved arrow shows the direction of the rotor. F – migratory path of the PS. Adapted from Umapathy, 2010.

Limitations of phase analysis

Despite phase analysis representing a highly sophisticated method to assess spatiotemporal patterns of electrical activation there are important limitations in phase analysis. Phase analysis is dependent on the ability to derive local unipolar electrograms by integrating the electric potential over a small volume of adjacent tissue. Hence, they require a high density of electrogram sampling, and even this may be insufficient for highly localized activation patterns. Although data interpolation is used to fill gaps between electrodes, the accuracy of this technique is very dependent on the sampling distances of actual recorded electrograms. Far field electrograms (such as found in areas of scar) need to be automatically removed from the data to avoid contamination. The reliability of phase analysis depends upon how accurately activation is detected, and (in the case of Hilbert transformation this requires the mean potential over each activation cycle to be subtracted from the electrogram.

Chapter 2 - Methodology

The following studies form the basis of this thesis:

- Study 1 - The effect of psychological stress on APD in normal hearts undergoing invasive electrophysiology studies
- Study 2 - The effect of psychological stress on APD in diseased hearts during ambulatory non-invasive studies
- Study 3 - A proof of concept study that an activation-repolarization time metric algorithm could be used clinically to predict the site of a clinical re-entry tachycardia
- Study 4 - High-density contact mapping during AF to identify the underlying mechanism in persistent AF

The methodologies employed for these studies are very different from each other and are described in order.

2.1 Methodology 1 - The effect of psychological stress on APD in normal hearts undergoing invasive electrophysiology studies

Background

As discussed in detail in the literature review there is a poorly understood association between mental stress and cardiac arrhythmia and SCD (chapter 1.7.1) (Taggart, 2011). The main purpose of this study was to examine the effect of mental stress on ventricular APD and haemodynamics. In addition mental stress and emotion are known to strongly influence the pattern of respiration (Homma, 2008; Gomez 2005; Rainville, 2006), which influences brainstem autonomic neural outflow and potentially cardiac electrophysiology. This study was designed to examine the effect of mental stress on ventricular APD independent of respiration.

Method

Studies were performed in patients undergoing cardiac ablation for atrial fibrillation. These patients had normal volumes and ejection fractions on echocardiogram, and aside from their AF were considered to have normal healthy ventricles. This study was approved by the Guy's and St Thomas' Hospital Ethics Committee and conformed to the standards set by the Declaration of Helsinki (1996 amendment). Written informed consent was obtained from all subjects. Antiarrhythmic medication was discontinued 5 days prior to the study.

Subjects remained un-sedated throughout the protocol, though local anaesthetic was administered prior to femoral venous access for catheter insertion. Unipolar electrograms were recorded using 2 decapolar electrode catheters (St. Jude Medical, St. Paul, MN, USA) with 2-5-2 mm spacing (35 mm total span). One of these was positioned in the left ventricle (through an atrial trans-septal approach) in a base-apex orientation on the postero-inferior endocardial wall. The second catheter was positioned in a base-apex orientation on the anterior septal wall of the right ventricle. Constant rate pacing was applied in order to remove heart rate variability as a confounding factor. The pacing rate was set at about 10 to 20 beats per minute above the subject's intrinsic heart rate; the smallest increase sufficient to minimise the likelihood of breakthrough of the intrinsic rhythm. Breakthrough beats occurred infrequently but were detected and removed from the analysis, along with the successive beat. If these beats constituted more than 10% of any series, the series was rejected. We employed right ventricular rather than atrial pacing, as in previous studies (eg. Hanson, 2009), which produces a more clearly defined T wave in the electrogram and facilitates accurate measurement of the ARI (Figure 11). A stabilisation period of at least 2 minutes was observed at the constant pacing rate prior to electrogram recordings being taken. The reference electrode for all 20 unipolar electrograms was a large skin-surface electrode at the position of the umbilicus. Arterial blood pressure was measured from the right femoral artery with a catheter transducer (TruWave PX600F, Edwards Lifesciences, Irvine, Ca, USA). Rate of pressure development (RPD) was calculated post-hoc from this recording (after low-pass filtering at cut-off frequency of 60 Hz), taking the maximum upward slope of the pressure increase during systole.

Figure 11: Unipolar electrogram recordings during invasive stress study

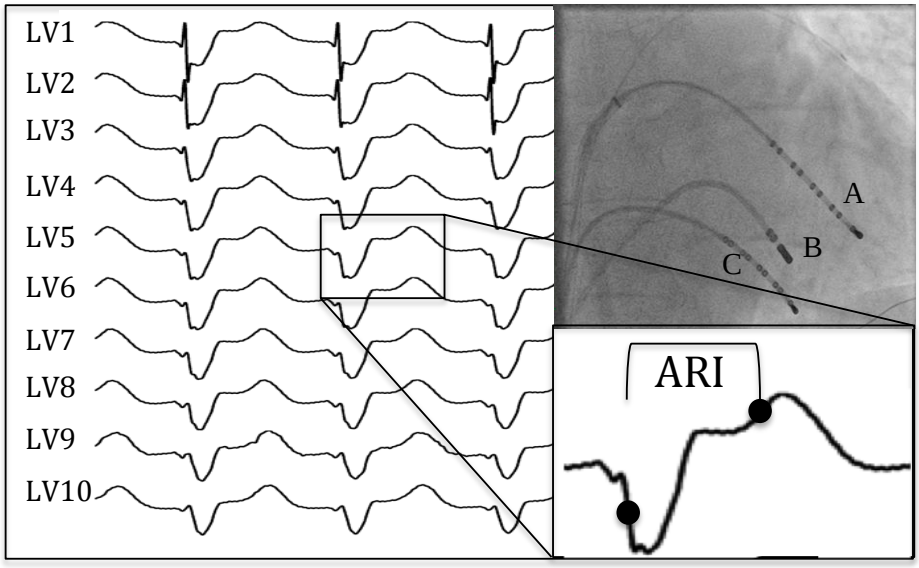

Figure 11. Left hand panel: Intracardiac unipolar electrograms taken from the decapolar catheter (A) within the left ventricle during constant ventricular pacing (RV electrograms not shown in illustration). Top right – position of catheters on fluoroscopy (A – LV decapolar catheter, B Pacing catheter at RV apex, C – RV decapolar catheter). Bottom right – Illustration of Activation Recovery Interval calculated by the Wyatt method (Wyatt, 1981).

Respiration was measured using a custom-adapted tension sensor (adapted from a RESPeRATE device, InterCure Inc., New York, NY, USA) fixed to an expandable elastic band placed around the subject's abdomen. Tension in the elastic band was directly proportional to circumference, and hence inspiration, and was digitized and recorded at a sample frequency of 1200Hz, and synchronized to the electrogram and blood pressure recordings (Ensite 3000 system, Endocardial solutions Inc). Subjects remained non-sedated and watched a 19-inch backlit LCD screen positioned approximately 30cm over their head in direct line of vision, with sound delivered through personal headphones.

In order to investigate the effect of respiratory pattern on ARI recordings, a novel protocol was employed to create a “control period” in which the subject replicated the same respiratory pattern as the movie period, but in the absence of the psychological stress. This was achieved as follows: Following the movie the subjects watched a coloured moving ball on the video for a 5-minute relaxation period. During this time the subjects' respiration pattern during the movie-clip presentation was analysed. The respiration trace was then played back to the subject via an animated graphical display (implemented in LabVIEW software, National Instruments Corp., Austin, TX, USA): the subject's variation in chest volume with time was displayed on a moving chart, showing the timing and magnitude of each respiratory cycle as it occurred during the movie-clip. A clear indicator highlighted the current state showing inspiration or expiration and the subjects were further guided by verbal breathing instructions provided by the investigator. A short training period was given prior to the investigation and the subject’s compliance was verified during the control period.

Mental stress / arousal was solicited by presentation of a short movie clip (4 minutes 30 seconds) depicting a rock climbing accident (“Vertical Limit”, Columbia Pictures, 2000). This particular movie clip was selected as it was perceived to contain a suitable sequence beginning with a minute of low-stress, building gradually up to maximum psychological stress at the end. The movie clip had been previously rated by a group of 18 healthy volunteers as moderately stressful (averaging 7 out of 10 on a standardized scale from 0: “no stress” to 10: “maximum possible stress”) and accompanied by an increase in

systolic blood pressure of 10-15mmHg and increase in heart rate of 10-15 beats per minute (Taggart P, MD DSc, unpublished data, 2010), in keeping with most laboratory-based mental stress protocols (Callister, 1992; Niizeki 2012; Lackner, 2011).

Activation–recovery intervals (ARI), as an estimate of APD were calculated automatically by the Wyatt method (Wyatt, 1981) (Figure 11) using the algorithm described by Western et al (Western, 2012), from automated custom algorithms implemented off-line (Matlab Mathworks, US). Blood pressure, rate of systolic pressure development (dp/dt max) and respiration rates were calculated from custom algorithms using Matlab.

All statistics were performed using SPSS Statistics, version 20 (IBM SPSS, New York, USA). Measurements were recorded during 3 separate 1-minute intervals at start, middle and end of the movie and control. A 2 way ANOVA with repeat measures (from a general linear model) was used to compare the effects seen during the period of stress (movie) with control (repeat breathing period). Measurements were recorded during 3 separate 1-minute intervals at start, middle and end of the movie and control.

2.2 Methodology 2 - The effect of psychological stress on APD in diseased hearts during ambulatory non-invasive studies

Background

Developing the theme from methodology 1 we were keen to explore the effect of mental stress on diseased hearts, in which the majority of ventricular arrhythmias and SCD occur. In addition, there are significant difficulties in trying to reproduce “everyday” psychological stress during an invasive electrophysiology study, which may in itself be a stressful event. We developed a novel methodology to allow precise intracardiac electrogram, continuous blood pressure and respiration measurements to be made entirely non-invasively during a variety of visually evoked psychological stresses in a more real-world environment.

Methods

Studies were performed in patients with a history of myocardial dysfunction (ischemic or non-ischemic) who were treated with a cardiac resynchronisation therapy pacemaker, implanted for at least 6 months prior to the study. Beta-blockers were stopped 72 hours prior to the study. The local Research Ethics Committee approved this study and written informed consent was given. Unlike the laboratory-based studies, all recordings were acquired non-invasively with the patient sat upright comfortably watching a high quality audio-visual display (approximately 1m diagonal width, at a distance of 2.2m) wearing over-the-ear headphones in a quiet room with dimmed lighting, designed to be more representative of real-life stressful situations.

Patients all had a Quartet left ventricular pacing lead (St. Jude Medical, USA), from which we were able to record individual 30-second intervals of unipolar electrograms from the left ventricular pacing lead non-invasively and remotely via the standard device programmer, sampled at 512Hz. The programmer allowed 5 separate 30 second recordings to be stored on each occasion, which could be timed to include over-lapping segments for a longer continuous recording. All patients had undergone cardiac resynchronisation therapy at least 6 months prior to stress studies, and echocardiographic data was available post device insertion.

Respiration was monitored through the same custom-adapted tension sensor used in the invasive studies (2.1 - Methodology 1). Continuous blood pressure was recorded non-invasively through a finger-cuff (Finometer pro, Finapress Medical Systems BV, Netherlands), digitized and sampled at 1kHz. Galvanic skin response was used when available as an objective measure of sympathetic psychological stress. These physiological recordings were synchronised using a short-duration electrical spike, which was recorded simultaneously across all measurement devices.

Patients were paced from their right ventricle at a constant rate 10% faster than their intrinsic heart rate, in order to maintain a constant cycle length and minimise any breakthrough intrinsic heart-beats, whilst unipolar left ventricular electrograms were recorded. Following any changes in pacing parameters (such as following a previous download) at least 2 minutes of continuous pacing was allowed to pass before any measurements were taken to allow for ARI

equilibration. Patients remained in their own clothes and aside from the respiration band around their abdomen, the galvanic skin stickers and the finger-cuff the study was designed to reproduce a normal television watching experience.

Patients then underwent both the following 2 stress protocols:

1. International Affective Picture System

The International Affective Picture System (IAPS) is a standardized series of photographic stimuli that have been designed, and subsequently well validated (Lang, 1999) in studies including global cardiovascular autonomic function (Aue, 2007; Bernat, 2006; Codispoti 2007), to provide a set of emotional stimuli for experimental research studies (see literature review 1.8.2). Different categories of stimuli have been demonstrated to elicit different emotional responses, including pleasant, threatening and disgust (Figure 12), which have differing effects on autonomic response (Kreibig, 2010).

Figure 12: Sample pictures from the International Affective Picture System

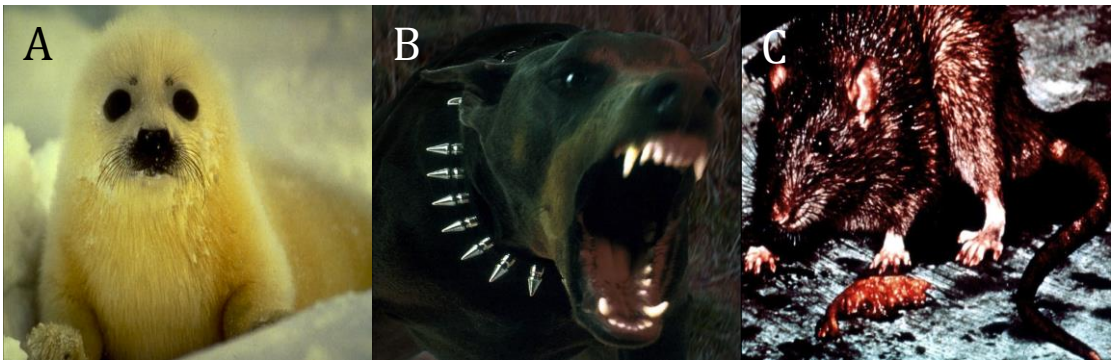

Figure 12. A – example of picture graded as pleasant. B – example of picture graded as threatening. C – example of picture graded as disgusting. Adapted from the IAPS (Lang, 1999).

Patients watched a 5-minute slide show consisting of photograph sequences adapted from the IAPS with each picture appearing for a period of 2 seconds. This slide show was divided into separate 1-minute picture categories with the pleasant IAPS sequences (control) starting at 0, 2 and 4 minutes and the fear and disgust sequences at 1 and 3 minutes. The order of the fear and disgust sequences was reversed in half of the patients to remove the effect of order as a source of bias. The final 30 seconds of each 1-minute sequence was recorded and used for analysis.

2. Movie Sequence Stress

Patients then watched an abridged horror movie film (The Shining, Warner Brothers, 1980 – condensed into a 20 minute clip). This film was chosen due to the periods of increasing anticipation and suspense leading up to stressful events. This film has previously been validated as causing high levels of

negative emotion (Schaefer, 2010). Whilst haemodynamic measurements could be made continually the intracardiac electrograms had to be recorded as groups of 5 individual successive 30-second intervals. At the end of each sequence the temporary pacing settings had to be restored and the data downloaded before the programmer would allow further recordings. Our initial protocol allowed for 2 separate sequences to be recorded, but as the study progressed we were able to add an additional sequence in 9 patients, whilst still maintaining the required 2 minutes equilibrating time when the pacing is restarted after the previous sequence had been downloaded. Briefly, sequence 1 and 2 initially started with periods of low stress with gradually increasing stress throughout of a violent and threatening nature. Sequence 3 was chosen to be slightly different and consisted of the first half the sequence where there was low activity and increasing suspense, followed by a sudden violent action designed to startle the subject.

Each patient was asked to report how stressful they found the study (score 0 low to 10 high).

ARI and Haemodynamic Measurements

ARI were measured with the Wyatt method (Wyatt, 1999) using the same automated custom algorithms employed in methodology 1 (Matlab Mathworks, US). An additional manual check plotting and visually expecting each electrogram was performed (Microsoft Excel 2011, Microsoft corporation, US), to validate the algorithms ability to exclude unwanted beats (e.g. ectopic,

intrinsic break-through and fusion beats) (see appendix A). Abnormal beats were removed from analysis together with the successive beat. Linear interpolation was applied to fill in missing beats, and the recording was rejected if more than 10% of the total number of beats were rejected from analysis.

Statistics

All statistics were performed using SPSS statistics, version 20 (IBM SPSS, New York). Measurements were recorded during the 30-second IAPS sequences, and the movie sequences (5 separate overlapping 30 second recordings, which were combined to allow approximately 90 seconds of continuous recordings). The movie sequences were then divided into quartiles for further analysis. A paired samples T test was used to compare the effects seen during periods of stress (stress pictures, movie sequence quartiles and entire movie) with periods of control (3 separate control IAPS sequences). Spectral analysis using the Periodogram function (Malab, Mathworks, Natick, USA) was performed to explore oscillating changes in ARI and blood pressure measurements.

2.3 Methodology 3 - A proof of concept study that an activation-repolarization time metric could be used clinically to predict the site of a clinical re-entry tachycardia

Background

The ability to accurately risk-stratify patients at risk of ventricular tachycardia is limited even with an invasive electrophysiology study, as discussed in detail in the literature review (chapter 1.6.2). Current methods of arrhythmia prediction and localization focus on activation, and neglect repolarisation properties, which at least experimentally are recognised as an essential aspect of initiating and maintaining re-entry arrhythmias, such as ischemic ventricular tachycardia (chapter 1.16).

Recent experimental work has demonstrated a mathematical relationship between the relative timing of depolarization and repolarization at upstream and downstream sites located either side of the line of block, and is discussed in detail in the literature review (chapter 1.17) (Coronel, 2009). In this study we investigated the hypothesis that an algorithm, which calculates this time interval between every feasible pair of recording sites in a multi-electrode map of activation and repolarization times obtained during simple premature stimulation, would successfully identify the site of re-entry upon more aggressive arrhythmia induction. We have designated this time interval the Re-entry Vulnerability Index-RVI, replacing the previous term Fibrillation Factor as its use is in determining re-entry and not fibrillation.

Methods

We sought to develop an algorithm that could map the RVI globally, thus identifying spatial regions with high susceptibility to re-entry.

Principles of the RVI algorithm:

The key electrophysiological principles of this algorithm are illustrated in Figure 8 (chapter 1.17) of the literature review.

Development of the algorithm for measurement and mapping of RVI

We consequently developed an algorithm based on a matrix analysis of multiple points and the spatial relationship between subsequent activation and repolarization intervals between pairs of electrodes during S1-S2 stimulation.

For each recording location RVI is calculated as follows:

First, the S2 beat is identified and the activation and repolarization times from each recording site are measured. For each recording position, neighbouring sites are then identified within a pre-defined radius. Those sites that are activated later than the reference site are identified as “downstream” sites (Figure 13 – *Left*). For each pair of sites, the RVI is then calculated using the algorithm below:

$$RVI_{i,j} = RT_i - AT_j$$

RVI_{ij} = Re-entry Vulnerability Index between electrodes *i* and *j*

RTi = Repolarization time of electrode *i* (proximal)

AT_j = Activation time of electrode *j* (distal) (Figure 4).

Figure 13: RVI mapping

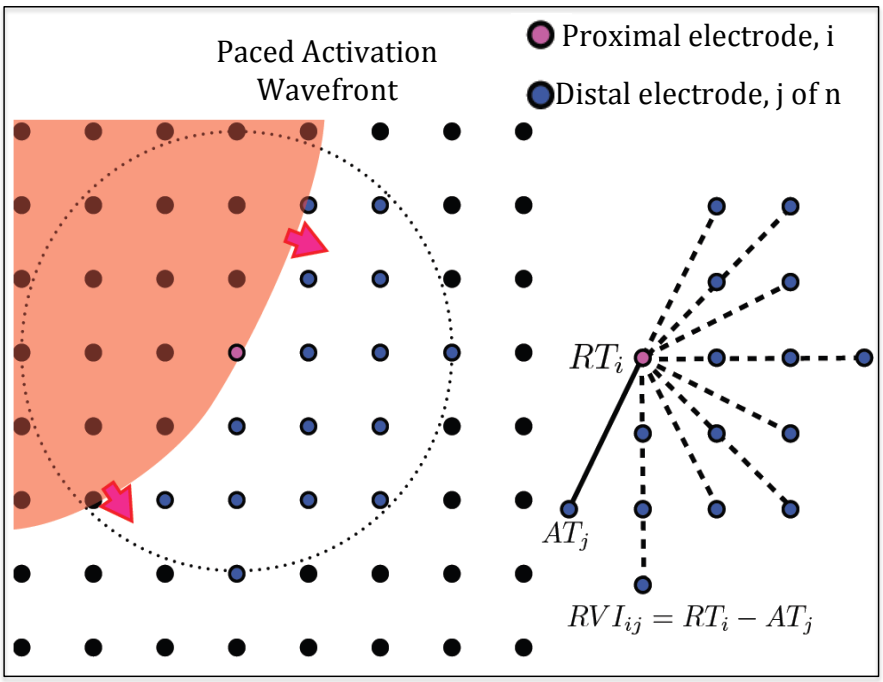

Figure 13. *Left* - Activation wave (red) shown propagating through region of a recording electrode grid (black circles), with the current proximal recording electrode shown in pink. All downstream distal electrodes within a set radius are shown in blue. *Right* - RVI_{ij} is calculated as the difference between the repolarization time of the *i*th proximal electrode (RT_i) and the activation time of each *j*th distal electrode (AT_j) on the S2 beat.

This results in a mesh of lines between pairs of points. An RVI map image is then produced from this mesh of lines by associating each RVI value with the

geometric mid-point between pairs of points, and plotting the final RVI value as the mean of all values associated with the same location. A color-map is then used in order to highlight small or negative RVI values to reveal the regions most susceptible to re-entry.

Validation of the algorithm in animal models

Langendorff porcine model

We initially tested our algorithm on data from an established animal heart model of repolarization heterogeneity involving a region of shortened APD at the stimulus site and a region of prolonged APD (the original data from the Langerdorff porcine hearts used by Coronel et al, 2010).

In Langendorff pig hearts steep gradients of repolarization were created by infusion of sotalol into the aortic cannula which produced APD prolongation, and pinacidil into the LAD which produced APD shortening in the LAD territory, thereby inducing a repolarization gradient between the 2 areas. Premature stimulation (S2) was performed from the region with short APD. Unipolar electrograms were recorded from a grid of 121 electrodes (2mm inter-electrode distance) positioned over the interface between the 2 different perfusion beds. Activation times and repolarization times for each beat were measured from the unipolar electrogram at every mapping electrode site using the Wyatt method (Wyatt, 1991). The RVI mapping algorithm was applied under conditions when re-entry did and did not occur.

Optical mapping on sheep heart

To further validate this algorithm in an additional animal model optical mapping was performed by colleagues using coronary-perfused sheep right ventricular wedges using a voltage-sensitive fluorescent dye during induction of re-entry.

A heart was acquired from a sheep (40 – 55 kg) in accordance with the guidelines from Directive 2010/63/EU of the European Parliament on the protection of animals used for scientific purposes and the local ethical committee. The sheep was pre-medicated with ketamine (20 mg/kg) and acepromazine (Calmivet, 1mL/50kg). Anaesthesia was induced with sodium pentobarbital (10 mg/kg) and maintained under isofluorane, 2%, in 100% O_2. The sheep was euthanized by sodium pentobarbital (40 mL, from 50 mg/ mL of stock) and the heart rapidly excised, cannulated and flushed with cold cardioplegic solution, containing (mM): NaCl, 110; $CaCl_2$, 1.2; KCl, 16; $MgCL_2$, 16; $NaHCO_3$, 10 and glucose, 9.01 at 4°C. The right ventricular region was dissected, coronary-perfused and leaks were carefully tied-off under cold cardioplegic solution. The preparation was mounted on to a frame to stretch and expose the endocardial surface then submersed and perfused with a saline solution containing (mM): NaCl, 130; $NaHCO_3$, 24; NH_2PO_4, 1.2; $MgCl_2$, 1; glucose, 5.6; KCl, 4; $CaCl_2$, 1.8, at 37°C. We placed 2 platinum line electrodes (5cm long, Cardialen, Inc) 4cm apart. One electrode was placed at the right ventricular base parallel to the right coronary artery and the other electrode was placed at the right ventricular apex. We stimulated at the mid-lateral side and

induced reentry by applying a cross-field pulse between the basal (+) and apical (-) line electrodes.

For optical recordings the preparation was loaded with the voltage-sensitive dye Di-4-ANBDQBS which was excited by illumination of the endocardial surface using monochromatic LEDs at 660 nm (Cain Research Ltd, Kent, UK). Optical images (100x100 pixels) of signals passed through a 715nm long-pass filter were acquired using a Micam Ultima CMOS camera (SciMedia USA Ltd, CA, USA) at 1 kHz with a spatial resolution of 0.7x0.7mm. Optical signals were filtered using a low-pass frequency filter at 120Hz followed by spatial averaging (kernel 1.2mm) and temporal averaging (kernel 3ms).

Optimisation of the RVI algorithm and computational simulations

Prior to its use on human data, the parameters used in the algorithm were optimized using a theoretical analysis of their effect upon the calculated RVI between a pair of electrodes in collaboration with our biomedical engineering colleagues.

Electrical activation was simulated using a monodomain representation of human ventricular tissue over a 2D sheet measuring 10x10cm. Ionic parameters were adjusted to produce a region of prolonged APD in the lower half of the tissue, with shortened APD in the upper half. Simulations were performed with the Cardiac Arrhythmia Research Package (http://carp.medunigraz.at) by our biomedical engineering colleagues.

Application to the human heart

To determine whether this algorithm could be applied in clinical practice using current technologies we performed a first in man proof of concept study during a clinical ablation. A 63-year old man with a background of ischemic heart disease with recurrent hemodynamically tolerated VT was admitted for a VT ablation. In addition to the standard ablation procedure, a short pacing programme including premature stimulation was used for a post-procedure analysis. He had a background of a prior inferior myocardial infarction and had severely impaired systolic function. Antiarrhythmic medications were stopped prior to the procedure. The patient gave informed consent and the local ethics committee approved the study.

The pacing protocol involved pacing from the LV apex using the mapping catheter with an 8 beat S1 drive train with a cycle length of 600ms, followed by an S2 at 500ms. Unipolar electrograms were recorded from a decapolar catheter (Saint Jude Medical, 2mm inter-electrode distance and 5mm spacing between each electrode pair) positioned in the LV. The electrograms and position of electrodes were recorded with Carto3 (Biosense Webster, Ca) with the mapping catheter remaining at the apex as the decapolar catheter was sequentially repositioned to 20 different LV locations to cover the entire endocardial surface (200 recording sites) (figure 14). The same pacing protocol was applied after each repositioning of the decapolar catheter. Low amplitude electrograms with complex morphologies (as typically seen within the perimeter of the scar) were not recorded as these would invalidate the algorithm, with

care taken to record normal electrograms just outside these regions. These measurements did not elicit any VT and the procedure subsequently continued its routine clinical course. Activation and repolarization times were measured using the same semi-automated system used in the previous methods.

Figure 14: Unipolar electrogram recordings during human VT case

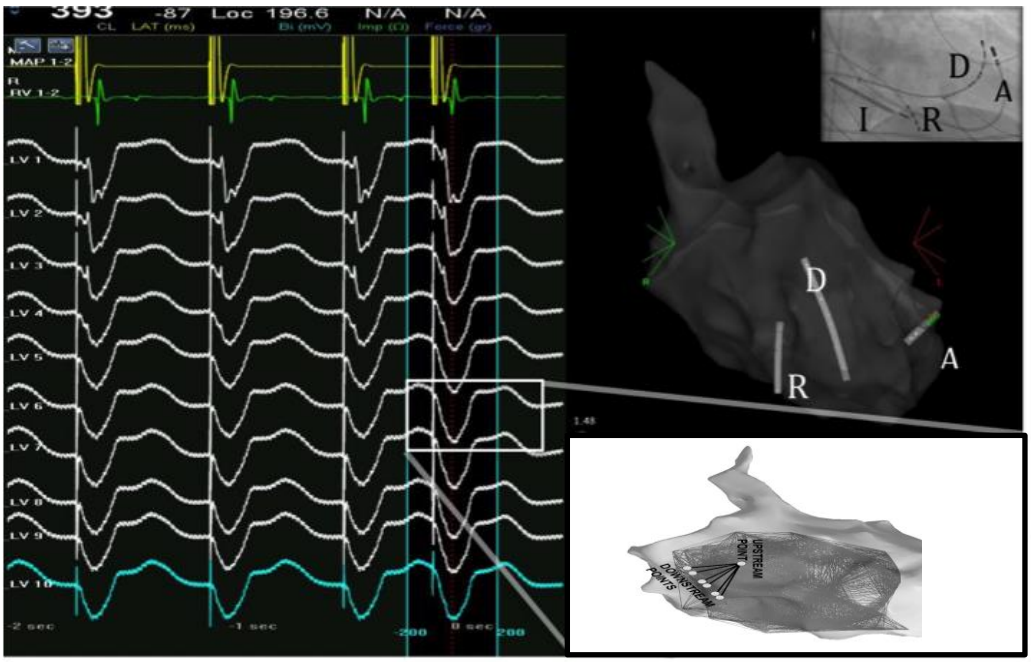

Figure 14: Left hand panel: Example electrograms recorded during clinical case. Top yellow channel – Ablation (A) catheter used to pace ventricle with an S7/S8 protocol. Green channel – distal right ventricular catheter. White channels – recorded unipolar electrograms for the 10 decapole (D) electrodes (LV10 in blue) showing the last 3 beats of the fixed rate S1 pacing followed by the premature S2 beat. Top right – position of catheters by both 3D electroanatomic mapping and fluoroscopy (A – ablation catheter, D – decapole catheter, R – RV apex catheter, I – ICD lead). Bottom right – RVI is then calculated by measuring the activation times of the downstream points relative to the repolarization time of the upstream point as previously described.

2.4 Methodology 4 - High-density contact mapping during AF to identify the underlying mechanism in persistent AF

Background

Despite persistent AF (PsAF) remaining a common clinical condition the underlying mechanism underlying the arrhythmia remains debated and contreversial as discussed in depth in the literature review. The aim of this study was to further understand the predominant mechanism that sustains PsAF in the human heart. We hypothesised that that there would be reproducible electrical mechanisms that would explain the maintenance of the atrial arrhythmia, and that these would be identifiable using phase analysis techniques.

Methods

Study design and recruitment

The STARLIGHT study (NCT01765075) was a non-randomized multi-centre observational study to collect and analyse high-density intracardiac electrograms immediately preceding cardiac ablation for PsAF. Patients were included in the study if they were due to undergo a clinically indicated ablation procedure for the treatment of PsAF. The main exclusion criteria were standard clinical AF ablation contraindications and additional criteria in which basket catheters may be associated with increased clinical risk, including the presence

of permanent pacemaker leads, severely stenotic tricuspid and mitral valves and other abnormal atrial anatomy which would not be suitable for the Constellation™ catheters (Boston Scientific, St Paul, Minnesota, size 48, 60 and 75mm). Enrolment occurred in 2 European centers (Guys and St Thomas' Hospital, London and Na Homoice Hospital, Prague) between 28/5/13 and 31/12/2013. Class I and class III antiarrhythmic medications were withheld for 5 days prior to ablation, whilst amiodarone was continued. All patients gave informed consent and the study was approved by the local ethics committee.

Data collection

Biatrial high-density recordings of unfiltered atrial electrograms were performed with 64-pole Constellation™ basket catheters prior to AF ablation (Figure 15 A&B). The atria were sized pre-procedure for optimum catheter size using on-table echocardography. Following transeptal puncture IV heparin was infused to achieve activated clotting times of >350 seconds. The catheters were fully expanded in each atria, verified by fluoroscopy and transoesophageal echocardiography.

Recordings were taken during baseline AF (presenting or induced), using the Ensite™ Velocity cardiac mapping system (St. Jude Medical) using 2 CathLink modules (providing a total of 128 electrode inputs) (Fig 14 C&D). In patients presenting in sinus rhythm (representing persistent AF patients having undergone recent cardioversion) AF was initiated using rapid atrial pacing manoeuvres in keeping with recent similar study techniques (Narayan, 2013).

Electrograms were recorded continuously for 1 minute at a sampling rate of 2000 Hz (Figure 15). Patients then proceeded to their clinical AF ablation using standard techniques.

Figure 15: Set-up for high-density contact mapping of AF

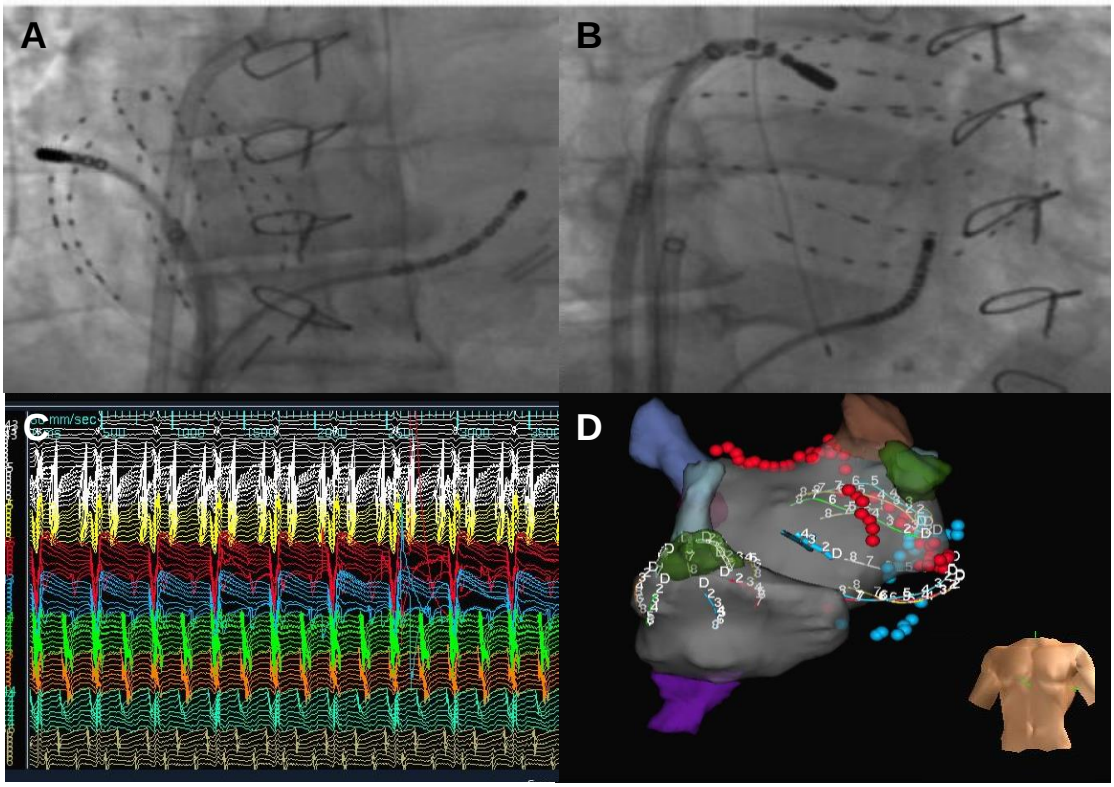

Figure 15. A - Constellation™ basket catheter (Boston Scientific, Natick, MA, USA) deployed in the right atrium (coronary sinus catheter and sternotomy wires also present) in the AP projection. B –Constellation Catheter™ deployed in left atrium in the same patient. C – 64 simultaneous electrograms recorded from a single constellation catheter to deliver high-density atria mapping. D - 3D visualization of the same catheters within the anatomical shell using Velocity.

Data processing

Electroanatomical data (unipolar electrograms and their associated 3-dimensional (3D) co-ordinates), in addition to anatomical shells and surface electrograms) were exported and processed using Matlab (Mathworks, Natick, USA). The atrial electrograms then required a series of processing steps to transform them into phase in order to allow spatiotemporal mapping. These steps are summarized below and shown in Figure 16 and were performed by Professor Clayton as previously described.

Figure 16:Stepwise approach to converting atrial electrograms into phase

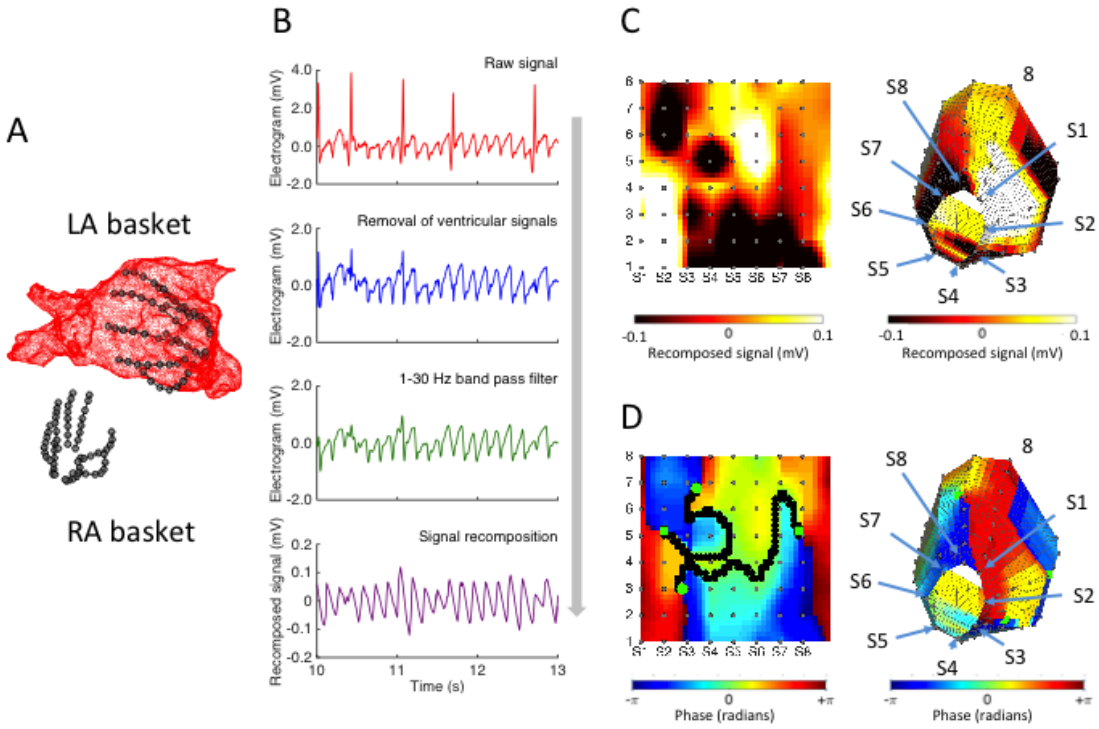

Figure 16. A – The recording electrodes are located in 3D geometry. B – The atrial electrograms undergo a series of filters and are recomposed (described in more detail in the main text). C – The recomposed signals are interpolated into the 8x8 grid and subsequent 3D locations. D – The Hilbert transformation is then used to construct phase maps for the recomposed data.

The timing of each ventricular beat was identified from reference electrodes (Fig 15B) using threshold crossing. An average ventricular beat was then calculated for each of the atrial electrodes by extracting signal segments with a duration equal to the average cycle length, aligned so that the start of the window preceded the timing of the ventricular beat by 0.3 of the average cycle length. The average ventricular beat was then subtracted from each atrial signal. The atrial signals were then filtered with a 4th order Butterworth band pass filter with passband from 1 to 30 Hz, applied in forward and reverse mode so as to minimise phase distortion. The dominant frequency of the electrogram at each electrode was identified from signal spectra obtained using the Welch method. Briefly, the 10 s recordings were divided into 4 epochs, each overlapping the preceding epoch by half its length. Each epoch was windowed with the Hanning function, and the fast Fourier transform of each windowed epoch was used to create an averaged spectrum. The dominant frequency was then the frequency corresponding to the largest spectral peak.

Signals with low amplitude or exhibiting significant electrical noise were removed from the analysis and replaced with the average of signals recorded at the nearest neighbours in the basket.

Filtered signals were then recomposed using a method described previously (Kuklik, 2015). The recomposed signals were then interpolated for each 8 x 8 grid of electrodes using linear interpolation onto a new grid of 36 x 42 where each electrode was separated from its neighbour by 4 interpolated points, and included interpolation between spline 1 and spline 8 of the catheter system. The

alignment of the interpolated grid within the LA and RA anatomy is shown in Figure 16.

The interpolated and recomposed signals were transformed into phase by calculating the Hilbert transform of each signal, producing a phase map (Figure 16D). Phase singularities and wavefronts were then calculated using methods described previously (Nash, 2006; Clayton, 2015).

In each frame, location of each phase singularity was compared with locations in the previous frame (10 ms earlier). Phase singularities separated by a threshold distance of 4 points on the interpolated grid were considered to be identical, and so we were able to estimate not only phase singularity lifetimes, but also the number of rotations supported by each phase singularity.

Data analysis

We selected 10 s epochs of AF recordings from baseline investigation prior to any ablation procedure. Each 10 s recording was processed as described above. All statistics were performed using SPSS Statistics, version 21 (IBM SPSS, New York). Results are presented as mean ± standard deviation, and a student t-test was used to compare RA and LA results.

Chapter 3: Results - The effect of psychological stress on APD in normal hearts undergoing invasive electrophysiology studies

Studies were performed in 19 patients and baseline demographics are presented in Table 1. Mean age was 57.7 years (range 42-75 years) and most patients were male (17/19). The majority of patients had PAF (14/19), and patients all had normal ejection fractions. No patient had a clinical history of ischemic heart disease.

Table 1: Baseline demographics

Case no	Age (years)	Male	AF duration (years)	PAF/ PsAF	Prior PVI	EF (%)
1	49	1	6	PAF	1	60
2	63	1	20	PAF	1	60
3	52	1	6	PAF	0	60
4	55	1	7	PAF	0	60
5	75	1	7	PAF	1	60
6	66	1	4	PAF	0	55
7	42	1		PsAF	0	50
8	64	1		PsAF	0	60
9	57	1	2	PAF	1	55
10	55	1	6	PAF	0	60
11	46	0	4	PAF	0	60
12	63	1	4	PAF	0	60
13	58	1	6	PsAF	0	60
14	58	1		PAF	0	60
15	61	1	3	PAF	0	60
16	48	0		PAF	1	60
17	52	1	3	PsAF	0	55
18	63	1	5	PAF	0	60
19	70	1		PsAF	0	60

PAF – paroxysmal AF, PsAF – persistent AF, EF – ejection fraction

Haemodynamics

All of the haemodynamic measurements increased during the high stress mid and end movie periods, compared to both the low stress start of movie period and the repeat breathing control period (p values 0.001 – 0.002). For example systolic blood pressure (mm Hg) increased from 146 ± 20 at the start of the movie to 153 ±22 and 156 ±22 at the mid and end movie periods respectively. There was no significant change in haemodynamics comparing the different repeat control periods with different respiration rates (Table 2 & Figure 17). The increases in haemodynamic measurements seen during the end movie period compared to the matched breathing control period were; systolic blood pressure (mmHg) 11±7 mmHg, diastolic blood pressure 5±4(mmHg), mean arterial pressure 7±5(mmHg), and rate of pressure development 89±82 (mmHg/s).

Table 2: Change in Haemodynamics

	Start		Mid		End		
	Movie	Control	Movie	Control	Movie	Control	p
SBP BP (mm Hg)	146.4 ± 20.2	146.5 ± 21.9	153.3 ± 22.3	146.5 ± 21.9	155.3 ± 21.8	144.4 ± 21.0	0.001
DBP (mm Hg)	91.6 ± 12.1	90.4 ± 12.6	94.3 ± 13.2	89.7 ± 12.3	95.5 ± 13.2	90.1 ± 12.2	0.002
MAP (mm Hg)	109.9 ± 13.6	109.0 ± 14.9	114.0 ± 15.2	108.3 ± 14.1	115.5 ± 15.3	108.2 ± 14.0	0.001
RPD (mm Hg/s)	1133 ± 485	1173 ± 451	1204. ± 466	1168 ±447	1218 ± 447	1129 ± 47	0.001
RR (breaths / min)	15.0 ± 5.9	16.1 ±5.8	15.7 ± 6.3	16.1 ± 6.2	17.2 ± 5.6	16.8 ± 4.5	0.08

SBP – systolic blood pressure, DBP – diastolic blood pressure, MAP – mean arterial pressure, RPD – rate of pressure development, RR – respiratory rate

Figure 17: Change in haemodynamic and respiration rates during the movie sequence

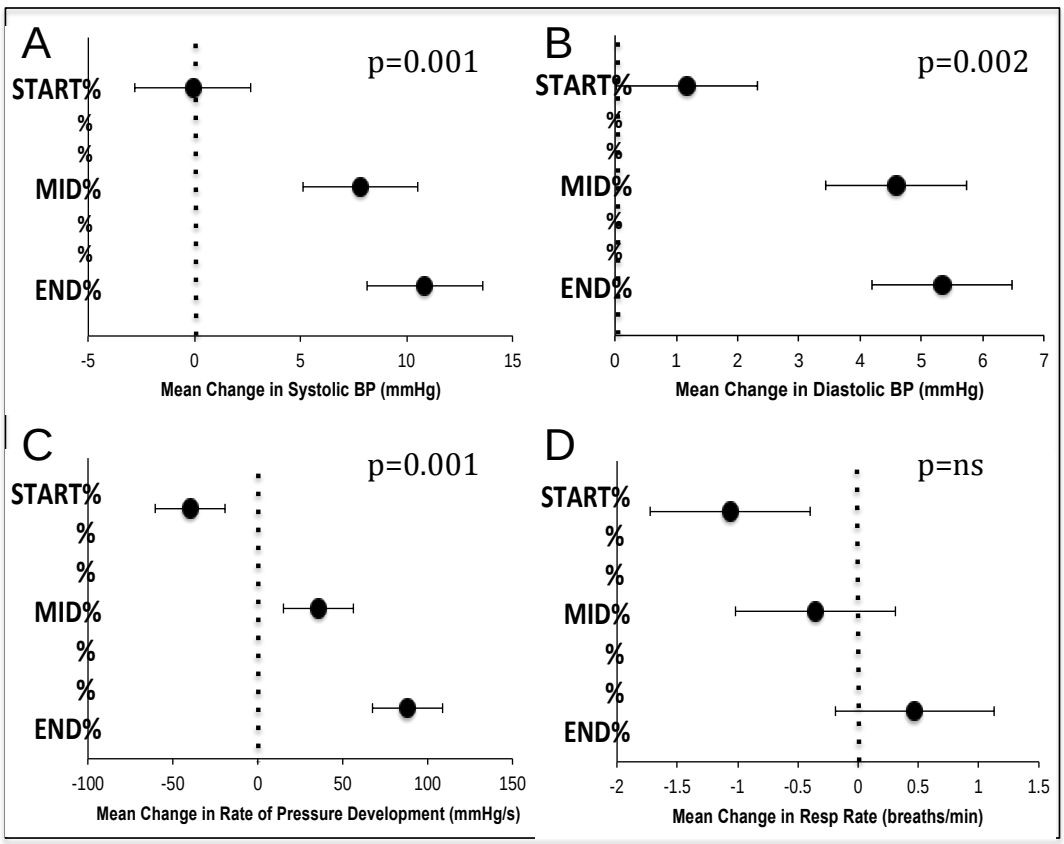

Figure 17. Change in systolic blood pressure (A), diastolic blood pressure (B), rate of pressure development (C) and respiration rate (D) during the start, mid and end of movie sequence compared to the repeat control period. During mid and end movie all heamodynamics show a significant increase. ns=non-significant.

Respiration

As expected mean respiration rates were very similar between the different movie periods and their respective copied breathing control period (Table 2). The average discrepancy between the movie and control period was 0.24 ± 2 breaths/minute. There was a significant increase in the respiration rate seen

from the start to the end of the movie (p=0.001). The increase in respiration tended to occur at approximately the same time as the blood pressure increased, as depicted in an example case in Figure 18, corresponding to an increase in sympathetic activation (increase in galvanic skin response) occurring during the movie sequence as the element of stress increases.

Figure 18: Example patient with haemodynamic, respiration and GSR response to psychological stress from movie sequence

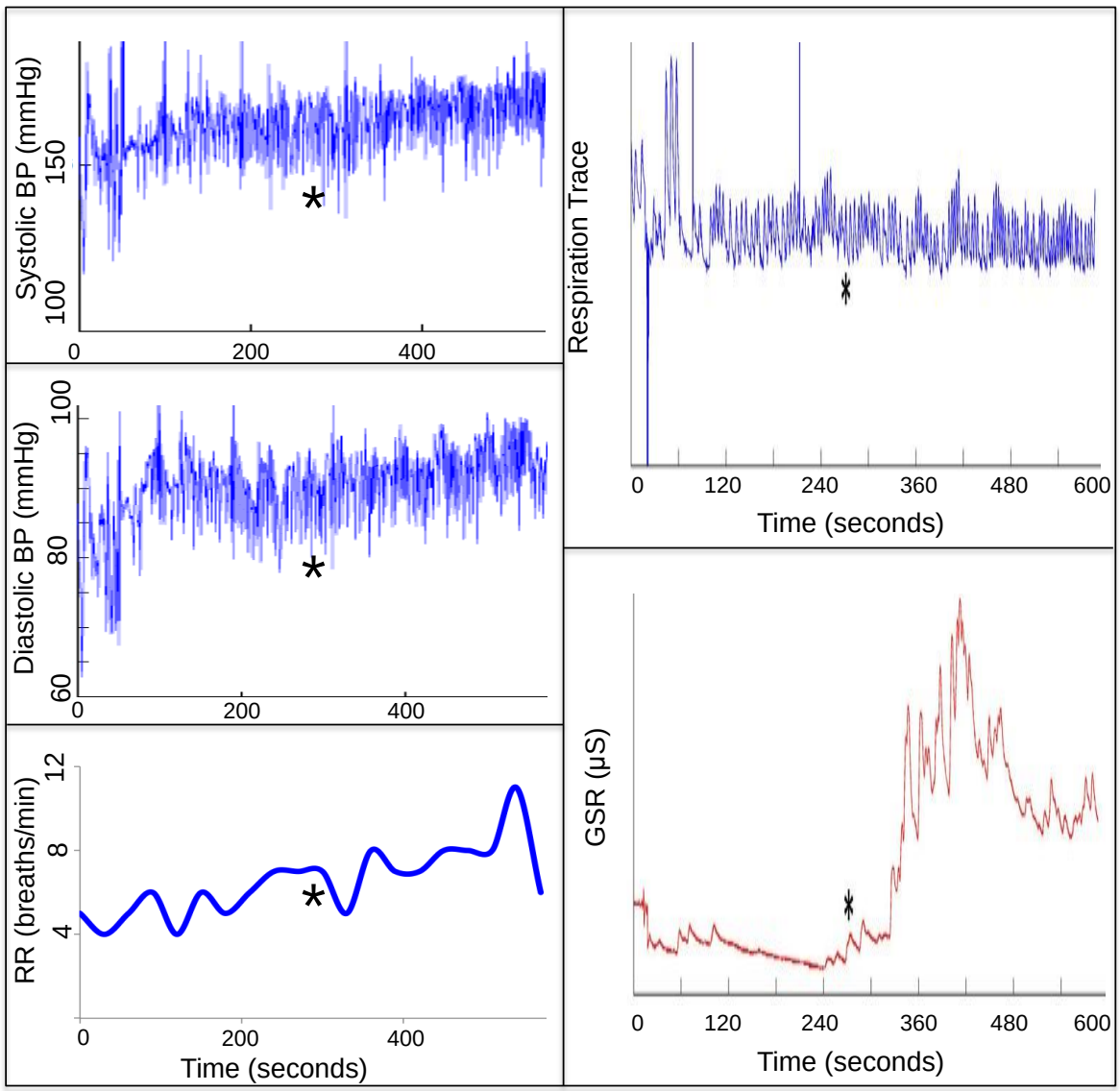

Figure 18. Haemodynamic Response to movie psychological stress. Left hand panels – systolic blood pressure, diastolic pressure and respiration rate all increase during the movie sequence. Top right – raw respiration trace. Bottom right – GSR response. After 280 seconds there is a surge in SNS activation measured by GSR, which coincides with an increase in the haemodynamic measurements.

Action potential duration (as measured by ARI)

Mean Global Change in ARI

Mean values of ARI over the 10 electrodes decreased during the movie compared to the repeat breathing control in both the LV and RV ($p=0.004$). At the start of the movie there was little change between control (LV 202.2 RV 197.5) and movie (LV 202.9 RV 195.7). In the mid movie (LV control 201.2 vs movie 200.1, RV control 197.6 versus movie 194.6ms) and end-movie (LV control 201.6 versus movie 199.8, RV control 198.0 versus movie 193.8ms) there was a small but consistent statistically significant shortening of global ARI. (Figure 19, Table 3). A similar shortening of ARI is also seen when comparing the movie sequence start (low-stress relaxed sequence) to the high stress movie mid and end segments ($p<0.001$). This change in ARI is not seen when comparing the different control periods with different repeated breathing rates ($p=0.4$).

Figure 19: Change in ARI during movie sequence compared to control

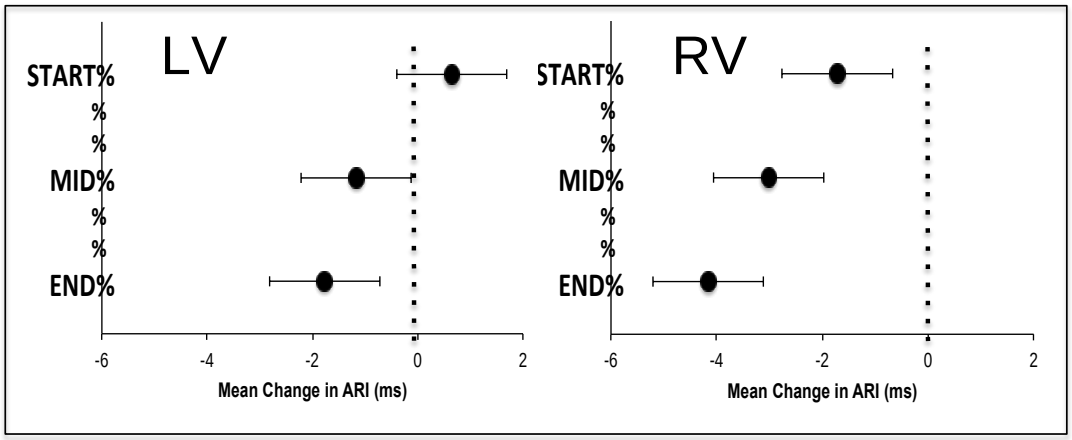

Figure 19. Change in Activation recovery intervals (ARI) for left and right ventricles during the movie clip compared to the matched repeat breathing control. Data are displayed as mean difference compared to breathing control and 95% CI.

Table 3: Change in mean ARI during the Movie compared to the repeat breathing control period

	START		MID		END		p
	Mean (SD)	Change (95% CI)	Mean (SD)	Change (95% CI)	Mean (SD)	Change (95% CI)	
LV ARI (ms)							
Movie	203 (17)	0.6 (-0.4, 1.7)	200 (15)	-1.2 (-2.2,-0.1)	200 (16)	-1.8 (-2.8,-0.7)	
Control	202 (14)		201 (15)		202 (15)		
RV ARI (ms)							0.004
Movie	196 (14)	-1.7 (-2.7, -0.7)	195 (14)	-3.0 (-4.0,-2.0)	194 (14)	-4.2 (-5.2,-3.2)	
Control	197 (13)		198 (13)		198 (13)		

Mean ARI values, SD, change in ARI (and 95% CI) are shown.

Between-subject variability

There was considerable variability between subjects in the overall mean ARI response. ARI changes in the RV ranged from lengthening 3.9 ms to shortening by 8.5 ms, and in the left ventricle ranged from increasing 2.4 ms to shortening by 12.2 ms. Larger overall changes in ARI were moderately correlated with a greater haemodynamic response (assessed using RPD - RV r=0.569 p=0.001, LV r=0.614 p=0.001). ARI changes at individual recording sites ranged from lengthening by 7.7 ms to shortening by 15.3 ms.

Regional variability

Similar responses in global ARI shortening were closely correlated between the right and left ventricles ($r=0.78$, $p<0.001$), ie super-responders in 1 ventricle showed a similar response in the other ventricle. However the global degree of ARI shortening during mid/end movie was significantly greater in the in the RV compared to the LV ($p=0.01$) (Figure 20).

Electrode measurements were recorded along the decapolar catheter to assess intra-ventricular regional variation between the base and apex. Mean ARI shortening at each electrode with 95% CI is shown in Figure 20. Overall there was no significant association between electrode position and degree of ARI shortening ($p=0.5$).

Figure 20. Change in Activation recovery intervals (ARI) illustrated by recording electrode.

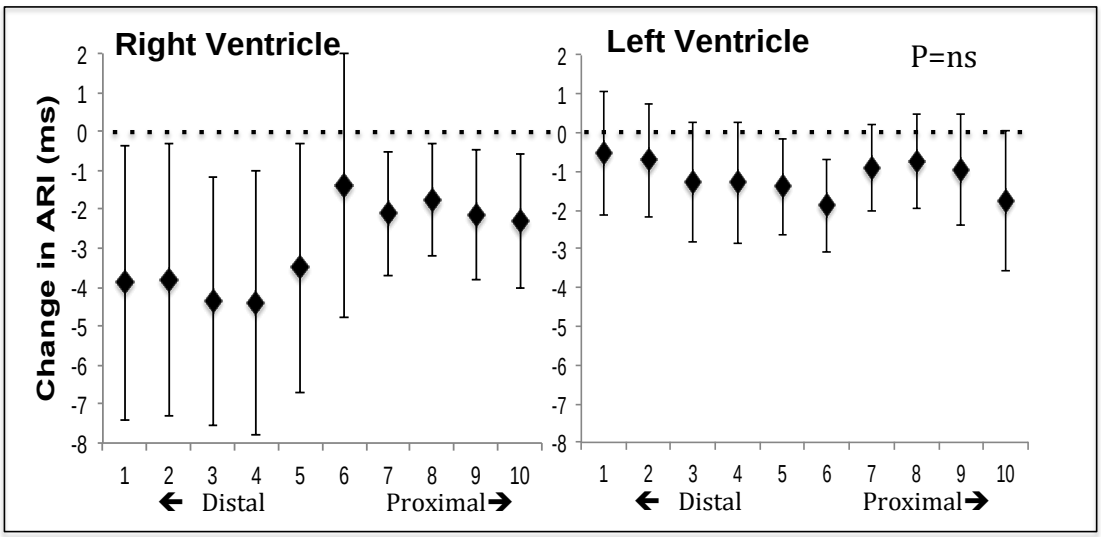

Figure 20. There is limited intra-ventricular variability in ARI response (p=n/s). Values represent mean difference from control repeat breathing period to movie period, and 95% CI.

Chapter 4: Results - The effect of psychological stress on APD in diseased hearts during ambulatory non-invasive studies

Studies were performed in 16 patients (mean age 68 +/- 8 years, 8 IHD vs 8 NICM, EF 39.9% +/- 14%) with a history of myocardial dysfunction who were treated with a cardiac resynchronisation therapy pacemaker, implanted for at least 6 months prior to the study. In one of these patients there were greater than 10% ectopic and fusion beats during the movie sequence, which was discounted, whilst the picture study remained. As such, IAPS studies were performed in 16 patients, and 15 of these patients went on to complete the movie protocol. ARI data was available for all these patients, whilst non-invasive blood pressure was only available in 12 patients (due to poor traces secondary to peripheral vascular disease). Galvanic skin response (which was introduced mid way through the study) was available in 7 patients.

3226 unipolar electrograms were analysed during the IAPS study (1.5% ectopic beats, 2.3% fusion beats). The pacing rate was increased in patients with significant abnormal beats prior to the movie sequences. During the movie sequences 5258 unipolar electrograms were analysed (including 1.7% ectopic beats and 0.15% fusion beats).

Baseline demographics are presented in Table 4. The mean subjective rating for the degree of psychological stress provoked by the study was 5.1 out of 10 (range 1 – 7.5).

Table 4: Baseline Demographics

Case no	Age (years)	Male	EF (%)	IHD/ NICM	Months since CRT	Rating (0-10)
1 *	74	1	40	IHD	16	1
2	77	1	15	NICM	6	6
3	67	1	30	NICM	12	4
4	69	1	35	ICM	66	7
5	77	1	32	ICM	12	7
6	61	1	55	ICM	10	3.5
7	63	1	45	NICM	30	2
8	63	1	45	ICM	18	6.5
9	68	1	40	ICM	11	5
10	67	1	37	NICM	9	6
11	80	1	40	ICM	13	1
12	72	1	65	NICM	15	6
13	69	0	50	NICM	18	5
14	80	1	60	NICM	9	7
15	48	1	39	NICM	7	7.5
16	69	1	36	ICM	10	7

EF – ejection fraction. IHD – ischemic heart disease. NICM – non-ischemic heart disease. CRT – cardiac resynchronisation. * denotes patient who only underwent IAPS study

IAPS Picture Study

Respiration and Haemodynamics

The respiration rate increased during both threatening (15.3 ± 3.3 breaths/min) and disgust sequences (15.1 ± 3.6 breaths/min) compared to the 3 separate control sequences (control 1 14.1 ± 3.4, p=0.14 and 0.14, control 2 14.1 ± 2.9 p= 0.02 and 0.06, control 3 13.6 ± 3.5 p=0.01 and 0.01). This was only significant when comparing the 2nd and 3rd control period (see Figure 21). Both SBP and DBP showed either a significant increase, or a strong trend towards higher values, during both stress sequences compared to the second and third control period. Systolic blood pressure rose by 3.8mmHg and 4.1mmHg during the threatening sequence (p=0.01, 0.07 respectively) and by 3.4mmHg and 3.1mmHg during the disgust sequences (p=0.05 and 0.2). Diastolic blood pressure was 1.8mmHg and 2.0mmHg higher during the threatening sequence (p=0.09, 0.12) and 2.2mmHg and 2.5mmHg during the disgusting sequences (p=0.11, 0.16). Similar to the respiration result this effect was not seen compared to the initial control period. GSR was not significantly different between picture sequences (n=7, p>0.05).

Table 5: Effect of IAPS sequence on Respiration, Blood Pressure and ARI

	Control 1	Threatening	Control 2	Disgusting	Control 3
RR (breaths/minute)	14.1±3.4	15.3±3.3*$	14.1±3.0	15.1±3.6*$	13.6±3.5
SBP (mmHg)	137.3±37	135.7±37*	131.8±35	135.2±37*	133.4±42
DBP (mmHg)	82.8±26	81.6±26	79.8±24	81.9±25.9	81.4±28
ARI (ms)	262.8±30	262.5±31	261.8±30	260.8±30**	265.7±29.6

RR - respiration rate, SBP - systolic blood pressure, DBP – diastolic blood pressure, ARI – activation recovery interval. *denotes significant mean change compared to control period 2. $ denotes significant mean change compared to control period 3. ** denotes significant change to all 3 control periods

Activation Recovery Interval

ARI was significantly lower in the disgusting IAPS sequences compared to all of the control sequences (260.8 ± 29 ms vs Control 1 262.8 ± 30 msec, p=0.001, Control 2 261.8 ± 29 msec, p=0.03, and Control 3 265.6 ± 29 msec, p=0.03). However, the threatening IAPS sequences were not significantly different to any of the control sequences (p>0.05). In addition, the ARI during the disgusting photograph sequences were significantly lower than during the threatening sequences (260.8 ± 30 vs 262.5 ± 21 msec, p=0.007).

Figure 21: Effect of IAPS sequence on Respiration, Blood Pressure and ARI

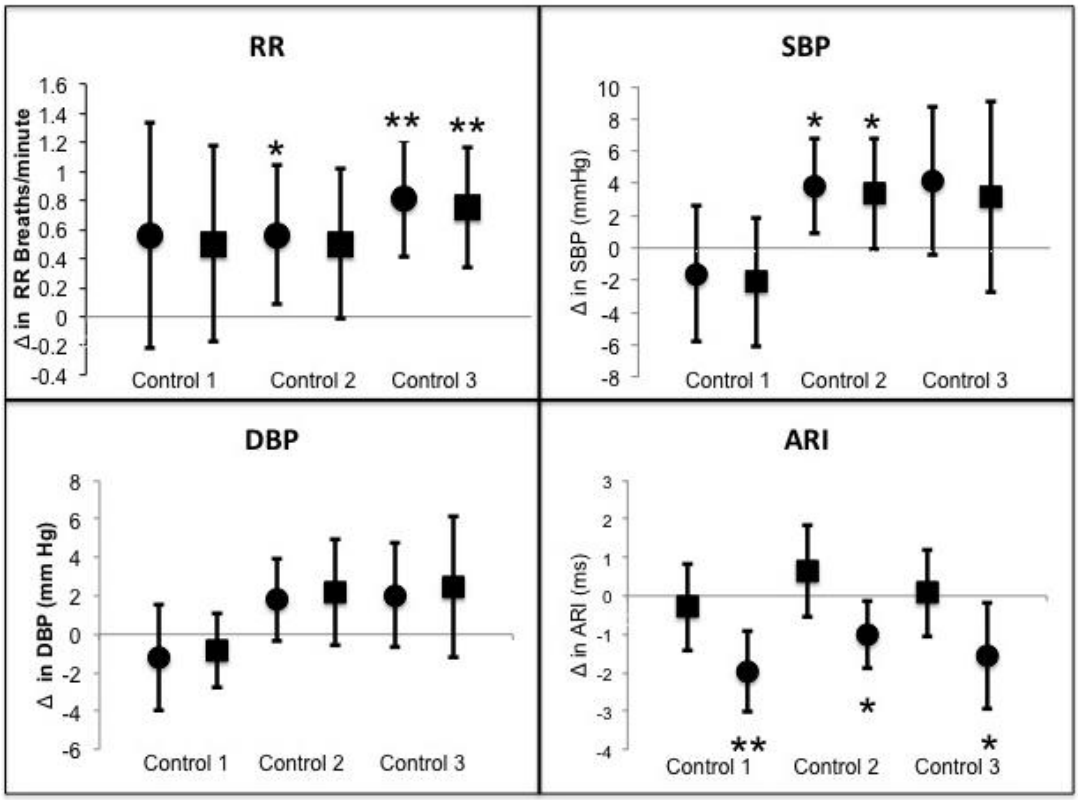

Figure 21. Changes in Respiration, Blood Pressure and ARI with different IAPS sequences. Square markers – threatening sequence, circle markers- disgusting sequence. RR -respiration rate. SPB -systolic blood pressure, DBP - diastolic blood pressure, ARI -Activation Recovery Interval. * = $p<0.05$. **$p<0.01$.

Emotionally charged Movie sequences

Respiration

Respiration rates were significantly higher during sequence 1 and sequence 2 than the control picture sequences (movie sequence 1 18.6 ± 3.0, movie sequence 2 17.1 ± 3.0 vs control 14.1 ± 3.0 breaths/ minute, p= <0.01 and <0.01 respectively. Respiration rates did not significantly increase during movie sequence 3 (15.6 ± 1.9 breaths/ minute p>0.05) (Table 6 and figure 23). During movie sequence 1 and 2 there was an increase in respiration rates during the middle part of the movie (Q2 and Q3 which corresponds to the period designed to contain maximum stress) compared to the start and the end, but this only reached statistical significance when comparing to the end of the sequence (sequence 1 Q2 19.0 ± 2.7 breaths/ minute, Q3 19.7 ± 4.3 breaths/ minute vs Q4 17.2 ± 3.6 breaths/ minute, p= 0.12 (ns), 0.04 respectively; sequence 2 Q2 16.1 ± 5.2 breaths/ minute, Q3 16.7 ± 5.7 breaths/ minute vs Q4 15.1 ± 4.8 breaths/ minute, p= 0.05, <0.01 respectively). Respiration rates during movie sequence 3 were more heterogeneous and did not show any significant changes either compared to the control sequences or during the different periods of the movie sequence.

Blood Pressure

Systolic and diastolic blood pressure both increased during the movie sequences compared to the control picture periods. Systolic pressure

increased by 7.4 ± 9.5, 9.7 ± 13.0, 14.7 ± 10.7 mmHg compared to the mean over all the control period (p=0.08, 0.07 and <0.01 respectively). Diastolic blood pressure increased by 6.8 ± 9.0, 7.6 ± 8.2, 11.1 ± 7.7 compared to the control period (p=0.09, 0.02 and <0.01 respectively) (Table 6 and figure 23). Blood pressure response during the movie sequence was very heterogeneous and did not show an expected increase in systolic or diastolic blood pressure during the more stressful parts of the movie sequences (Q2 and Q3).

Galvanic skin response

Galvanic skin response increased during each stress movie sequence compared to the control period (control 1.41 ± 0.73 µS vs movie sequence 1 2.2 ± 1.4 µS p= 0.04; movie sequence 2 2.2 ± 1.4 µS p=0.04; movie sequence 3 2.2 ± 1.6 µS p=0.09 (ns)) (Table 6 and figure 23). GSR showed a trend towards increasing values during the 3rd and 4th quartile of each sequence, which was significant only when all 3 sequences were combined and compared to the start (Q1 1.99 ± 1.26 vs Q3 2.20 ± 1.30 µS p=0.003; vs Q4 2.46 ± 1.54 µS p=0.007).

Table 6: Effect of Movie Sequence on Respiration and Haemodynamics

	RR (breaths /minute)	SBP (mmHg)	DBP (mmHg)	GSR (μS)
Control	14.2 ± 2.9	134.8 ± 39.0	78.6 ± 19.5	1.41 ± 0.7
Sequence 1	18.5 ± 3.1*	142.2 ± 33.7	85.4 ± 19.9	2.2 ± 1.4*
Q1	18.3 ± 3.2	144.5 ± 39.1	86.7 ± 24.1	1.9 ± 1.2
Q2	19.0 ± 2.7	141.5 ± 34.3	84.7 ± 22.5	2.1 ± 1.3
Q3	19.7 ± 4.3$	141.6 ± 30.2	85.5 ± 21.3	2.1 ± 1.2
Q4	17.2 ± 3.6	141.3 ± 31.4	84.5 ± 22.5	2.5 ± 1.7
Sequence 2	17.1 ± 3.0*	144.5 ± 33.2	86.2 ± 27.2*	2.2 ± 1.4*
Q1	17.3 ± 4.8	146.2 ±39.2	88.1 ± 30.0	2.0 ± 1.1
Q2	17.3 ± 2.7$	143.6 ± 32.9	86.1 ± 27.9	2.1 ± 1.2
Q3	17.9 ± 3.5S	145.2 ± 37.7	86.1 ± 29.4	2.1 ± 1.1
Q4	16.2 ± 2.4	140.2 ± 27.2	84.7 ± 26.7	2.6 ± 1.7
Sequence 3	15.6 ± 1.9	149.5 ± 38.9*	89.7 ± 27.1*	2.2 ± 1.6
Q1	15.8 ± 1.8	149.2 ± 50.0	89.9 ± 31.0	2.1 ± 1.6
Q2	15.6 ± 3.2	149.3 ± 50.2	90.0 ± 30.5	2.0 ± 1.2
Q3	16.4 ± 3.3	149.5 ± 50.2	89.1 ± 31.2	2.3 ± 1.7
Q4	15.9 ± 2.9	150.1 ± 50.6	90.3 ± 32.0	2.2 ± 1.5

Effect of mental stress on haemodynamic measurements during movie sequence quartiles. RR – respiration rate, SBP – systolic blood pressure, DBP – diastolic blood pressure, GSR – galvanic skin response. * $p<0.05$ vs control period. $ $p<0.05$ vs final quartile.

Figure 22: Effect of mental stress on Respiration, blood pressure and Galvanic Skin Response

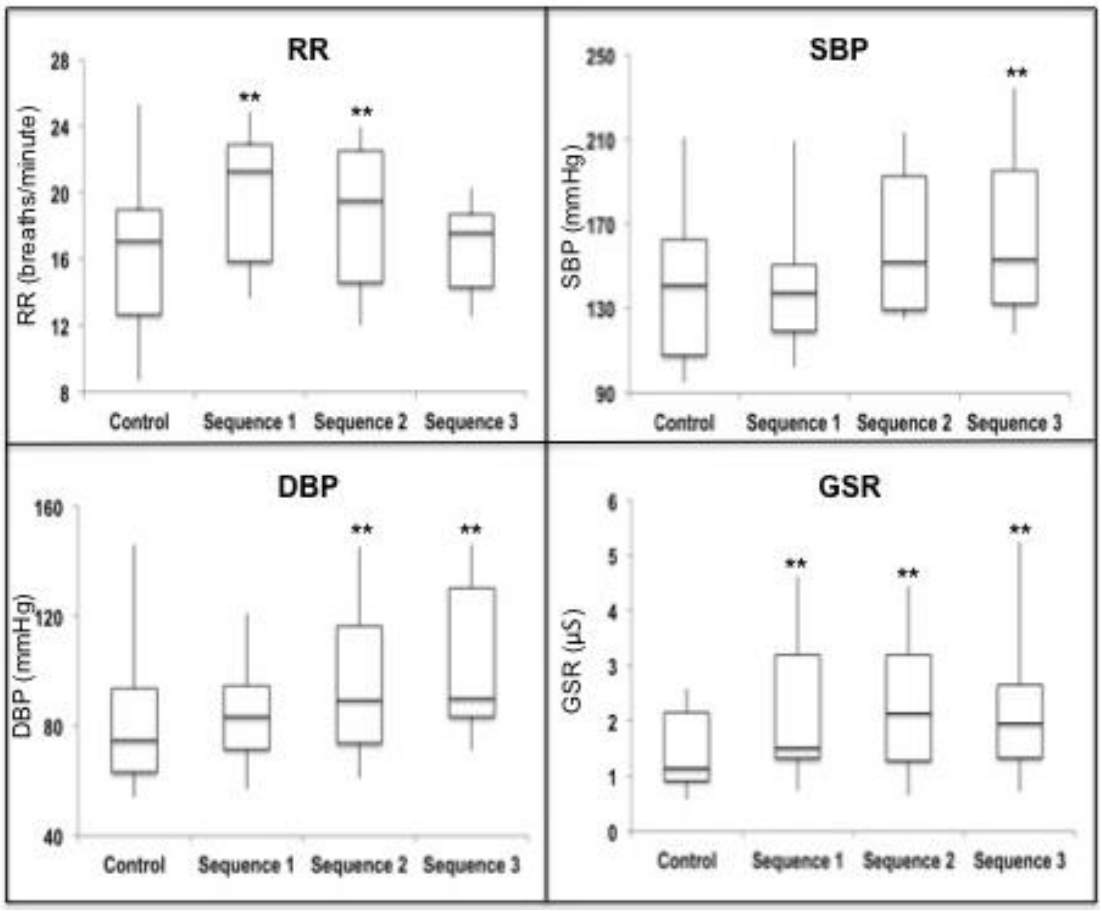

Figure 22. Box and whisker plot for respiration (RR), systolic blood pressure (SBP), diastolic blood pressure (DBP) and galvanic skin response (GSR) recorded during the control picture sequences compared to the movie sequences. **p<0.01.

Activation recovery interval

Mean activation recovery intervals were significantly shorter during each of the stressful movie sequences than during the control picture periods. During movie sequence 1 mean ARI shortened by 2.5 ± 3.2 ms, p=0.05; movie sequence 2 3.1 ± 5.2 ms, p=0.05; movie sequence 3 3.6 ± 5.0 ms, p=0.02 (Figure 23).

Changes in ARI were not related to underlying aetiology (ICM vs NICM), ejection fraction or self-reported stress score, but in subjects with a strong haemodynamic response to stress ARI shortened more than in those without (SBP > 5mmHg mean ARI change 5.8 ± 5.3 ms vs -0.2 ± 1.3 ms p=0.015, GSR >10% increase mean ARI change 4.1 ± 2.5 ms vs 1.6 ± 3.2 p=0. 09). There was no significant change in measures of ARI dispersion, including standard deviation and root-mean square standard deviation (RMMSD).

Overall intra-sequence ARI responses were heterogeous and overall there was no significant difference in ARI response during the 4 quartiles of each sequence. On subgroup analysis during the 3 stressful movie sequences ARI values shortened slightly from the relatively low stress start of the movie (Q1 264.3 ± 29.5) to the higher stress middle component (Q2 263.5 ± 29.3, p= 0.09 (ns); Q3 263.4 ± 28.9, p= 0.05). The mean ARI lengthened again during the final portion of movie (264.1 ± 30.0), also considered relatively low stress, but was not statistically significant (p=0.3 vs Q2, p=0.15 vs Q3).

Figure 23: The effect of Movie Stress on the activation recovery interval

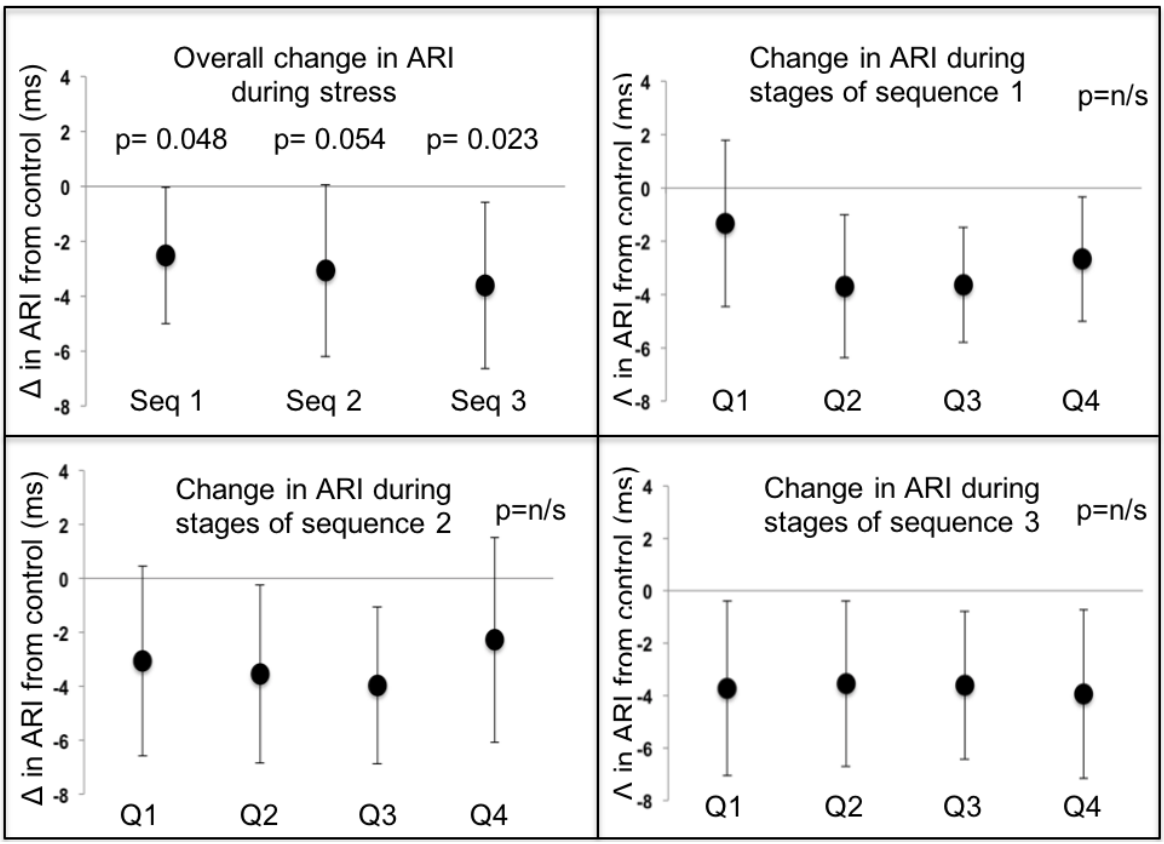

Figure 23. Top Left – The effect of movie stress on activation recovery interval (ARI) during each movie sequence compared to control – mean ARI change and 95% confidence interval. ARI significantly decreased during sequence 1 and 3, and there was a strong trend to shorter ARI in sequence 2. Top right - ARI changes in in different periods of sequence 1 (the clip was divided into quarters). Bottom left and right – The same quarters for sequence 2 and 3. There was no significant difference in the degree of ARI shortening observed in different quartiles of the movie sequence.

Timing and frequency of ectopic beats

Overall the frequency of ectopic beats were very low in both the IAPS study (48 out of 3226 beats, 1.5%) and the movie sequence (89 out of 5161 beats, 1.7%) and occurred with similar frequency both in the stressful picture sequences and the movie sequences compared to the control picture sequences (p=ns). There was also no significant difference in the frequency overall of ectopic beats in different quartiles of the movie sequences.

There was however an interesting observation noted in sequence 3 of the movie sequence (depicting a period of low activity but increasing suspense as a character walks carefully down a corridor looking for the murderer, followed by a sudden surprise as the murderer jumps out and kills him with an axe). In 5 out of 14 patients there was at least 1 ectopic beat that occurred very close to this sudden change in the sequence (figure 24). There was a higher frequency of ectopic beats in the 10 seconds either side of the key moment, than in the rest of the sequence (ectopic frequency 2.9 ± 4.4 vs 0.8 ± 1.4%, p=0.05). This observation was independent of any sudden changes in preceding ARI.

Figure 24: Example of ectopic beats occurring at time of surprise

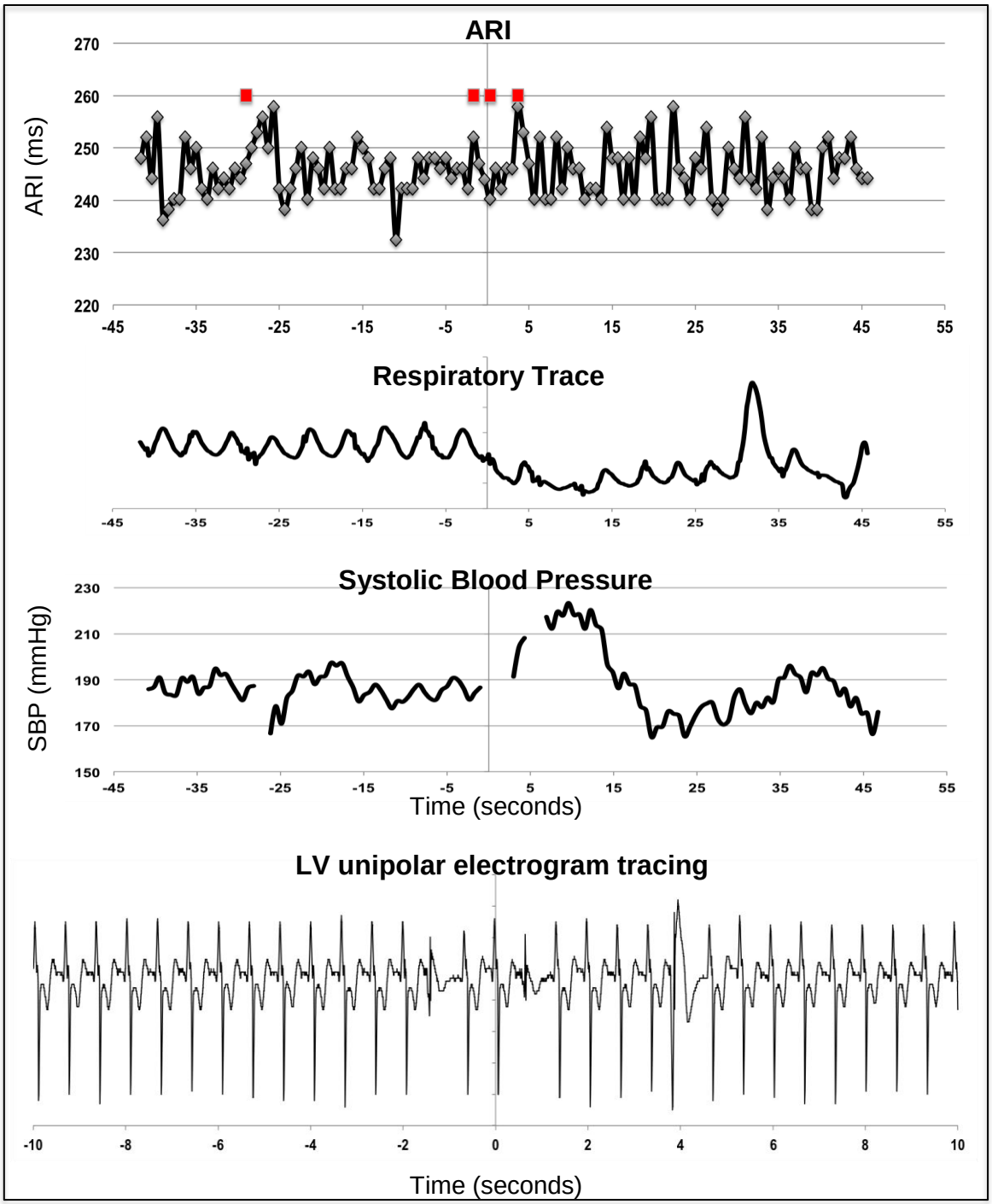

Example of response to sudden shock mid sequence (0 seconds). As well as a change in respiratory pattern and increase in systolic blood pressure there are 3 ectopic beats occuring all within a short period at the time of shock. From the top - ARI (red dots illustrate timing of ectopic beats), Respiratory pattern, systolic blood pressure and LV electrogram tracing (over a 20 second period). ARI - activation recovery interval, SBP systolic blood pressure.

Oscillations in ARI and Blood Pressure recordings during stress

The results of the ARI and blood pressure measurements throughout the movie stress sequences were frequently found to exhibit repetitive oscillatory behaviour. Whilst this has previously been observed in blood pressure recordings this was a suprising finding as ARI oscillations had not previously been reported. Time-frequency analysis was used to further explore these oscillations which were were oberved both at the respiratory frequency (figure 24) and at a slower frequency of approxametely 0.1 Hz, consistent with previously reported oscillations in sympathetic nerve traffic and termed Mayer waves (0.04 – 0.15Hz) (Hanson 2014) (Figure 25). In subjects with a relatively constant respiratory rate during the movie sequences (defined as a clear peak in the time-frequency periodogram and found during 25 movie sequences) SBP was found to be oscillating at the respiratory frequency in 10 recordings (40%) and ARI in 13 (52%) recordings. In addition low frequency oscillations (0.04 – 0.15 Hz) in SBP were found in 32% of sequences and low frequency ARI oscillations in 55%. Oscillations at both the respiratory and Mayer wave frequency were often seen within the same recording (blood pressure recordings 8%, ARI recordings 32%) (Figure 26).

Figure 25 - Example of the relationship between respiration and activation recovery interval (ARI) and systolic blood pressure (SBP)

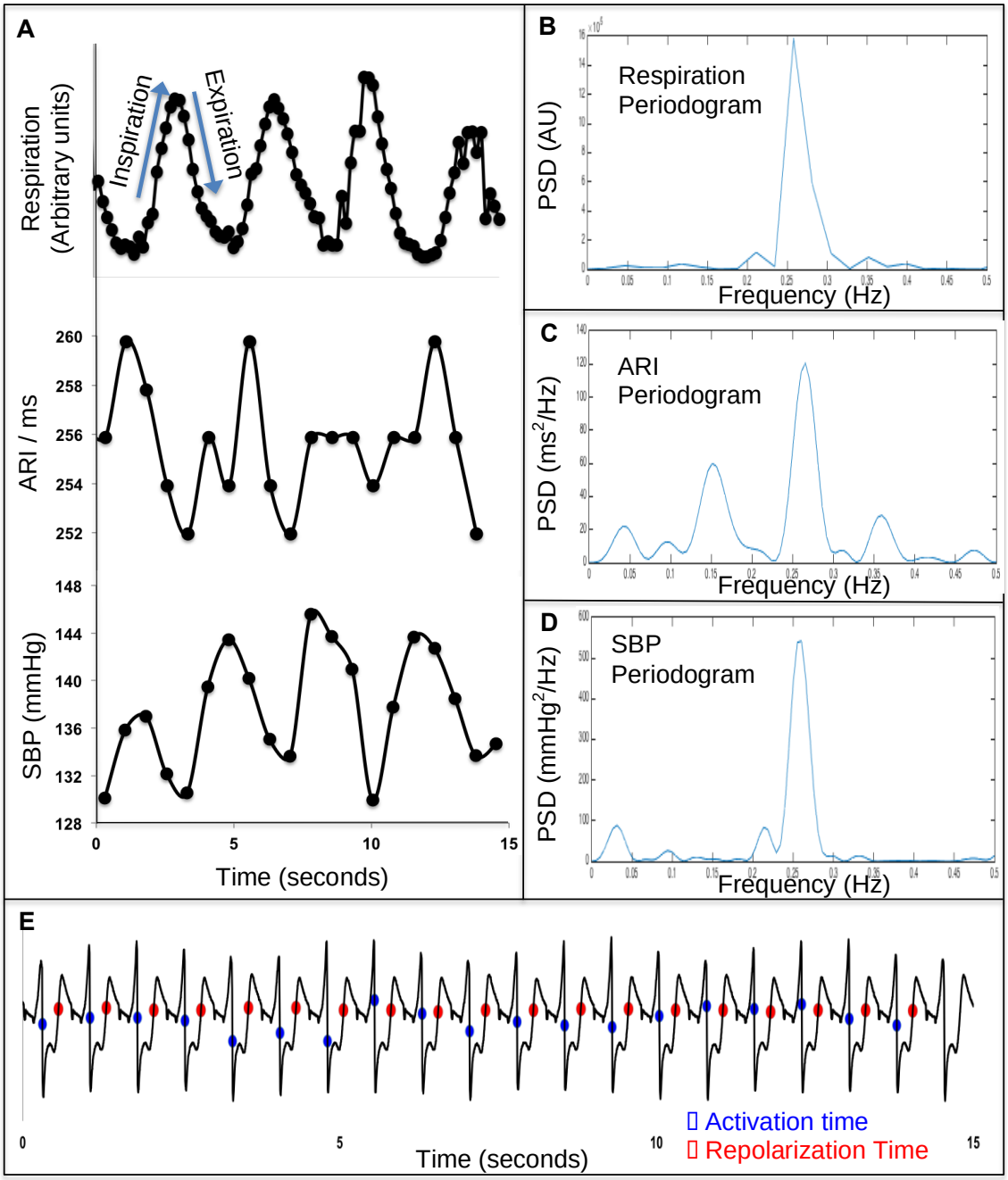

Figure 25. A – A 15 second synchronous period of respiration, ARI, and SBP measurements. During inspiration the ARI is seen to be higher and the SBP lower. B-D Time spectral analysis demonstrating all 3 phyiological measurements are oscillating at the respiratory frequency (0.27Hz in this case). E – The corresponding EGM recording (blue dots represent activation time, red dots repolarisation time calculated automatically using MATLAB).

Figure 26 – Example showing oscillations in ARI at both respiratory and Mayer wave frequencies

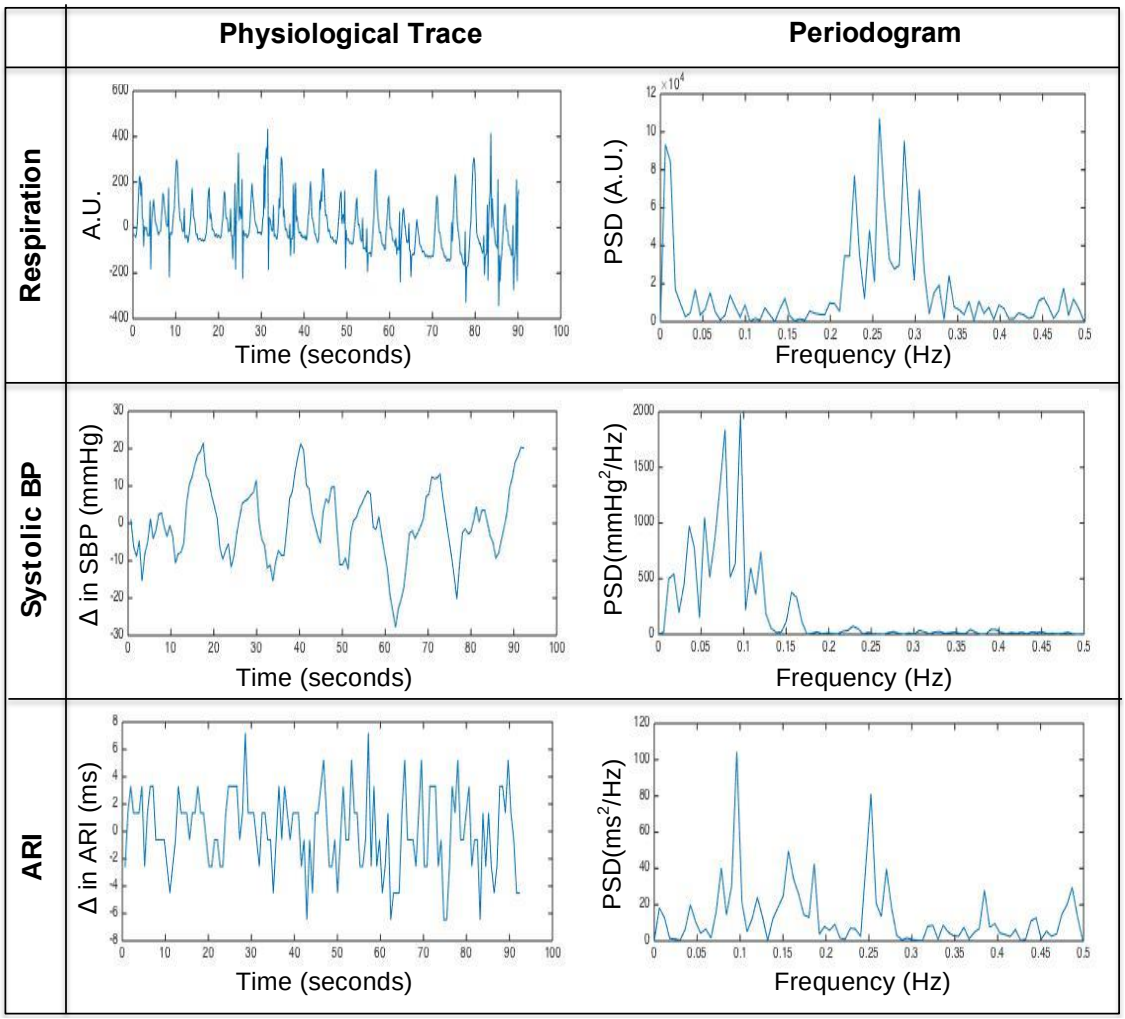

Figure 26. Respiratory, systolic blood pressure and activation recovery tracings during a 90 second stress movie sequence. Physiological tracings are shown on the left and time-frequency analysis using the periodogram function is shown on the right. The respiration tracing displays a relatively consistent respiratory rate corresponding to a peak frequency between 0.25-0.3Hz. The blood pressure recording shows a slower oscillating pattern at the Mayer wave frequency of 0.1Hz, and the ARI recording, which has peaks at both the respiratory and the 0.1Hz frequencies.

Chapter 5 – Results: A proof of concept study that an activation-repolarization time metric algorithm could be used clinically to predict the site of a clinical re-entry tachycardia

Optimisation of RVI algorithm

Prior to its use on animal or human data, the parameters used in the algorithm were optimized using a theoretical analysis of their effect upon the calculated RVI between a pair of electrodes in collaboration with our biomedical engineering colleagues. A full description of the results of this analysis is found in the paper by Hill et al, 2016. Briefly, the search radius of neighboring downstream sites and the spatial resolution of recording electrodes were identified as parameters that could be adjusted to maximize the sensitivity of the algorithm to discriminate between high and low re-entry vulnerability (Figure 27 for details).

Figure 27: Theoretical Optimisation of RVI algorithm

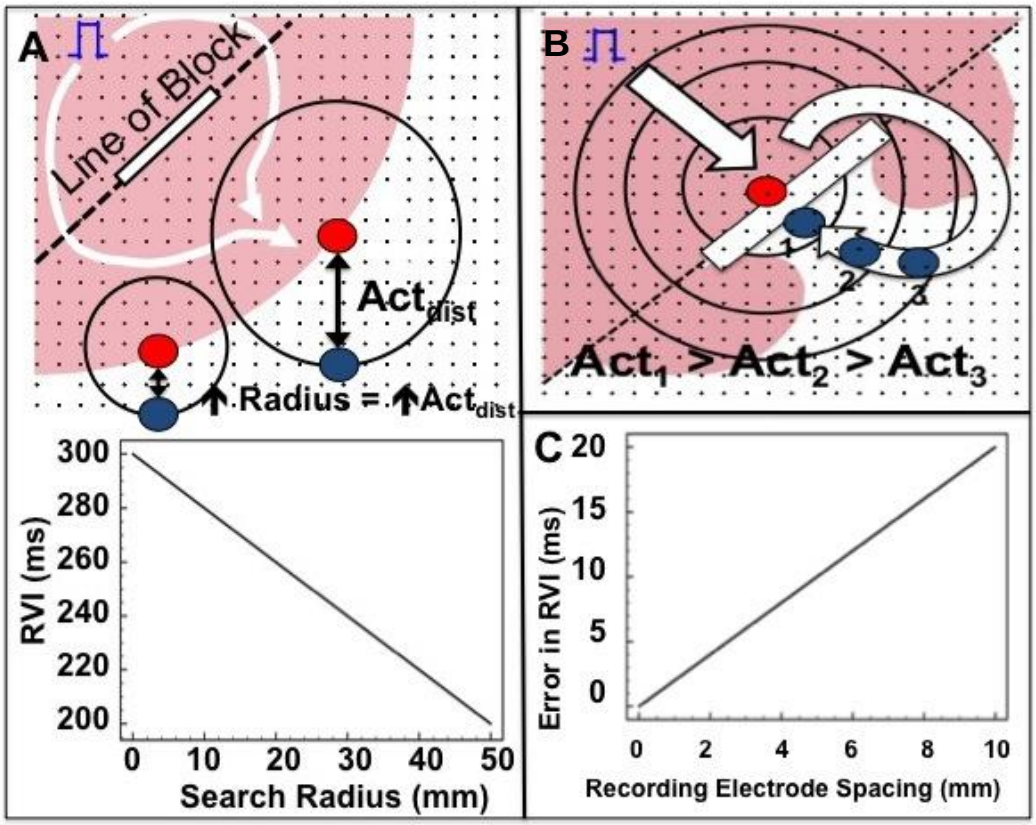

Figure 27. The RVI is calculated using the formula previously described. In A – as the distal point is activated later (blue) this leads to a lower RVI as a result of an increased activation time. B – In tissue spanning the conduction block the area nearest the re-entry has the longest Activation time and hence lowest RVI (dot 1). Whilst radius size increases distal activation times occur earlier (dot 2 & 3) and hence RVI increases, but the lowest RVI will remain unchanged. C – RVI measurement error increases as electrode spacing increases.

Computational Simulations

Figure 28 shows an example of a premature (Case (ii), re-entry initiated) and slightly less premature (Case (i), bidirectional block) S2 beat simulated within a heterogeneous 2D sheet. The respective voltage map images (panels A & D) and activation maps (panels B, E, F) show similar wavefront and wavetail dynamics compared to the experimental preparation. In both Cases (i) and (ii), the S2 wavefront is initially blocked as it encounters refractory tissue in the region of long APD, travelling around the line of block and eventually entering the distal region of prolonged APD as it recovers. In Case (ii), the wavefront is able to propagate into recovered tissue at the site of initial block to successfully re-enter (panel F), whereas the tissue remains refractory in Case (i) and bidirectional block occurs. Panel G shows the computed RVI map for Case (ii), highlighting that the region of low RVI is distinctly co-located with the site of initial block and re-entry. Importantly, the corresponding RVI map for the case of failed re-entry (Case (i)) also shows low RVI values in a similar site (panel C). Finally, for the case of sustained re-entry (Case (ii)), a 'hot-spot' map of cumulative phase singularity locations is shown (panel H), highlighting that the region of spiral wave rotor clustering occurs adjacent to the region of low RVI.

Figure 28: Computational simulations

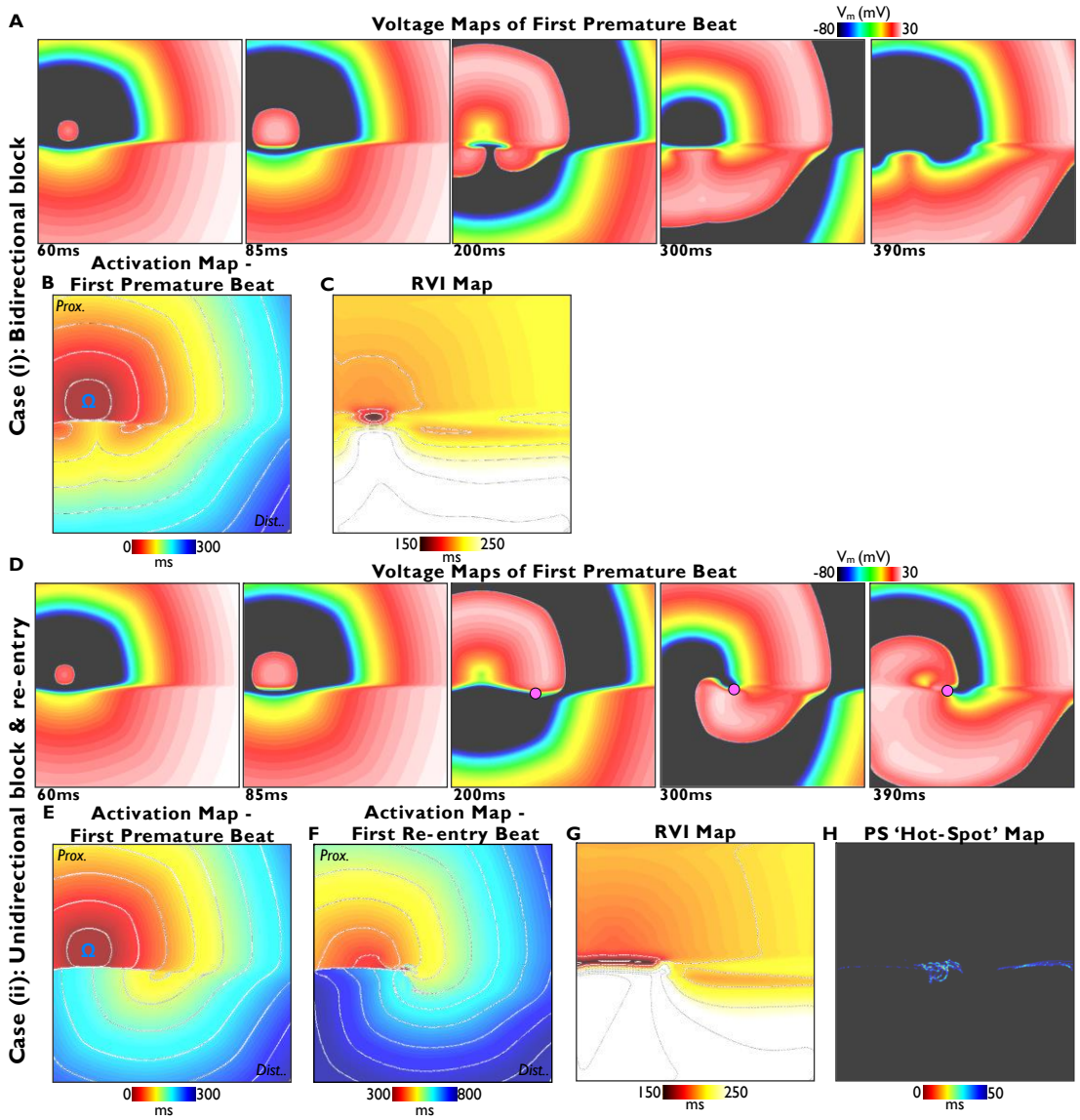

Figure 28. Simulations of premature S2 beats in the cases of bidirectional block (S2 interval 350ms, upper panels) and unidirectional block and re-entry (S2 interval 340ms, lower panels). In each case voltage maps showing activation sequences (A, D), activation maps (B, E, F) and calculated RVI maps (C, G) are shown. Phase singularities are shown as pink circles in panel D. In the case of re-entry, a 'hot-spot' map showing cumulative spatial phase singularity locations is shown (panel H). All timings shown are relative to S2 application.

Validation of the algorithm in the animal models

Porcine model

The RVI mapping algorithm was applied under conditions when re-entry did and did not occur and was shown to accurately predict the occurrence of re-entry (Figure 29)

Figure 29: Porcine model results

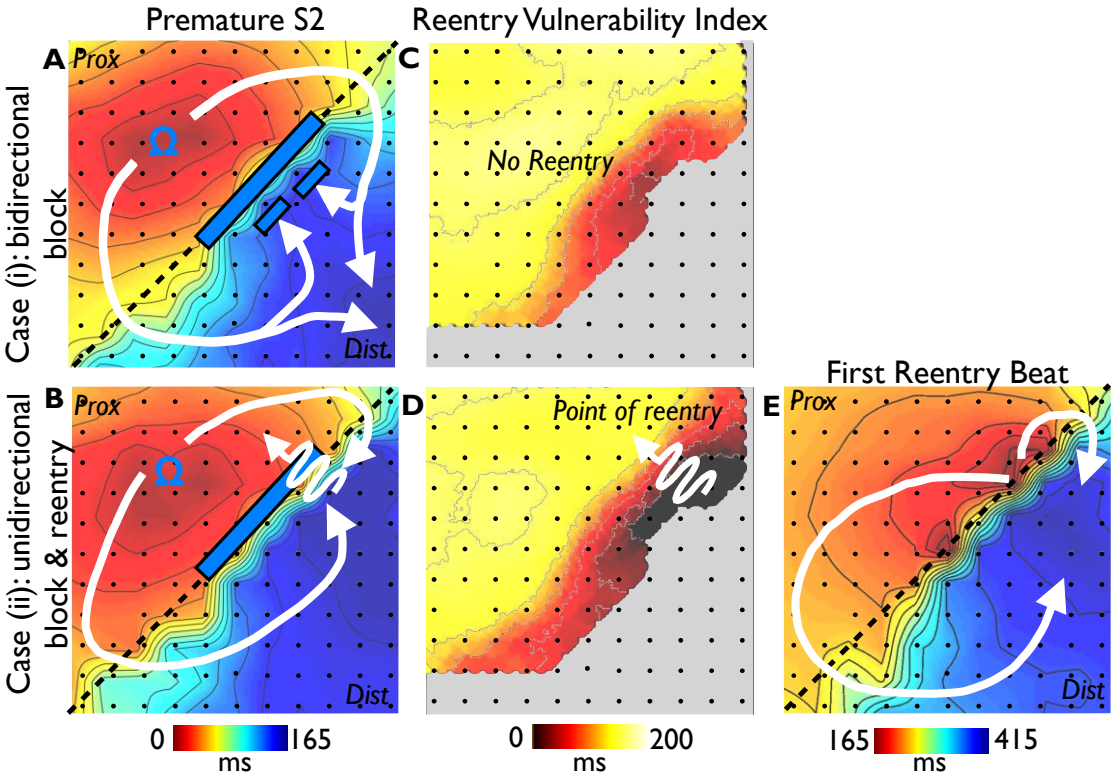

Figure 29. Activation sequence after premature stimulation (S2) from an experiment in a Langendorff pig heart model of inhomogeneous repolarization (APD shortened by Pinacidil above the dashed line and prolonged by sotalol below the dashed line) in the cases of unsuccessful (A) and successful (B) re-entry. The premature wavefront propagates from the stimulation site (Ω) and is recorded by the electrode grid (electrodes represented by dots). C & D show corresponding RVI maps, with the critical area of low RVI identified in D. E shows activation sequence of the first re-entrant beat.

In the case where re-entry did not occur (Figure 29A), activation spread downwards from the stimulus site (Ω) and blocked as it entered the region of prolonged refractoriness (blue bar). The wavefront then travelled around the region of block (shown as curved white arrows) and arrived at the distal side while the proximal region was still refractory. It was thus unable to establish re-entry) Figure 2B and 29E shows a similar situation, but in this case the time of arrival of the wavefront at the distal side was later relative to the time of proximal repolarization, and the wave was able to complete a re-entry circuit.

Figures 29C and 29D show the results of RVI mapping corresponding to Figures 29A and 29B respectively. In Figure 29D, the algorithm identified a region where the RVI is very short and re-entry successfully occurred (minimum RVI value -16ms); in Figure 29C, RVI measures were longer and re-entry did not occur (minimum RVI value 29ms). Note, however, that the critical area of susceptibility was still correctly identified even when re-entry did not occur (Figure 29C).

Optical Mapping

Figure 30 shows sequential fluorescent images (panel A) and corresponding activation maps (panel B and C) for the premature S2 beat during a case of induced re-entry in the experimental coronary-perfused sheep right ventricular preparation, described above. The S2 wavefront is initially blocked (110ms image), but eventually propagates around this region of block and re-enters (220ms). Panel D shows example optical APs from two pixels located proximal

(blue triangle) and distal (green star) to the line of block. Finally, panel E shows the computed RVI map; as expected the region of low RVI is co-located with the site of initial block and re-entry.

Figure 30: Optical mapping

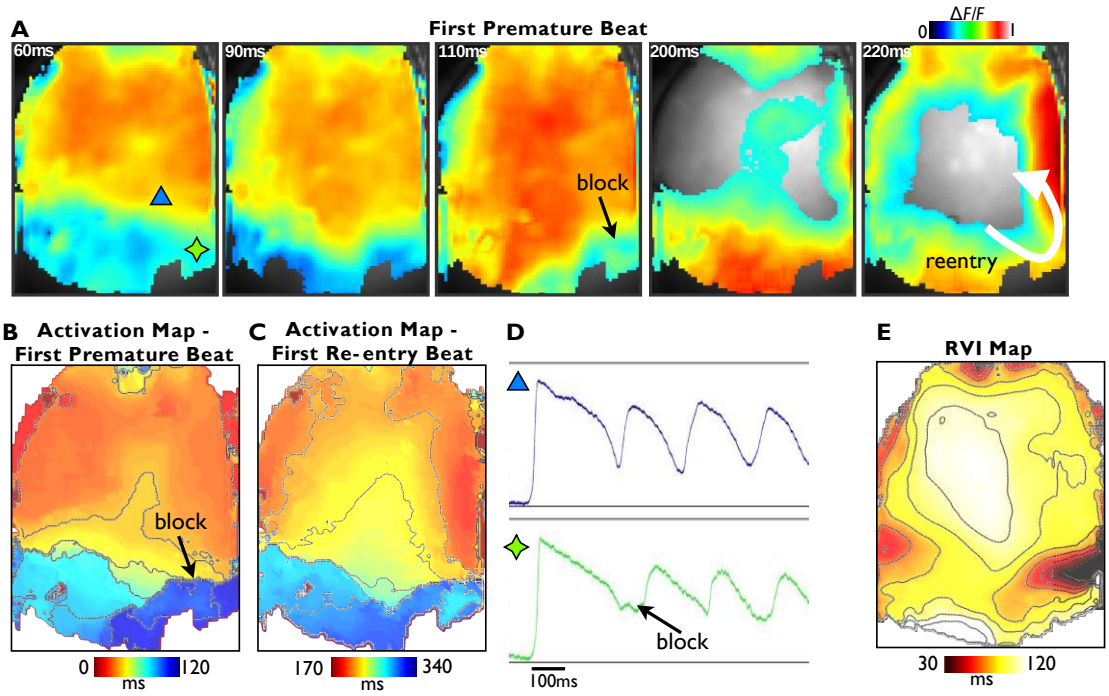

Figure 30. Normalized fluorescent voltage maps showing activation sequence (panel A), activation maps (panel B, & C) and calculated RVI map (panel E) following a premature S2 beat that successfully initiated re-entry. Panel D shows example fluorescent traces from a region proximal (blue) and distal (green) to the line of block. All timings shown are relative to S2 application. (green trace, green star). Exact locations are shown by triangle and star in 4.96s image of panel A. (E) RVI map calculated with a search radius of 20 voxels (~4mm). Region of low RVI is seen to very closely correlate with both the region of initial block and the ensuing reentry.

RVI map to predict location of exit point in a patient undergoing VT ablation

In order to test the feasibility of RVI mapping during clinical procedures, the algorithm was applied to the activation/ repolarization mapping data obtained at 200 LV endocardial sites in a patient with a previous myocardial infarction undergoing a routine VT ablation procedure. Care was taken to acquire high quality unipolar electrograms and fractionated electrograms were excluded from analysis (the algorithm requires electrograms with clear activation and repolarization times). This was particularly important around the scar borderzone where electrograms are typically more complex and fractionated and in these cases unsatisfactory electrograms were removed and the catheter moved gradually away from borderzone until satisfactory electrograms were obtained.

Figure 31 shows the spatial distribution of the RVI calculated based-on the S1-S2 protocol that did not result in the induction of an arrhythmia. The shortest values, which represent sites of highest susceptibility to re-entry (dark red), are confluent in the postero-basal region.

Figure 31: Clinical RVI map

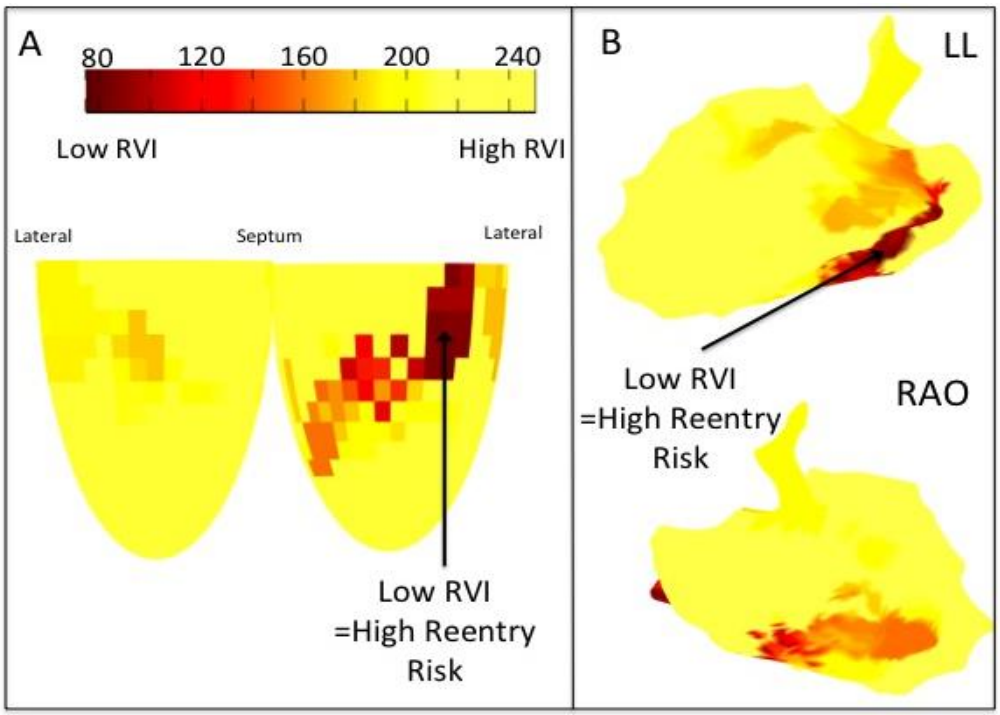

Figure 31. A – Diagrammatic hammerplot representation of the LV showing a map of the spatial distribution of the RVI. B – RVI mapped on the 3D Carto geometry, displayed in the left lateral and right anterior oblique projections.

Subsequently, a spontaneous hemodynamically tolerated VT was induced following an isoprenaline bolus, with the same cycle length (CL 430ms) as the clinical VT. The VT circuit was identified during the arrhythmia through a combination of activation mapping (Figure 32 and 33) and locating diastolic potentials (Figure 34). It was also demonstrated that entrainment occurred with concealed fusion with a post-pacing interval only slightly longer than the VT cycle length and a similar stimulus to QRS time as electrogram to QRS at pacing termination (S-QRS 88ms, EGM-QRS 70ms) (Figure 35). In addition the S-QRS time was relatively short (20% of the VT CL) indicating proximity to the exit point of the circuit (Stevenson, 1997). Radiofrequency ablation was performed in this region (Figure 36) terminating the VT, which was then no

longer inducible and there has been no further VT episodes since. Superimposition of the RVI with scar, and circuit exit point is shown in Figure 37 shows how applying the RVI algorithm during sinus rhythm pacing in this patient would have successfully identified the site of re-entry.

Figure 32: Voltage and activation maps of clinical VT in EP lab

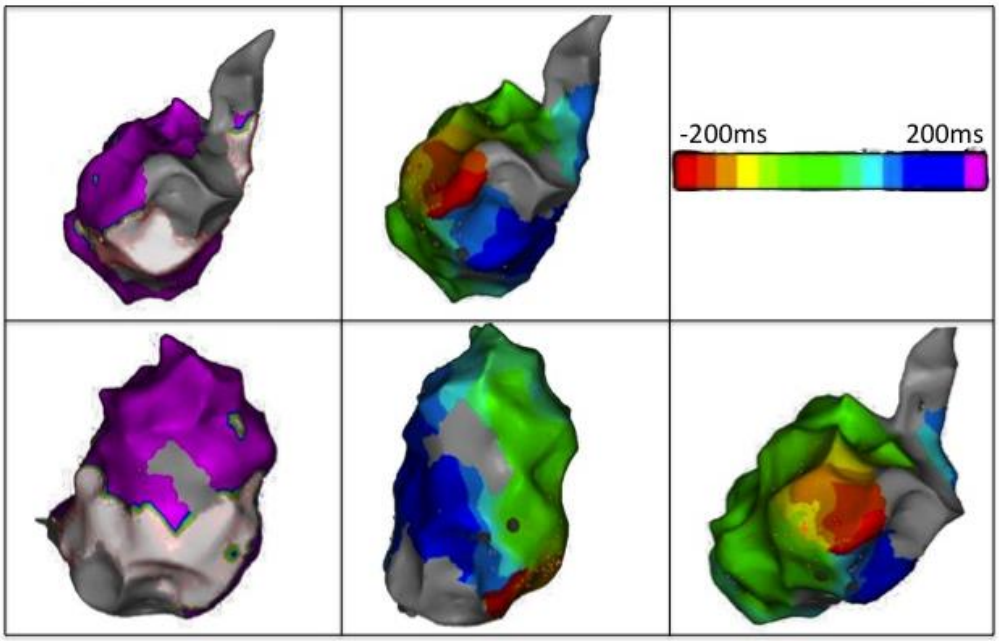

Figure 32. Left – Voltage maps (scar <0.5mV white) in left anterior oblique (LAO) (Top) and inferior projection (bottom) showing inferior dense scar. Middle - VT activation maps in LAO (Top), inferior (bottom) and (bottom right) left lateral projections identifying a counter-clockwise circuit which is shortest over the lateral inferior free wall. Activation map scale -200 ms to 200ms, with VT cycle length 430ms.

Figure 33: Reconstructed activation time map

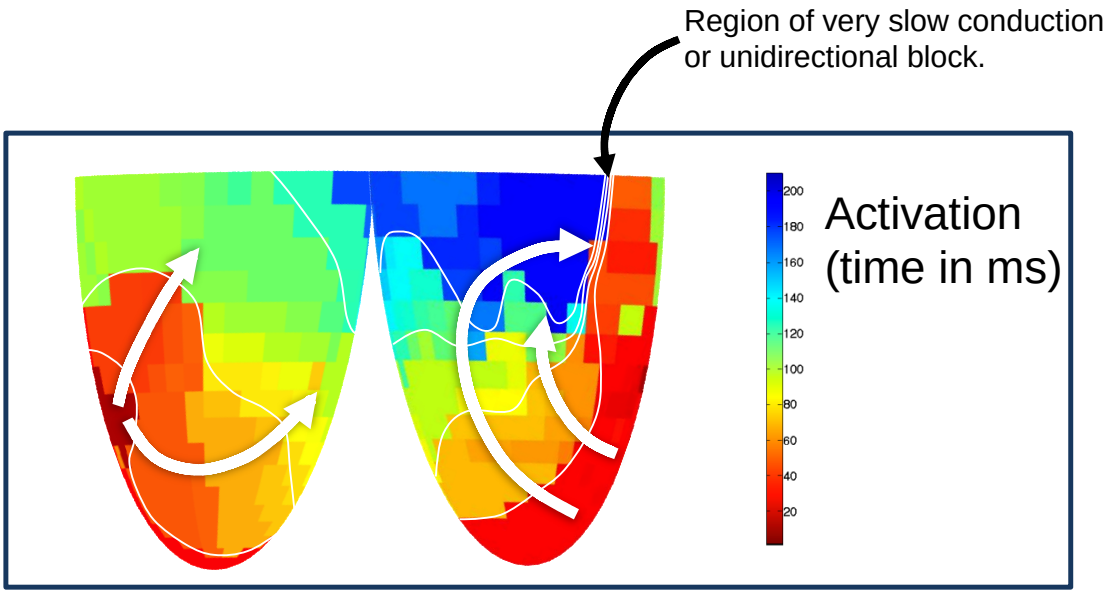

Figure 33. This reconstructed activation time map produced from clinical electrogram data, along with isochrones to identify region of slowed conduction/ block in the same hammerplot as the RVI figure in Figure 32.

Figure 34: Diastolic potentials during VT

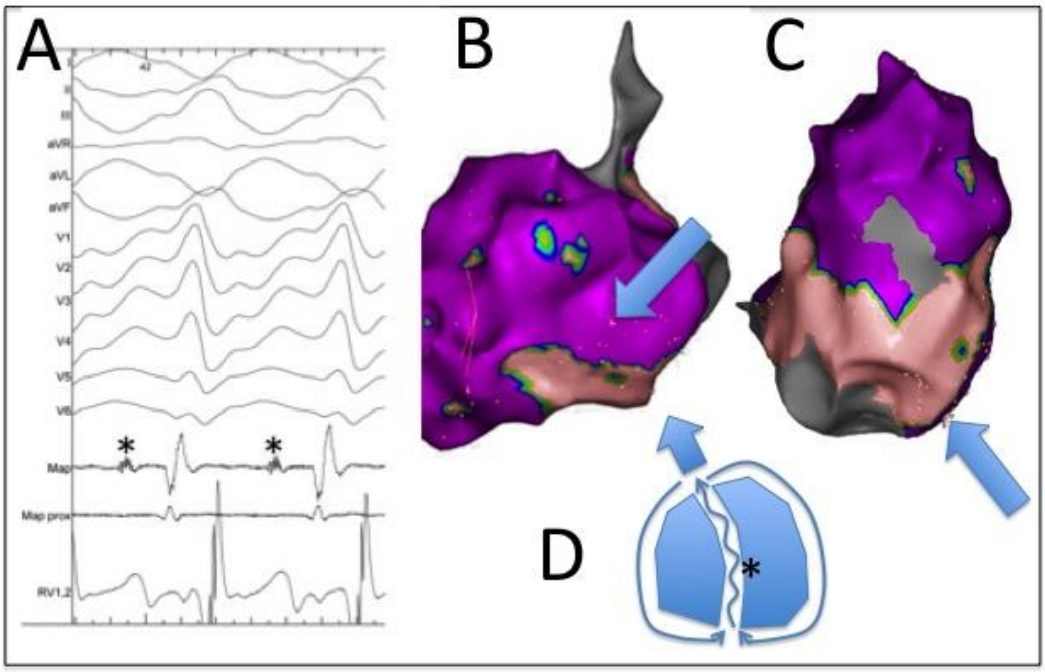

Figure 34. A – Diastolic potentials (*) identified on the mapping catheter in the basal lateral scar. B&C Left lateral and inferior projection from Carto with exact position corresponding to electrograms from A (marked on Carto with a small red cross and highlighted with arrow for illustration). D – diagrammatic representation of slow conducting channel where diastolic potentials (*) are located.

Figure 35: Entrainment during VT

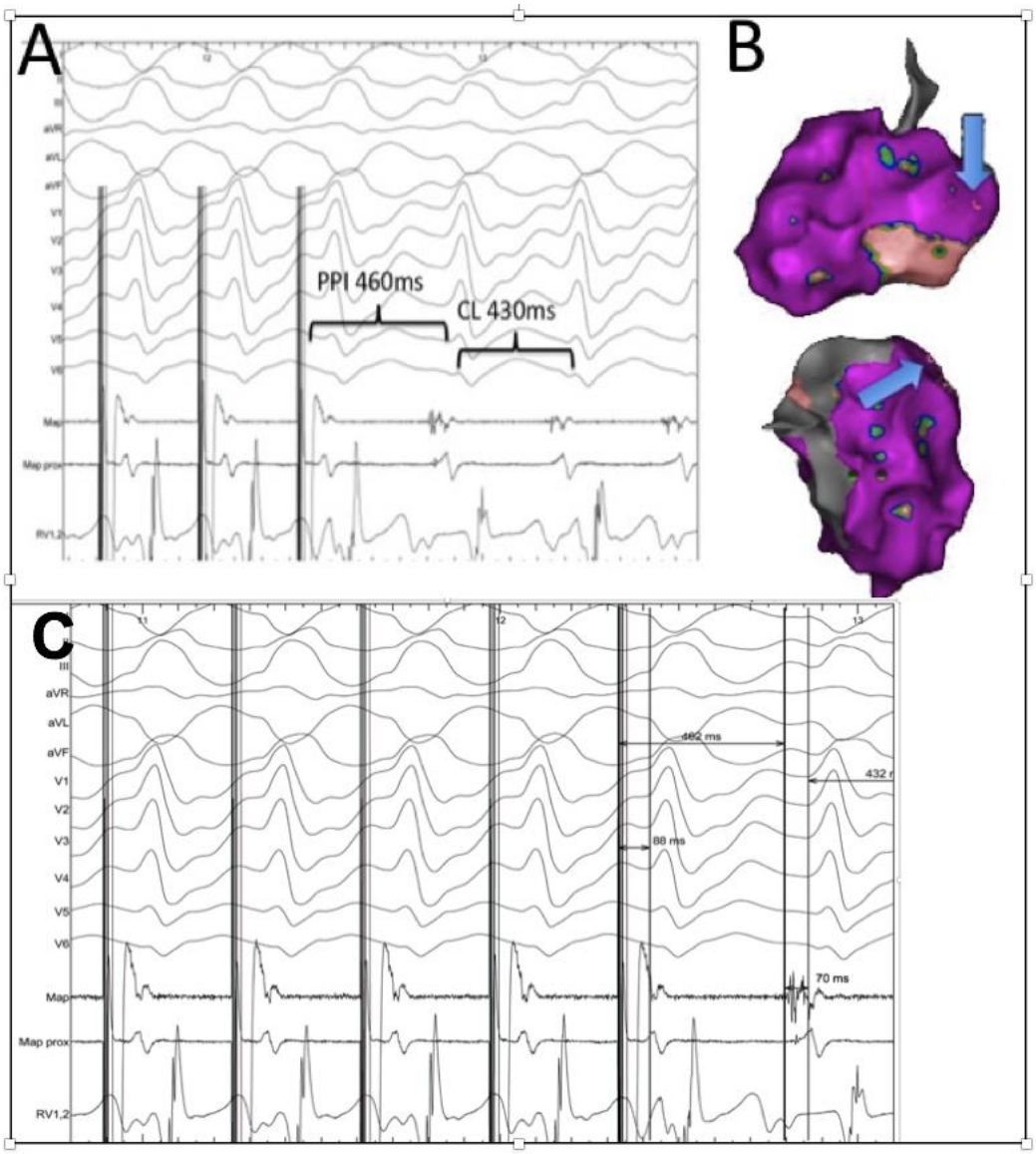

Figure 35. Entrainment during VT. A – Surface and intracardiac electrograms during entrainment from the lateral free wall. Pacing from within or very close to the VT circuit during re-entry results in concealed fusion and a post pacing interval (PPI – 460 ms) which is nearly the same as the VT cycle length (430ms). B – Exact Carto location corresponding to electrograms in A, seen in left anterior oblique and Superior views (marked by Carto with a small red dot, and highlighted for illustration with the arrow). C – Termination of pacing during VT demonstrating a stimulus to QRS time of 88ms and an electrogram to QRS time of 70ms satisfying criteria of being within the VT circuit (<20ms difference). The S-QRS time is 2-% of the VT CL suggesting a location at the exit of the isthmus (Stevenson, 1997).

Figure 36: Sites of Radiofrequency ablation

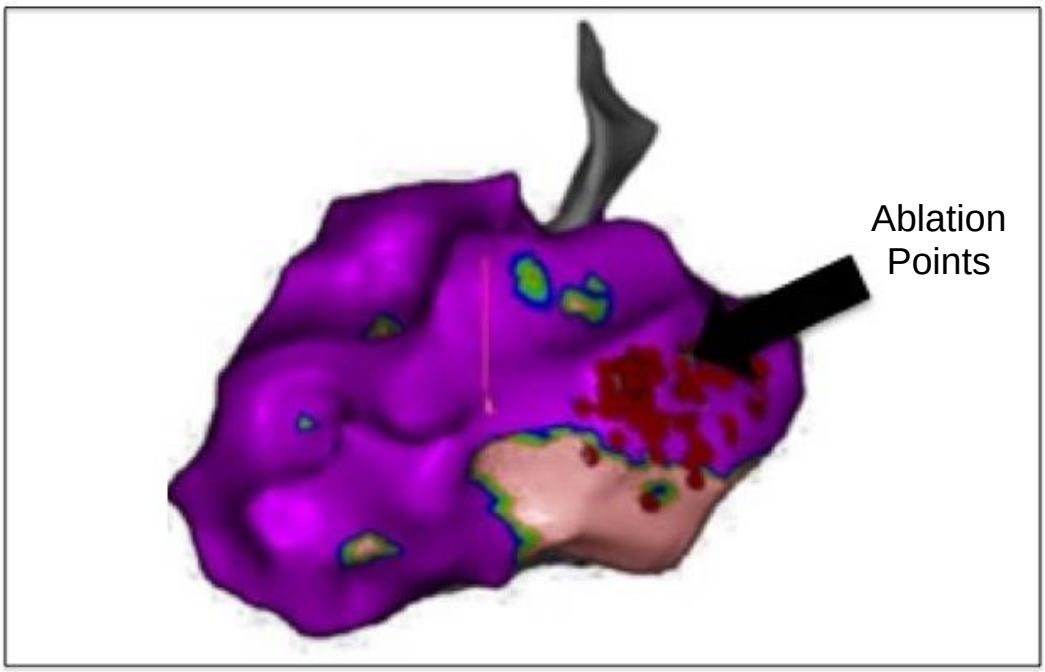

Figure 36. Radiofrequency ablation was applied to the basal lateral free wall in the region of the scar border and more basally. Red dots from Carto illustrate areas of ablation in the left lateral projection.

Figure 37: Correlation of RVI with VT

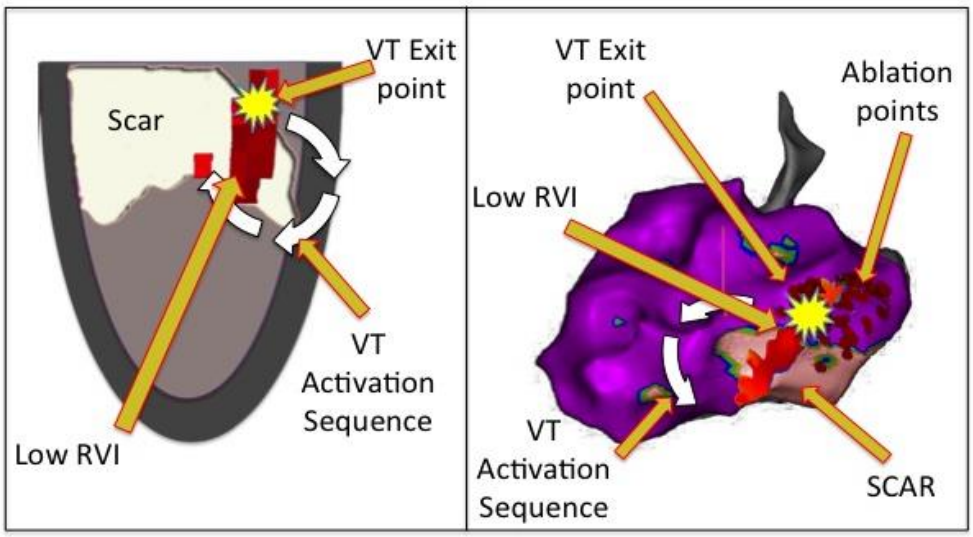

Figure 37. Left – Diagrammatic representation showing superimposed scar (white), activation sequence (white arrow) and area of low RVI (dark red area) co-localizing with VT exit point (yellow). Right – Carto geometry with the same features displayed on the left lateral projection of the 3D geometry. Small red dots show areas of endocardial ablation which resulted in termination and non-inducibility of the VT. White arrow represents the direction of circuit on leaving the exit point deduced from the activation map.

Chapter 6 – Results: High-density contact mapping during AF to identify the underlying mechanism in persistent AF

Recruitment

Recordings from 14 patients were analysed (mean age 61±8 years, LVEF 59±10%, LA size 46 x 58mm, RA size 42 x 55mm). Baseline demographics are presented in Table 7. Two patients had previously undergone AF ablations and 1 patient was on amiodarone. The mean duration of PsAF was 36 months. 8 patients presented in SR in whom AF was induced prior to mapping by rapid pacing. Biatrial basket catheters were successfully positioned in each patient and basket sizes are shown in table 7.

.

Table 7. Baseline demographics

Study no	Age (years)	Gender	EF	NYHA	Prior atrial ablation	Outcomes at 30 days	LA size (mm)	LA Basket (mm)	RA size (mm)	RA Basket (mm)
1	51	Female	55	2	No	SR	43x52	48	38x50	48
2	75	Male	39	2	No	AFL	45x43	48	33x44	48
3	61	Male	41	1	No	SR	61x51	60	72x43	60
4	45	Male	63	1	No	SR	45x45	48	46x46	48
5	63	Male	71	1	No	SR	56x45	60	55x42	60
6	59	Male	74	1	No	SR	51x40	48	50x40	48
7	59	Male	65	3	No	SR	65x48	60	56x52	60
8	50	Male	58	1	No	SR	56x42	60	55x38	60
9	68	Male	60	1	No	SR	61x39	60	49x34	48
10	68	Female	60	1	No	AF	75x48	60	64x49	60
11	61	Male	60	1	No	AFL	65x47	60	62x46	60
12	56	Male	55	1	Yes	AF	55x45	60	53x39	48
13	75	Male	67	2	Yes	SR	61x53	60	57x44	60
14	63	Male	60	2	No	SR	64x54	60	63x43	60

EF – Ejection Fraction, NYHA – New York Heart Association heart failure score, LA - left atrium, RA - right atrium, SR – sinus rhythm, AF – atrial fibrillation, AFL – atrial flutter

Dominant frequency

The mean dominant frequency recorded over all 64 electrodes in the RA and LA is shown in Table 8. Overall, there was no significant difference between LA and RA dominant frequency.

Table 8. Dominant Frequency

Patient	LA dominant frequency (Hz)		RA dominant frequency (Hz)	
	Mean	SD	Mean	SD
1	5.5	1.4	4.9	0.5
2	5.1	0.4	5.1	0.3
3	3.8	0.4	4.7	2.8
4	6.9	3.6	7.3	4.6
5	5.3	1.6	4.7	0.7
6	5.4	0.9	5.1	0.6
7	4.5	0.3	4.9	0.8
8	9.2	2.7	12.8	4.1
9	3.5	0.6	3.4	0.4
10	6.5	2.1	6.5	2.7
11	6.5	0.2	6.0	0.6
12	6.0	0.6	5.4	0.7
13	4.6	0.3	4.7	0.4
14	4.5	0.6	4.5	0.6
Overall	5.5		5.7	

LA – left atrium, RA – right atrium

Identification of phase singularities

In Figure 38, a single phase singularity (PS) is illustrated which was present for 0.93s, showing snapshots of recomposed voltage and phase, as well as the raw electrograms from four electrodes surrounding the phase singularity location. These electrograms are consistent with sequential depolarisation around the phase singularity, followed by regular activity as the phase singularity moves away from this quartet of electrodes.

Figure 38: Example of a rotor in the right atrium

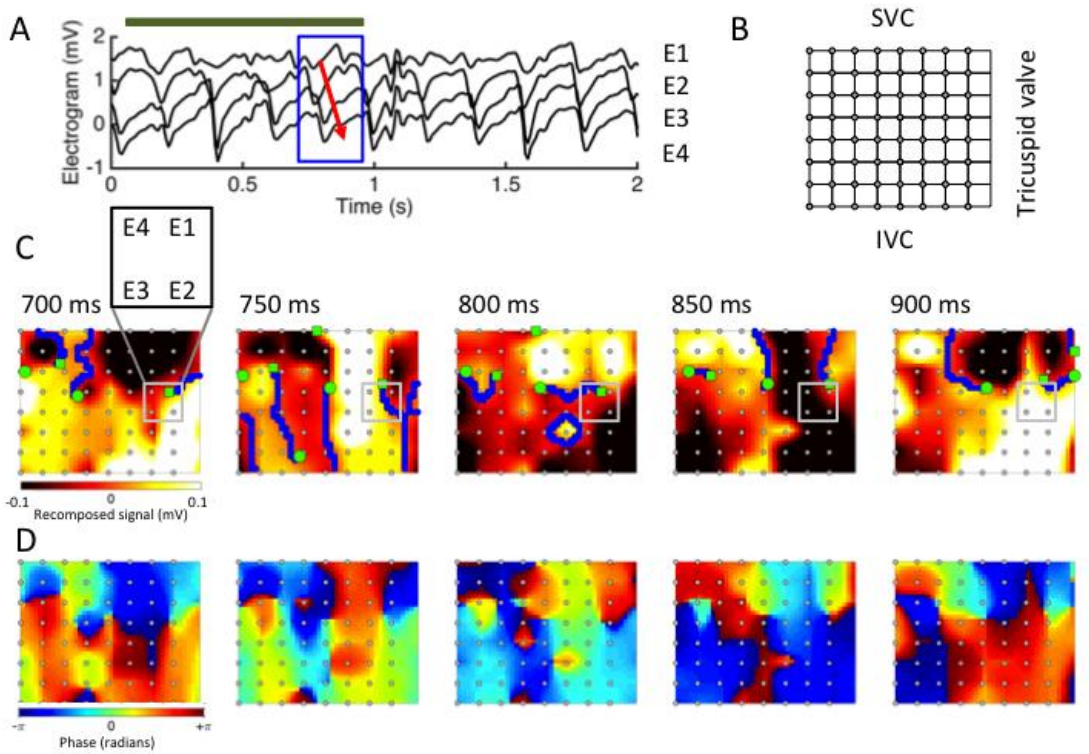

Figure 38. A- Raw electrode signals recorded at locations E1-E4. Blue box indicates the time interval highlighted in C and D, red arrow shows sequential activation at E1-E4, and green line shows lifetime of re-entry. B- Anatomical landmarks for interpolated grid shown in C and D. C- Snapshots of recomposed electrode voltage, showing phase singularities (green: circles anticlockwise, squares clockwise), and wavefronts (blue). Grey boxes show location of

electrodes E1-E4. 3D- Snapshots of phase corresponding to recomposed voltage in C.

Number of phase singularities

We identified PS in both atria, and the total number of PS detected in each atrium for each patient over the 10 s recording period is shown in Table 9. Over all 14 patients, the total number of PS detected in the LA over the 10 s analysis period was higher than the number detected in the RA (779 ± 302 vs 552 ± 235, $p = 0.015$ from paired t-test). To compensate for differences in the catheter deployment, we calculated the total area covered by each basket. The number of PS per unit area is also given in Table 9, and as for the uncorrected numbers, the PS density was higher in the LA compared to the RA (0.166 ± 0.11 PS/mm^2 vs 0.07±0.04 PS/mm^2, $p = 0.0018$ from paired t-test).

Table 9: Number of phase singularities detected in each patient over each 10 s analysis period

Patient	LA			RA		
	Number of PS	PS per unit area (mm^{-2})	Lifetime > 200 ms	Number of PS	PS per unit area (mm^{-2})	Lifetime > 200 ms
1	1232	0.196	9	686	0.064	22
2	950	0.172	3	775	0.142	4
3	441	0.046	3	564	0.043	10
4	733	0.292	0	1151	0.155	2
5	666	0.163	10	534	0.045	12
6	1014	0.443	10	752	0.121	18
7	910	0.309	39	366	0.057	10
8	389	0.122	0	475	0.074	0
9	544	0.105	59	327	0.045	50
10	206	0.061	13	203	0.048	13
11	897	0.145	12	515	0.052	12
12	1211	0.133	19	568	0.061	20
13	908	0.083	45	433	0.033	33
14	813	0.054	40	386	0.040	18
Average	779	0.166	18.7	552	0.070	16

Lifetime of phase singularities

Overall, there were more PS in the LA compared to the RA, but PS detected in the RA tended to have a longer lifetime (Mean lifetime RA 45.9 ± 22.0 ms, LA 38.4 ± 17.1 ms, p=0.009 from paired t-test). Figure 39A shows a histogram of PS lifetimes in the LA and RA, indicating fewer short-lived PS in the RA compared to the LA. Figure 38B shows that the fraction of PS with lifetimes longer than 200 ms was higher in the RA compared to the LA (RA mean 3.77%, LA mean 2.74%, p=0.023 from paired t-test).

Figure 39: Lifetime of Phase Singularity

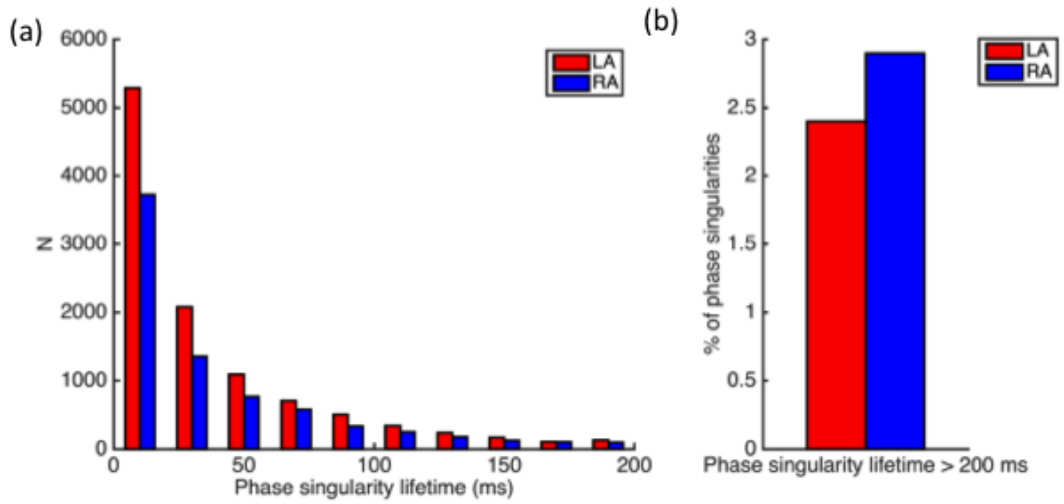

Figure 39. a - Histogram of phase singularity lifetimes in left atrium (red) and right atrium (red). b - Percentage of phase singularities in left atrium (red) and right atrium (blue) with lifetime longer than 200 ms.

However, the number of PS with lifetimes longer than 200 ms was small; in the LA we found 262 PS with lifetime longer than 200 ms, and 14 with a lifetime longer than 500 ms. In the RA we found 224 PS with a lifetime longer than 200

ms, and 19 with a lifetime longer than 500 ms. One patient had no PS in either RA or LA with a lifetime longer than 200 ms, and one further patient had no PS with a lifetime longer than 200 ms in the LA, but has two PS with a lifetime longer than 200 ms in the RA. The longest lasting PS in the entire cohort had a lifetime of only 1150 ms.

LA and RA PS lifetime were strongly correlated (Pearson Correlation (PC) 0.95, $p<0.001$).

Location and clustering of phase singularities

The position of each PS was initially mapped onto an 8x8 2-dimensional array. This was then converted to a 3-dimensional reconstruction based on the 3D co-ordinates of each electrode. There was significant heterogeneity in the geometric distribution of PS distribution with some patients showing clustering of PS locations and others demonstrating a much more uniform distribution of PS spread throughout the atrium (examples in Figure 40).

Figure 40: Examples of Phase singularities

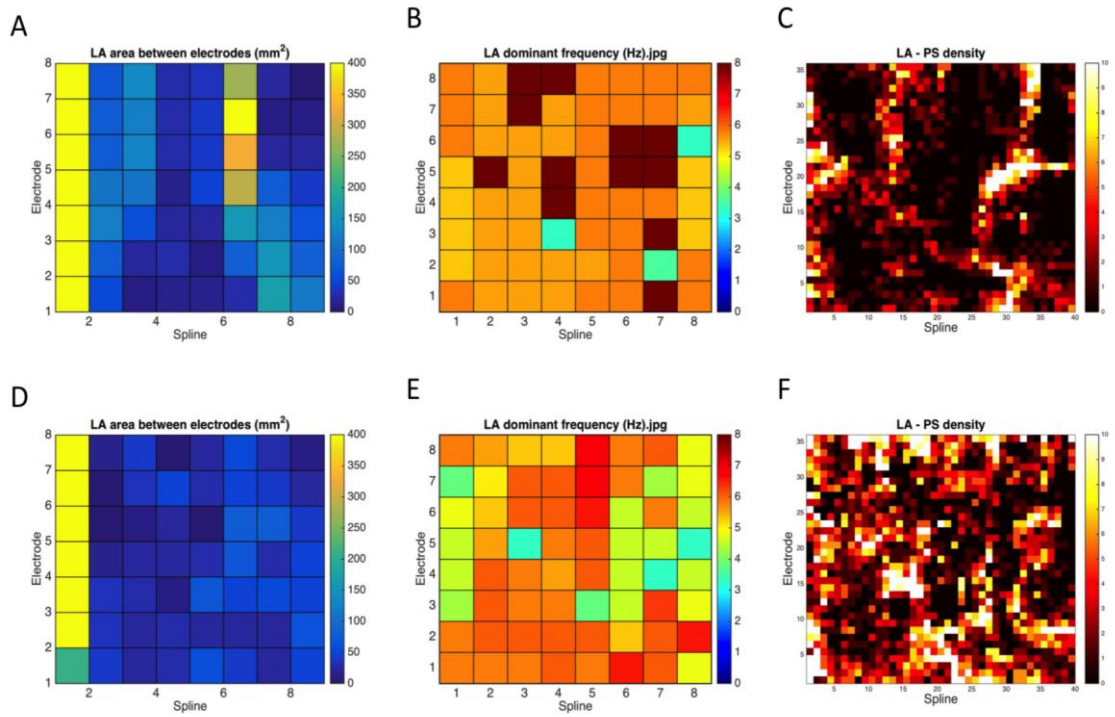

Figure 40. Examples of phase singularity locations in a patient where there was uniform distribution of phase singularities (top row, A-C), and in a patient where there was clustering (bottom row, D-F).

Anatomical location of Phase singularities

There were no long lasting PS (longest PS duration 1150ms) so there is no merit on commenting on likely anatomical positions of rotors. PS were distributed globally throughout both chambers with no clear anatomical predisposition, irrespective of PS duration length (Figure 41).

Figure 41: Anatomical location of rotors

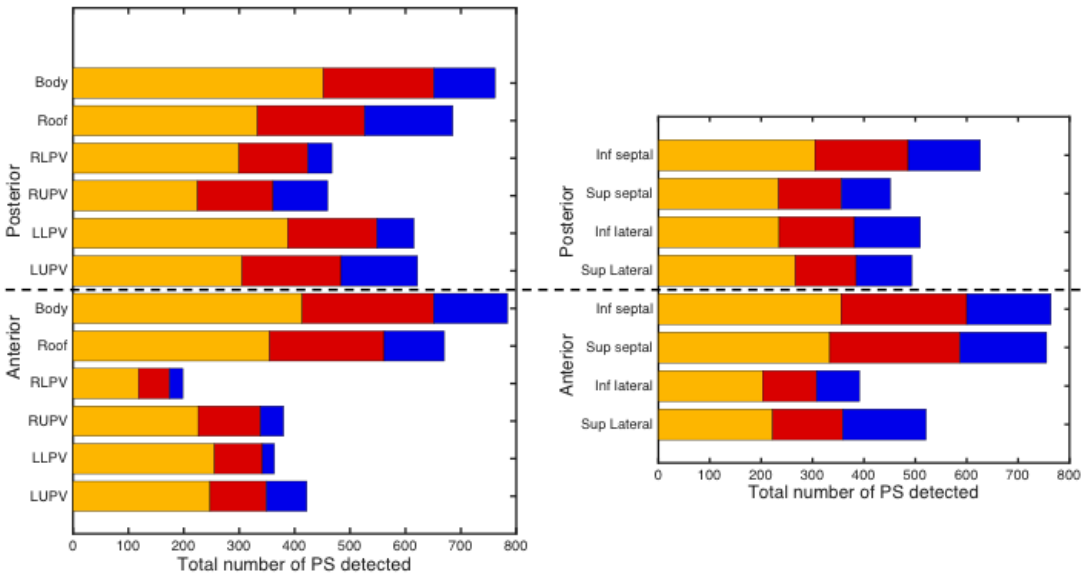

Figure 41. Anatomical location of PS in LA (left) and RA (right) regions. Each bar shows the number of PS detected over a 10 s period in each anatomical location, normalised by the number of electrodes and summed over all 14 patients. The bar colours indicate PS with lifetime more than 200 ms (blue), between 100 and 200 ms (red), and less than 100 ms (yellow).

Atrial size

LA short axis size was significantly correlated with PS lifetime duration (p=0.01), max PS lifetime duration (PC 0.70, p=0.005), and mean number of rotations (PC 0.59, p=0.025). RA short axis was not associated with any PS/rotation parameters. These results were not related to the size of the basket used.

Chapter 7 - Discussion and Limitations

This thesis aimed to investigate a number of key unanswered mechanistic principles thought to be important in arrhythmia initiation, maintenance and potential therapy and risk stratification.

The effect of psychological stress on intracardiac electrical properties

This was studied both invasively in subjects with otherwise normal hearts and non-invasively in those with diseased hearts in 2 separate experimental protocols. In both studies psychological stress was shown to result in small but significant reductions in the activation recovery interval, from which is inferred shortening of APD and hence refractoriness. In both studies this effect was independent of heart rate response to psychological stress (controlled for by pacing at a fixed rate above the intrinsic heart rate).

For the invasive study, in patients with otherwise normal hearts the direct effect of an emotionally-charged movie clip on cardiac repolarization was assessed from multiple endocardial electrodes in the left and right ventricle in fully conscious adults prior to an invasive electrophysiology study. In addition, central arterial blood pressure, RPD, and respiration were recorded. As expected, there was an increase in mean, systolic and diastolic blood pressure and RPD during the mental stress, compared to the control periods. We were able to demonstrate in our invasive study that in relatively non-diseased human hearts there was a small consistent shortening of the ARI in both ventricles

(change at maximal stress of 4.8ms in the RV and 1.8ms in the LV) (Child, 2014). There was no significant variability between the degree of ARI shortening and distal/ proximal position of recording electrodes in these patients with relatively normal hearts. The changes in ARI provide direct quantitative evidence for an effect of mental challenge on intracardiac repolarisation and had not previously been reported.

In the non-invasive study, subjects with significantly diseased hearts were studied entirely non-invasively, again measuring haemodynamics, respiration (and galvanic skin response in 8 patients) and left ventricular intracardiac epicardial electrograms recorded from the left ventricular lead in patients with a cardiac resynchronisation therapy pacemaker. There were significant increases in respiration, blood pressure and GSR during periods of stress compared to the control period in both the threatening and disgusting picture sequences and the movie sequences. Whilst ARI significantly shortened during the disgusting picture sequence (by an average of 2.6ms) there was no significant change in ARI during the threatening picture sequence, raising the possibility that certain negative emotions have more of an effect on ARI, whilst more global haemodynamic responses were similar (see later). In the movie sequences a consistent small reduction in ARI (mean change 2.5 to 3.6ms) were seen in all 3 sequences when compared to the relaxing picture controls.

Shortening in ARI as a consequence of sympathetic stimulation is consistent with the known effects of adrenergic stimulation (Heijman, 2011; Terrenoire,

2005). Animal models have reported APD or effective refractory period (ERP) shortening in the region of 4 to 20 ms during direct left, right or bilateral sympathetic nerve stimulation in canines, and ERP lengthening in the region of 4 to 10 ms following sympathetic nerve section (Haws, 1978; Martins, 1980; Garcia-Calvo, 1992; Schwartz, 2001; Vaseghi, 2012). Shortening of ARI in both our studies were less pronounced than in these animal studies which may be due to a lower intensity of the film/picture stimuli compared to electrical stimulation in activating the sympathetic nervous system. This would be supported by a comparison of the response in systolic blood pressure, which increased by 28-36% following sympathetic nerve manipulation (Vaseghi, 2012) compared to 4.5% in the invasive study and a maximal increase of 9.8% in the non-invasive study. It is possible that a more-intense mental stress stimulus would have produced more pronounced APD shortening. A more recently published study by Finlay et al using mental stress tests reported ARI shortening of between 4 and 8ms (Finlay, 2016), which is broadly consistent with our results. Alternatively, this difference in ARI response may reflect a difference between species.

In our invasive studies ARI shortened more in the RV than in the LV. Several mechanisms might explain this observation, including the asymmetric autonomic innervation of the ventricles and asymmetric central input to the autonomic control system, both of which have been considered to play a possible role in inducing electrical heterogeneity and arrhythmogenesis (Taggart, 2011). However, in the study by Finlay et al (Finlay, 2016) the reverse

finding was described in which the shortening was greater in the LV and further studies would be useful in determining whether there is any consistent relationship.

Local changes in repolarisation caused by psychological stress may be important, as APD is a critical component of re-entry, which is a common form of clinical arrhythmias and sudden cardiac death. An improved understanding of the response of local refractoriness to psychological stress in the future may explain the increased risk of significant arrhythmias seen in response to psychological stress (Taggart, 2011, Aoki, 2012), and has the potential to improve risk stratification or target future therapies. Prior to this study we had hypothesized that any changes in ARI would be greater in diseased hearts than the relatively healthy hearts used in our first invasive study. During our non-invasive study in more severely diseased hearts we found a similar degree of ARI shortening as seen in the previous normal ejection fraction stress study and between those with moderate and severely impaired systolic function. Whilst this could be confounded by different degrees of psychological stress during the different studies, the fact that there were appropriate and similar changes in systolic blood pressure during both studies means this is unlikely.

In the IAPS study both stress picture sequences resulted in a similar increase in respiration, systolic and diastolic blood pressure but whilst the images associated with the disgust emotion resulted in a shortening of ARI, the pictures associated with the threatening emotion did not. Previous non-cardiac studies have demonstrated that different IAPS emotions result in different physiological

responses, despite being of similar intensity (Bernat, 2006; Yartz, 2002). This may be the result of the differing neurophysiology processes occurring in response to different stimuli. Functional MRI has demonstrated that the disgust and fear emotions are based in separate neural systems, components of which are found on different hemispheres, for example the left insula in the case of disgust (Sprengelmeyer, 1998). Whilst there is obviously considerable overlap both when these outputs converge in the frontal regions and at various plexi between the brain and the heart, this difference in hemisphere processing could theoretically result in same-side predominance (brain-heart laterality hypothesis chapter 1.8.4). This might explain why different ARI responses were seen from 2 negative emotions, which has not previously been reported and further studies would be useful to confirm and elaborate this finding.

The shortening of APD in response to psychological stress is independent of respiratory changes

Changes in respiration are known to affect cardiac activity due to the cardiorespiratory feedback loop (chapter 1.13). As expected, respiration rate increased during the stress protocols of both studies. Importantly, in the invasive study in normal hearts we were able to control for the effect of changes in respiration by incorporating a respiration playback system so that the subjects repeated the same breathing pattern that they developed during psychological stress during the control period. The repeated-breathing control period demonstrated that the haemodynamic and repolarisation changes we observed were not attributable to the alteration in breathing pattern alone,

suggesting that these were predominantly generated by the movie-induced psychological stress.

In the invasive study all subjects demonstrated an increase in respiratory rate during the movie consistent with other studies on the effect of a mental or emotional challenge (Hanson, 2009). Respiration is known to modulate autonomic activity and alters membrane potentials of preganglionic vagal and sympathetic neurones. Since mental stress is well known to affect both respiration and the autonomic nervous system (Bernardi, 2000) it has been uncertain as to their relative roles in mediating the electrophysiological effects of a mental challenge. Our results show that when the altered breathing pattern generated by the movie was copied by the subjects in the absence of the movie, the ventricular APD shortening seen during the movie did not occur. This suggests that the effect of mental challenge on APD was a direct effect via the autonomic nervous system.

Activation Recovery Interval shows cyclical variation at both the respiratory and sympathetic activity frequency

During our non-invasive study we observed that as well as the gross mean increases and decreases in blood pressure and ARI measurements there appeared to be a degree of regular cyclical oscillation in our physiological measurements. This is in keeping with most, if not all, biological systems but had not previously been reported in the case of ARI, and potentially adds to our understanding of the underlying systems governing cardiac repolarization.

Respiratory oscillations in blood pressure are well recognised, and are thought to be a combination of both mechanical forces and modulation of the vagal-cardiac nerve activity (Katona, 1970; Eckberg, 2000). More recently low frequency oscillations (0.1Hz) have been reported in blood pressure, which is thought to reflect the frequency of sympathetic nerve firing, termed the Mayer wave.

ARI oscillation at the respiratory frequency has previously been reported by our research group during fixed breathing protocols (Hanson, 2012). Our results corroborate this previous finding and this respiratory frequency of oscillation was found in approximately half of patients who had a relatively constant breathing rate when measured over the entire movie sequence. Possible mechanisms explaining this finding includes mechano-electrical coupling (reflecting changes in ventricular loading during different components of the respiration cycle) and a variety of nervous mechanisms including central respiratory networks gating the autonomic neural traffic to the myocardium (Hanson, 2012).

One previous limitation of the originally published data was that during respiration catheter position might move, which could account for the respiratory observations. This study used LV epicardial leads that had been implanted for a significant duration, and as such are generally regarded as entirely fixed structures, which would not be subject to respiratory movement and hence support the previous observations.

During this study ARI was found to show oscillations at a low frequency (Mayer waves), which had not previously been reported. Mayer oscillations are the result of oscillations of sympathetic nervous tone (Cevese, 2001; van de Borne, 2001). Studies were performed in patients in an upright position, which is known to facilitate sympathetic activation, and in a group of patients with heart failure in whom sympathetic activity is frequently overly active.

Further more detailed analysis was performed and published on 14 out of our 15 non-invasive study patients using time-frequency and coherence analysis (Hanson, 2014). This comprised much more complex statistical analysis primarily performed by our biomedical engineering collaborators, and as such is not included in the result section, but is described briefly below.

The initial identification of respiratory and low frequency oscillations in the results section was performed effectively over an average of the entire sequence, using the periodogram function in Matlab. The more complex analysis applied time-frequency analysis as a function of time for the respiratory oscillations, using the smoothed pseudo-Wigner Ville distribution, which has previously been validated in similar cardiovascular studies (Orini, 2012). This very complicated method is required to account for the time varying nature of these oscillations. As demonstrated in Figure 42 the time frequency spectrum is analysed continuously throughout time using this method. A Cross-Time-Frequency-Spectrum was then used to identify whether ARI was oscillating with respiration. A similar technique was then used to identify whether ARI was oscillating at the slower (0.1 Hz) frequency, and the relationship between blood

pressure and ARI oscillations. Determination of statistical significance was via time-frequency coherence testing, which determines whether these frequencies were occurring at much greater amplitude than expected by background noise (Figure 43).

Figure 42 - Illustration of time-frequency analysis of the respiratory signal and the definition of the respiratory frequency band

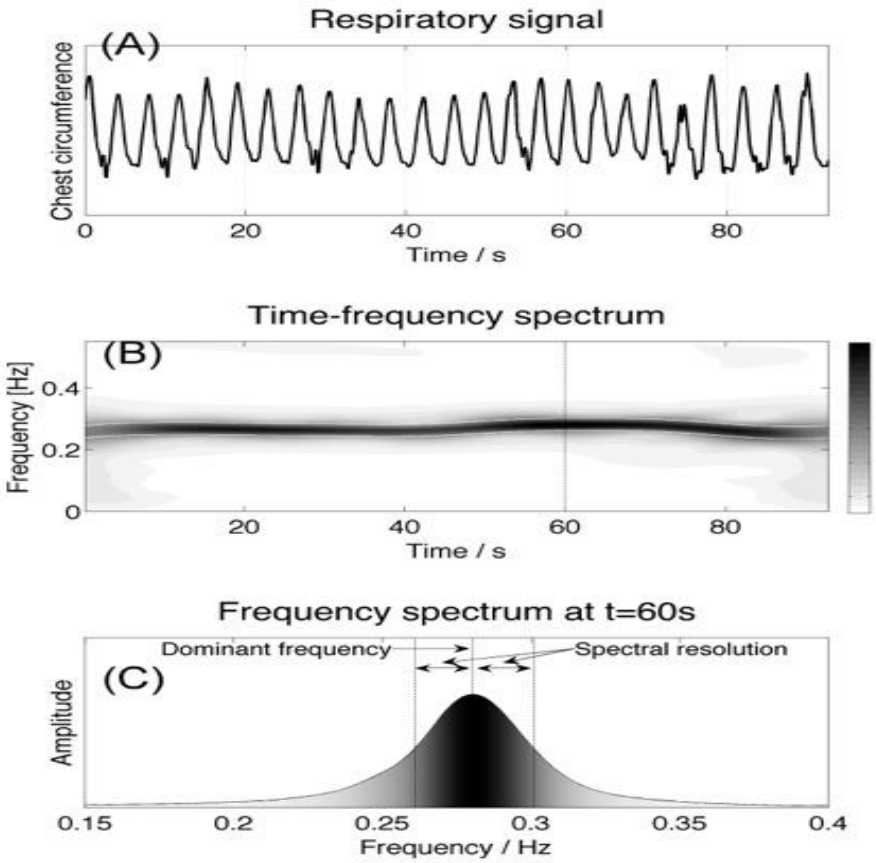

Figure 42. The upper panel (A) shows the time series of the respiratory signal. The corresponding time-frequency spectrum is presented in the middle panel (B). The intensity of a specific frequency is given by the grayscale (white: low intensity, black: high intensity). An enhanced frequency band is clearly visible at the respiratory frequency (approx. 0.28Hz in this example). The frequency spectrum (C) provides a cross-section of the time-frequency plot at 60s, shown by a dashed line in (B). The respiratory frequency band is defined by taking the maximum amplitude frequency ± the spectral resolution. (Adapted from Hanson, 2014).

Figure 43 - Example plot showing oscillations in the ARI signal at the respiratory frequency

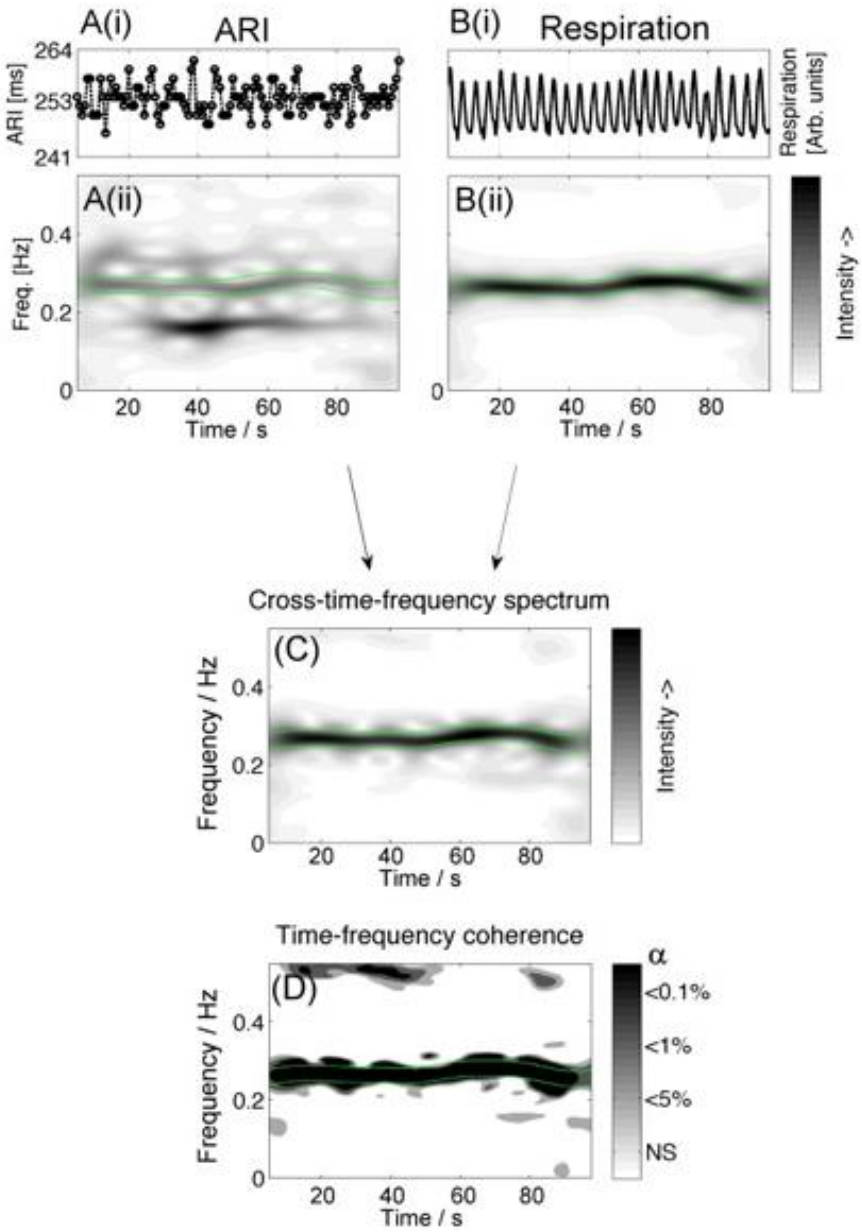

Figure 43. The top graphs A(i) and B(i) show the time series of ARI and respiration. The corresponding time-frequency spectra are plotted below, A(ii) and B(ii). The high intensity band in the time-frequency spectrum of the respiratory signal B(ii) represents the frequency of the respiratory signal (approx. 0.25Hz). High intensity is also seen in the ARI time-frequency plot A(ii) in this frequency band. The cross time- frequency spectrum (C) shows that the ARI and respiratory signal are correlated at the respiratory frequency. The

results of coherence analysis in the lower panel (D) show the coherence at the respiratory frequency is significant at $p < 0.001$, indicating that both signals are coupled at this frequency. NS = not significant. (Adapted from Hanson, 2014).

Using this more complex time-frequency analysis method, which measures over different points in time, all patients showed significant ARI oscillations at the respiratory frequency during part of the recording, with an average peak to peak differences of 5ms. In most patients coupling between ARI and respiration occurred intermittently during the recording (mean 43% of total recording), which is why this is a much more sophisticated method than our initial analysis. In addition, blood pressure Mayer waves were found in all patients, and in 46% of the ARI recordings. The average peak-to-peak ARI differences ranged from 2.9 to 9.2 ms, and again occurred intermittently.

The presence of significant coupling between ARI and systolic blood pressure at Mayer wave frequencies suggests that a similar mechanism might be acting on both systems. The mechanism underlying the slow frequency oscillation in ARI remains unclear and further studies will be required to further investigate this newly reported phenomenon. In particular, further studies looking at what happens to this oscillatory behaviour in and around diseased myocardium where sympathetic innervation might be reduced or even super-sensitive (chapter 1.9.2) might add valuable insight into the mechanism underlying ventricular arrhythmia generation. This finding of oscillatory ARI behaviour needs to be considered in future studies of ventricular refractoriness as it significantly complicates interpretation of any single measurement taken in time.

In an additional study by our research group (n=10) we were able to demonstrate that in subjects in whom ARI was oscillating at the respiratory frequency during a fixed rate breathing protocol, the addition of metoprolol resulted in a reduction in respiratory peak to peak difference in ARI and a reduced coherence between the 2 traces (van Duijvenboden, 2015). This finding confirms the interaction between respiration pattern and cardiac sympathetic innervation.

Methodological considerations and limitations of the stress studies

The methodologies employed in these studies were novel. In the invasive study the protocol was designed to combine electrical recordings from within the heart in conscious subjects undergoing a stressful stimulus unaccompanied by vocalisation (unlike methods such as serial 7 subtraction), which would have interrupted the natural pattern of respiration. We contrived a protocol to enable subjects undergoing routine cardiac catheterisation procedures to be shown film clips during the procedure.

One obvious limitation of this study was that a cardiac catheterisation procedure would in itself be considered a stressful situation and as such there is no real control element to the study. In order to overcome this the second study aimed to perform a similar psychological stress study using a combination of validated picture sequences and film clip whilst measuring haemodynamics and electrical recordings entirely non-invasively in a less stressful environment. This

approach allowed measurement of only a single epicardial electrode (from the patients LV epicardial pacing lead), as opposed to the 10 electrodes in each ventricle during the invasive study, and recordings had to be made in batches of 30-second epochs allowing only segments to be recorded at a time. Given our finding of oscillations in ARI it would have been very useful to have multiple electrode recordings in order to establish spatial heterogeneity, and longer recording times and future similar studies should consider this.

The fixed rate pacing protocols used in both studies allowed us to isolate changes in ARI as a result of psychological stress independent of rate-related effects. Film stimuli have several advantages over other stimuli including their dynamic nature, a sustained effect and the combination of visual and auditory inputs.

In these studies we chose blood pressure measurements to indicate sympathetic activation, which has previously been validated (Meyer, 2010), rather than plasma catecholamine sampling to better capture short-duration changes throughout both protocols. However, having identified the oscillations in blood pressure we decided this might confound our results so added in galvanic skin response as an additional measure that quickly identifies changes in sympathetic tone.

The use of Re-entry Vulnerability Index can successfully identify areas at risk of re-entry

We have developed a mapping algorithm able to identify localized regions of high susceptibility to conduction block and re-entry using a novel parameter referred to as the re-entry vulnerability index (RVI) based on our previous experimental work (Coronel, 2010). In an animal model of repolarization heterogeneity (mimicking the peri-infarct region) in which re-entry had been induced and mapped, the algorithm successfully identified the region of block and subsequent re-entry. It also performed similarly well in optical mapping experiments and computer simulations in which it also co-located regions of low RVI with spiral wave rotors. We then applied this technique to a patient undergoing radiofrequency VT ablation in whom activation and repolarization times were measured from 200 electrode sites in the LV during S1-S2 pacing that did not induce the arrhythmia. From these data points the algorithm generated a global map of RVI that could be co-registered with the anatomy. It is of note that the low RVI co-located with the VT exit site identified after induction of the arrhythmia.

Optimization and experimental validation of the RVI mapping algorithm

Theoretical sensitivity analysis of the dependence of the RVI metric magnitude with respect to parameters used in its calculation allowed us to optimize the algorithm to robustly distinguish regions of block/re-entry when applied to different experimental, modelling and clinical applications, and across different

species (sheep, porcine, man). In porcine experiments and computer simulations, re-entry was established due to an imposed intrinsic gradient of repolarization, whereas in the sheep optical mapping experiments, re-entry was established following a strong cross-field shock perpendicular to a uniform repolarization wave, setting-up initial conduction block. In all cases, however, the algorithm successfully identified the site of re-entry.

This algorithm has subsequently undergone extensive further computational modelling (Hill, 2016) and has been shown to be robust at predicting sites of re-entry even within complex and intramural scar anatomies with low-resolution clinical data acquisition.

Our approach links the classical views on re-entry posited by Mines (Mines, 1913), to those involving the more mathematical description of rotors, wavefront-wavetail interaction, and singularity points. The RVI is based on the interaction between the front and the tail of an activation wave across a region of block, being functional or structural in nature. We demonstrate that without addressing the underlying mechanism of re-entry (either leading circle or rotor based) the algorithm accurately identifies the site of re-entry. This is of clinical importance, because this is the site that is the target for ablation therapy.

Our RVI metric is based upon electrophysiological parameters that have a long established importance in arrhythmogenesis; activation time and repolarization time. The main significance of our index is that it allows identification of the site of initiation of re-entry without the need to actually induce the arrhythmia (which

is usually clinically hemodynamically not tolerated or inducible); in contrast, identifying phase singularities requires a rotor to be induced. In our simulations, we were also able to demonstrate a strong, but not exact, correlation of the region of low RVI with the site around which phase singularities associated with the rotor clustered. These regions could also be approximately identified from activation time maps where conduction velocity slowed near the rotor core. However, in addition to the fact that conduction velocity may be undefined at the site of block, the area identified as low RVI corresponded to a much smaller region than the area of slowed conduction, spanning only the line of block at the restricted area where re-entry occurs for the first time. We further note that our RVI approach will identify sites vulnerable to re-entry in situations in which singularity points are not always present, for example during anatomical re-entry, thus working equally well regardless of the underlying re-entry mechanism.

A low RVI is pro-arrhythmic and is enhanced by shorter APD of the premature S2 in the proximal zone. Repolarization in the proximal region is determined by the local APD restitution characteristics. Steep APD restitution in this region therefore would be potentially pro-arrhythmic (shorter RVI) and conversely flattening restitution would be potentially anti-arrhythmic (longer RVI). This would be in keeping with the classic restitution hypothesis (Riccio, 1999) and the known anti-fibrillatory effect of flattening APD restitution (Garfinkel, 2000), although the latter considerations are likely more relevant to non steady-state conditions. Our data also demonstrate that a slope of the restitution curve needs not to be lower than 1 to identify pro-arrhythmic conditions.

Clinical Application of the RVI algorithm

RVI mapping is clinically applicable in the treatment of VT by radiofrequency ablation, where success rates overall are unsatisfactory (Aliot, 2009). The majority of VT episodes following myocardial infarction are due to re-entry mechanisms, involving interaction between electrical activation and repolarization waves.

Clinical ablation procedures typically focus on activation times rather than measure repolarization times in order to localize the circuit, and when this is not possible anatomic mapping is usually performed (identifying areas with low amplitude signals, that may not be involved in a re-entrant circuit). The optimum ablation strategy aims to prevent the arrhythmia by interrupting the re-entry pathway by delivering radiofrequency energy to the isthmus and around the scar (Stevenson 2000). However, this is only possible in a minority of cases, either because the arrhythmia is not hemodynamically tolerated or the VT is non-inducible. Furthermore, multiple exits may exist that may remain undetected by these standard methods.

In ischemic cardiomyopathy, re-entrant arrhythmias are based on anatomic re-entry involving the scar region, which provides the electrophysiological requirements of heterogeneous activation and repolarization for initiating and maintaining the re-entry circuit. The re-entrant activation commonly involves conduction along channels of surviving myocardium that transect the infarcted

region. Although conduction velocity along these surviving fibers is typically normal, the tortuosity of the channels causes a relatively long pathway and thereby a long conduction delay (de Bakker, 1990). If the surviving fibers connect to non-infarcted myocardium, circular activation can be accomplished. The apparent 'focal' origin of the tachycardia in reality is the exit point where the re-entrant activation emanates from the infarcted tissue. Experiment and theory predict that the site of unidirectional block in post infarct VT is located near the exit point (Segal, 2010). Additional conduction delay is often provoked by a premature beat (Saumaraz 1992) and the completion of full re-entry depends on whether the normal tissue has regained excitability following the premature beat. These are the conditions identified by the RVI algorithm. The algorithm has the potential advantage that it does not require initiation of the tachycardia and employs non-critical prematurity of extra stimulation.

Limitations of the RVI algorithm

We cannot exclude the possibility that some variations in the post MI substrate such as post repolarization refractoriness might affect the clinical performance of the algorithm. Post repolarization refractoriness, if present, is likely to occur in the region of block; in which case, the normal correspondence between action potential repolarization and refractoriness may not exist. However, our algorithm does not incorporate the time of action potential repolarization in the downstream region of block, only the activation time in this region of the premature beat, together with the repolarization time of the premature beat in

the upstream region. Therefore, post repolarization refractoriness does not affect the efficacy of the RVI algorithm. The RVI algorithm requires relatively non-fractionated unipolar electrograms to accurately assign activation and repolarization times which is challenging in and immediately around the areas of scar which are the regions of particular interest.

The study in one patient was intended to verify the prediction that an RVI map could be generated in the human ventricle during the course of a clinical procedure and that the RVI map could be co-registered with geometry acquired using a Carto mapping system (Biosense Webster, Ca). No attempt is made at this stage to establish a role for RVI mapping as an aid to ablation other than to demonstrate its feasibility. Future work may identify the efficacy, sensitivity and specificity of this combined activation and repolarization mapping approach in radiofrequency ablation procedures in larger cohorts of patient with VT. Following on from this research we have now acquired research ethics for a further 10 clinical cases in order for us to further optimise the algorithm and streamline the clinical mapping protocol. Currently the measurement of RVI is performed post procedure, but clearly if it is to be of clinical use in the ablation of VT this will have to be developed with industry support to collaborate in developing the software so that it can be calculated in real-time during the index procedure.

Lack of long-lasting rotors in persistent AF

The main finding from our PsAF study is that despite using whole-chamber panoramic endocardial mapping and a sophisticated analysis method no sustained rotors or localized drivers were identified. Only very transient rotational activation was present, which by definition does not represent sources but likely the result of passive activation. This is despite using a comparable technique to that used previously by our group in successfully identifying rotors during ventricular fibrillation. The PS results are consistent with the multiple wavelet hypotheses, and are clearly not consistent with the rotor hypothesis.

Short-lived PS were identified in the majority of patients, reflecting the anatomical and functional electrical heterogeneities present in PsAF. However, such short-lived PS are not thought to play a role in sustaining AF, but secondary to passive activation. There was a greater density of PS in the LA compared to the RA, and also in larger left atriums, likely due to increased electrical and anatomical remodelling. The LA and RA PS lifetime was also strongly correlated suggesting that the same underlying process is occurring in both atria. PS duration was shorter in the LA than the RA, possibly due to increased wavefront collisions. PS were found throughout all areas of each respective chamber, in a seemingly random distribution.

Despite substantial cellular, animal and human studies in PsAF the underlying mechanism responsible for initiation and perpetuating the condition remains

non-defined and controversial. The importance of triggers originating from the pulmonary veins are well recognised, and underlie the basis for pulmonary vein isolation in PAF (Haissaguerre, 1998). However, in PsAF the atria myocardium is thought to play an important role and there are 2 main contrary hypotheses to explain the underlying mechanism; namely the multiple wavelet hypothesis (Moe, 1964) and the currently favoured localized source hypothesis in which organized re-entrant circuits (rotors) or focal impulses disorganize into AF (Narayan, 2012b).

Previous studies have yielded conflicting results as to the presence of rotors. Traditionally the favoured mechanism underlying PsAF was the multiple wavelet hypothesis, in which AF was perpetuated by several randomly wandering wavefronts that vary in position, number and size (Moe, 1964). This theory has been substantiated by a number of mapping studies from animals and humans and recent body surface mapping studies (Allessie, 1976; Cox, 1991; Cuculich, 2010).

However, over recent years the alternative hypothesis of localised sources, and in particular rapidly activating atrial re-entrant circuits (rotors) as the mechanism for maintaining AF has been strongly advocated (Vaquero, 2008). A substantial body of evidence is emerging substantiating this hypothesis using a variety of methodological techniques (Ganesan, 2013b; Skanes, 1998; Kalifa, 2006; Haissaguerre, 2014). In the CONFIRM study rotors and localised focal sources were present in almost all of their AF patients (98%, mean 2.3 +/- 1.1 concurrent rotors and focal sources) and that targeting these local areas with ablation can

terminate the arrhythmia and lead to improved clinical outcomes (Narayan, 2012b; Narayan, 2014). Yet despite such strong results, a number of other research groups have failed to collaborate the prevalence of rotors (Lee, 2014; Lin, 2013) or their stable nature (Cuculich, 2010). In a recent study by Benharash et al, 24 cases initially reported as having rotors from the initial CONFIRM study were reanalysed using alternative techniques and failed to show rotors (Benharash, 2015).

A rotor in mathematical terms is generally defined as a phase singularity in which the phase activation pattern cycles twice around (Umapathy, 2010) whilst in the clinical studies, most rotors are reported as stable over at least 30 minutes (thereby comprising thousands of rotations) (Skanes, 1998). During this study we used phase analysis algorithms to detect rotors, as unlike organised tachycardias it is not possible to temporally map activation from their original electrograms. Phase tracks progression of an area of myocardium through the action potential and is a thoroughly validated technique (Gray, 1998).

There are a number of similarities between our mapping and signal analysis method and the technique performed in the CONFIRM study, in that both studies used Constellation™ basket catheters (Narayan, 2014), in order to achieve high density mapping and one would predict the same degree of inter electrode signal interpolation. There are a number of technical considerations and difficulties involved with mapping AF in this way, which has previously been reported by our group (Laughner, 2016), and would have been similar across

studies. Both studies use phase-based algorithms but with important differences. There are inherent mathematical difficulties in performing the required Hilbert transformation for phase analysis from unipolar atrial fibrillatory electrograms because the intermittent nature of the electrogram trace does not fit the required sine wave. In our study this problem of the electrogram morphology was resolved by the novel method of recomposing the atrial electrogram signal into a sum of sine waves, as recently described by Kuklik et al (Kuklik, 2015), whereas the method employed by Narayan et al involves substituting individual fibrillatory waves for unipolar action potentials using a previously validated library, which have a morphology which is more suited to the Hilbert transformation. In addition, in further work completed after my period of research we were able to reproduce our results using a different previously published and validated method of AF phase analysis supporting the robustness of our methodology (Child, 2018).

Our observations on the electrophysiology of atrial fibrillation are in contrast to previous observations from our research group on ventricular fibrillation in humans (Nash, 2016; Bradley, 2011). In these studies VF was maintained by large coherent wavefronts interrupted by disorganised wavelet patterns. The conclusion from these studies was that human VF was driven by both mother rotor and multiple wavelet mechanisms. In the present study on atrial fibrillation evidence for rotor activity was minimal or absent. The explanation for these differences is at present unclear. Similar analytical methods were used in both studies. One possibility might be that the thicker walled ventricular myocardium

is more favourable to the formation and stability of rotors than the thinner walled atrium.

Limitations in our study of Persistent AF

Limitations of this study include a relatively small number of patients with PSAF, however this should still represent a large enough cohort to have demonstrated rotors given their previously reported near universal incidence (Narayan, 2012b). There are significant methodological differences between our method of data processing and phase transformation compared to the previously reported mechanism. However, our process used a mathematically robust method, previously validated in VF, and has been demonstrated to show short-lived rotational atrial activity (Figure 38). The electrogram sampling method is very similar to previous studies, using the same catheters and electroanatomic mapping systems (Narayan, 2012b). However, in the new Topera system (Abbot Electrophysiology, CA, USA) there are some minor changes in electrode spacing. Certainly equatorial bunching resulting in a range of inter-electrode spacing was observed in our cohort as previously described (Laughner, 2016), and is a universal problem with all studies. We have not attempted to assess how the process of ablation will affect the electrical wavefronts in this study.

Chapter 8: Conclusions

The movie and picture stress studies employed mild to moderate mental stress and resulted in a consistent but small decreases in activation recovery interval throughout the studies. Similar results were seen in patients with severely impaired cardiac function and those with good function, and between ischemic and non-ischemic disease. In addition to the small global changes seen in activation recovery interval during stress cyclical oscillations at both respiratory and sympathetic activity (0.1 Hz) frequency were frequently observed. These results provide further insight into the complex physiological balance that maintains optimal cardiac refractoriness in health, and potentially the mechanism for arrhythmia generation in disease.

The activation recovery interval algorithm was successfully validated both by computational modelling and 2 different animal models, prior to its successful implementation in a clinical case in which it successfully predicted the source of re-entry in ventricular tachycardia. Further work is required in order to bring this mathematical method into routine clinical use.

No long-lasting rotors or localized drivers were found in this cohort of PSAF. Whilst relatively short-lived PS were identified, given their short lifespan these are likely secondary to passive activation, and not a mechanism for maintaining PSAF. We conclude therefore that the predominant mechanism in PSAF is the multiple wavelet hypotheses.

Acknowledgements

I would like to express my sincere thanks to my supervisor Professor Jaswinder Gill who I have had the pleasure of working beside and continually learning from. This thesis is testament to his continued fascination to better understand the origins of arrhythmia.

I would also like to thank my second supervisor, Professor Reza Razavi, who has supported my studies and helped guide its progress.

I am extremely grateful to Professor Peter Taggart, Dr Ben Hanson, Dr Martin Bishop and Professor Richard Clayton, all of whom I have had the pleasure of collaborating with and have helped to direct this research by adding both additional skills and enthusiasm.

There are countless electrophysiology consultants, clinical and biomedical research fellows who I have had the pleasure of working alongside and sharing ideas.

I also thank the technical and nursing staff of the electrophysiology laboratory, for their support and time during the clinical studies

Lastly, I would like to thank the patients who volunteered for my studies, without whom this research would not have been possible.

Funding Sources

I was supported throughout my research by an educational grant from St Jude Medical. I also acknowledge financial support from the Department of Health via the National Institute for Health Research (NIHR) Comprehensive Biomedical Research Centre award to Guy's and St Thomas' NHS Foundation Trust in partnership with King's College London and King's College Hospital NHS Foundation Trust. Data collection for the persistent AF project was part of an industry sponsored and funded study by Boston Scientific.

Appendix – Manual comparison of the automated ARI calculation algorithm with visual inspection and manual ARI measurement

Background

Both psychological stress studies were performed in patients during right ventricular pacing, thus removing variable diastolic intervals prior to each beat, which is known to significantly affect ARI. In addition, pacing from the right ventricle has previously been shown to result in a clearly defined T wave in the unipolar electrogram, which allows accurate measurement of ARI (Hanson, 2009).

Patients in the invasive study were paced at 10-20 beats per minute above their resting heart rate in order to minimise the number of breakthrough intrinsic beats. The ARIs were calculated automatically using a custom algorithm, previously developed and validated by members of our team who specialize in computer engineering (Western, 2010). The method has been used in a variety of clinical studies and has previously been shown to be robust. The algorithm contains a number of automated checks to remove noise, indistinct T waves, and a variety of automated error checking steps, including discounting electrograms where the start of activation occurs earlier than expected to remove ectopic beats and intrinsic breakthrough. This is an automated process without the ability to manually check each complex to ensure that abnormal electrograms (ectopics, artefact etc) were not being incorrectly analysed and included in the ARI data.

Manual calculation of ARI and blood pressure

ARI could be calculated from the original data simply using the Wyatt method (chapter 1.2.6) simply by Microsoft excel (the slope of Vmin measured in a semi-automated fashion using the formula X-(X-1), Tup was calculated using the same technique but given the slower rate of increase the change in slope was averaged over 5 beats. Systolic and diastolic blood pressure was also measured manually using maximum and minimum values for each beat. Manual measurements of ARI and blood pressure proved very time consuming. As shown Figure 1 blood pressure measurements using both techniques were virtually identical, and although there was some variation between ARI values there was generally good concordance. The ARI activation times using this method closely matched the automated Vmin measurement and variation was due to the more precise way that the maximal upslope gradient was calculated for Tup.

Figure 1: Example comparison of ARI measured using both the entirely automated algorithm and the manual method

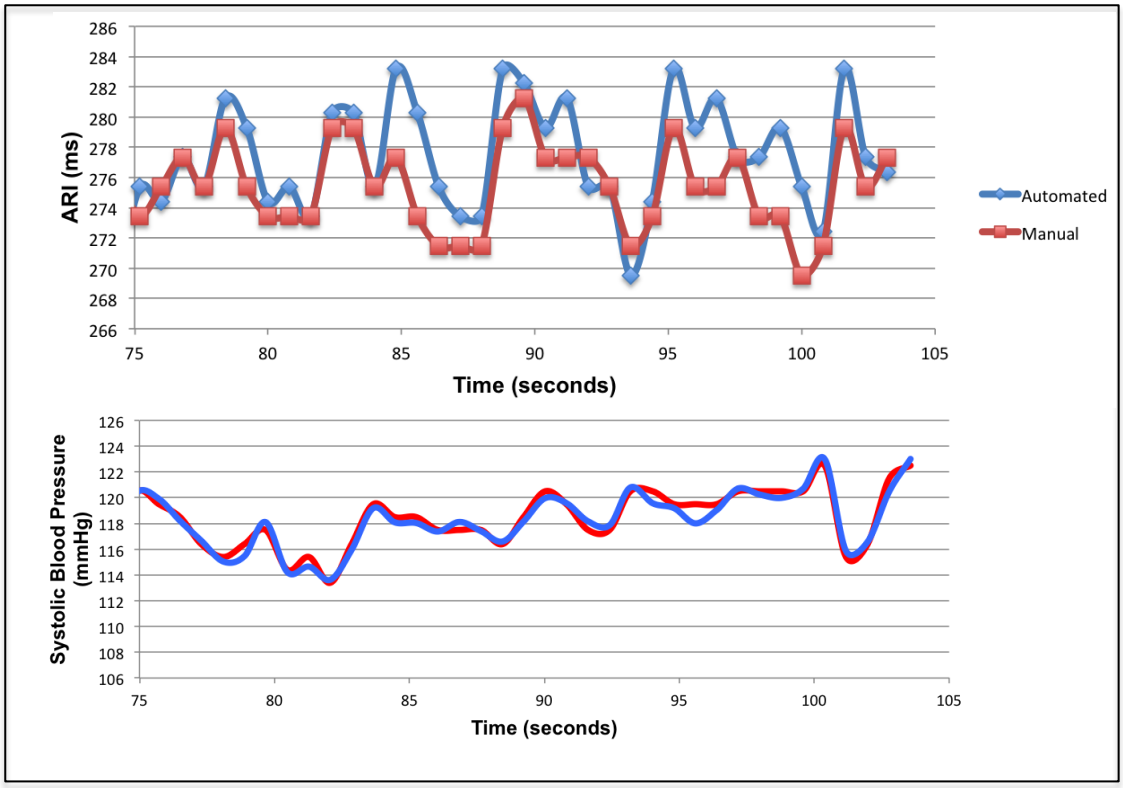

Comparison of automated ARI and SBP measurements with manually calculated measurements. Top – ARI, Bottom – SBP.

Performance of the automated algorithm in identifying and rejecting abnormal beats

By comparing the automated data to manual inspection of the electrograms the automated algorithm correctly identified all ectopic and intrinsic breakthrough beats and rejected them from the analysis (n=137 abnormal beats / 8484 total beats). However, unipolar electrograms with activation occurring when expected but with different electrogram morphologies (and hence ARIs that were different to the rest of the sequence) occurred in 82 out of 8484 beats and

the algorithm did not reject these automatically. These were presumably caused by fusion of paced and intrinsic rhythm and were subsequently manually removed and replaced with data by linear interpolation.

Conclusion

The automated Matlab software was able to calculate ARI accurately and appropriately identified and rejected all the ectopic and breakthrough beats. It was not successful however in removing other abnormal beats occurring at the expected activation time, presumably fusion beats, which required manual extraction.

References

Abdelghani SA, Rosenthal TM et al. Surface Electrocardiogram. Predictors of Sudden Cardiac Arrest. Ochsner Journal 2016;16(3): 280-289.

Al-Khatib SM, Arshad A et al. Risk Stratification for Arrhythmic Events in Patients With Asymptomatic Pre-Excitation: A Systematic Review for the 2015 ACC/AHA/HRS Guideline for the Management of Adult Patients With Supraventricular Tachycardia: A Report of the American College of Cardiology/American Heart Association Task Force on Clinical Practice Guidelines and the Heart Rhythm Society. Journal of the American College of Cardiology 2016;67(13): 1624-1638.

Al-Khatib SM, Sanders GD et al. Preventing tomorrow's sudden cardiac death today: part I: Current data on risk stratification for sudden cardiac death. American Heart Journal 2007;153(6): 941-950.

Aldhafeeri FM, Mackenzie I et al. Regional brain responses to pleasant and unpleasant IAPS pictures: different networks. Neuroscience Letters 2012;512(2): 94-98.

Aliot EM, Stevenson WG et al. EHRA/HRS Expert Consensus on Catheter Ablation of Ventricular Arrhythmias. Europace 2009;11(6): 771-817.

Allessie MA, Bonke FI et al. Circus movement in rabbit atrial muscle as a mechanism of tachycardia. II. The role of nonuniform recovery of excitability in the occurrence of unidirectional block, as studied with multiple microelectrodes. Circulation Research 1976;39:168-77.

Aoki T, Fukumoto Y et al. The Great East Japan Earthquake Disaster and cardiovascular diseases. European Heart Journal 2012;33(22): 2796-2803.

Aue T, Flykt A et al. First evidence for differential and sequential efferent effects of stimulus relevance and goal conduciveness appraisal. Biological Psychology 2007;74(3):347-357.

Azevedo ER, Newton GE et al. Cardiac and systemic sympathetic activity in response to clonidine in human heart failure. Journal of the American College of Cardiology 1999;33(1): 186-191.

Bai R, Di Biase L et al. (2011). Ablation of ventricular arrhythmias in arrhythmogenic right ventricular dysplasia/cardiomyopathy: arrhythmia-free survival after endo-epicardial substrate based mapping and ablation. Circulation Arrhythmia and Electrophysiology 2011;4(4): 478-485.

Bali A, Jaggi AS. Clinical experimental stress studies: methods and assessment. Reviews in the Neurosciences 2015;26(5): 555-579.

Banna M, Indik JH. Risk stratification and prevention of sudden death in patients with heart failure. Current Treatment Options in Cardiovascular Medicine 2011;13(6): 517-527.

Barber MJ, Mueller TM et al. Transmural myocardial infarction in the dog produces sympathectomy in noninfarcted myocardium. Circulation 1983;67(4): 787-796.

Barcroft H, Starr I. Comparison of the actions of adrenaline and noradrenaline on the cardiac output in man. Clinical Science 1951;10(3): 295-303.

Benharash P, Buch E et al. Quantitative analysis of localized sources identified by focal impulse and rotor modulation mapping in atrial fibrillation. Circulation Arrhythmia and Electrophysiology 2015; 8(3): 554-561.

Benjamin EJ, Wolf PA et al. Impact of atrial fibrillation on the risk of death: the Framingham Heart Study. Circulation 1998;98(10): 946-952.

Bernardi L, Wdowczyk-Szulc J et al. Effects of controlled breathing, mental activity and mental stress with or without verbalization on heart rate variability. Journal of the American College of Cardiology 2000;35:1462-1469.

Bernat E, Patrick C et al. Effects of picture content and intensity on affective physiological response. Psychophysiology 2006;43(1):93-103.

Bigger JT. Prophylactic use of implanted cardiac defibrillators in patients at high risk for ventricular arrhythmias after coronary-artery bypass graft surgery. Coronary Artery Bypass Graft (CABG) Patch Trial Investigators. New England Journal of Medicine 1997;337(22): 1569-1575.

Bourke JP, Richards DA et al. Routine programmed electrical stimulation in survivors of acute myocardial infarction for prediction of spontaneous ventricular tachyarrhythmias during follow-up: results, optimal stimulation protocol and cost-effective screening. Journal of the American College of Cardiology 11991;8(3): 780-788.

Bradley CP, Clayton RH et al. Human ventricular fibrillation during global ischemia and reperfusion: paradoxical changes in activation rate and wavefront complexity. Circulation Arrhythmia and electrophysiology 2011;4:684-91.

Brunner-La Rocca H, Esler MD et al. Effect of cardiac sympathetic nervous activity on mode of death in congestive heart failure. European Heart Journal 2001;22(13): 1136-1143.

Buch E, Share M et al. Long-term clinical outcomes of focal impulse and rotor modulation for treatment of atrial fibrillation: A multicenter experience. Heart Rhythm 2016;13(3): 636-641.

Caldwell JH, Link JM et al. Evidence for pre- to postsynaptic mismatch of the cardiac sympathetic nervous system in ischemic congestive heart failure. Journal of Nuclear Medicine 2008;49(2): 234-241.

Callister R, Suwarno NO et al. Sympathetic activity is influenced by task difficulty and stress perception during mental challenge in humans. Journal of Physiology 1992;**454**: p. 373-87.

Cao JM, Fishbein MC et al. Relationship between regional cardiac hyperinnervation and ventricular arrhythmia. Circulation 2000;101(16): 1960-1969.

Carroll D, Smith GD et al. Pressor reactions to psychological stress and prediction of future blood pressure: data from the Whitehall II Study. British Medical Journal 1995;310(6982): 771-776.

Cevese A, Gulli G et al. Baroreflex and oscillation of heart period at 0.1 Hz studied by alpha-blockade and cross-spectral analysis in healthy humans. Journal of Physiology 2001;531:235-244

Chen PS, Moser KM et al. Epicardial activation and repolarization patterns in patients with right ventricular hypertrophy. Circulation 1991;83(1): 104-118.

Chen PS, Chen LS et al. Sympathetic nerve sprouting, electrical remodeling and the mechanisms of sudden cardiac death. Cardiovascular Research 2001;50(2): 409-416.

Chen PS, Chen LS et al. Role of the autonomic nervous system in atrial fibrillation: pathophysiology and therapy. Circulation Research 2014;114(9):1500-1515.

Chen Z, Sohal M et al. Myocardial tissue characterization by cardiac magnetic resonance imaging using T1 mapping predicts ventricular arrhythmia in ischemic and non-ischemic cardiomyopathy patients with implantable cardioverter-defibrillators. Heart Rhythm 2015;12(4): 792-801.

Child N, Hanson B et al. Effect of mental challenge induced by movie clips on action potential duration in normal human subjects independent of heart rate. Circulation Arrhythmia and Electrophysiology 2014:7(3):518-523.

Child N, Bishop MJ et al. An activation time metric to predict localized regions of high susceptibility to re-entry. Heart Rhythm 2015 12;7:1644-53.

Child N, Clayton RH et al. Unravelling the Underlying Arrhythmia Mechanism in Persistent Atrial Fibrillation: Results from the STARLIGHT Study. Circulation Arrhythmia and Electrophysiology 2018 Jun;11(6). PMID: 29858382

Christie IC, Friedman BH.Autonomic specificity of discrete emotion and dimensions of affective space: a multivariate approach. International Journal of Psychophysiology 2004;51(2): 143-153.

Chugh SS, Jui J et al. Current burden of sudden cardiac death: multiple source surveillance versus retrospective death certificate-based review in a large U.S. community. Journal of the American College of Cardiology 2004;44(6): 1268-1275.

Chugh SS, Reinier K et al. Epidemiology of sudden cardiac death: clinical and research implications. Progress in Cardiovascular Diseases 2008;51(3): 213-228.

Chugh SS, Havmoeller R et al. Worldwide epidemiology of atrial fibrillation: a Global Burden of Disease 2010 Study. Circulation 2014;129(8): 837-847.

Clayton RH, Nash MP. Analysis of cardiac fibrillation using phase mapping. Cardiac Electrophysiology Clinics 2015;7(1):49-58

Codispoti M, De Cesarei A. Arousal and attention: picture size and emotional reactions. Psychophysiology 2007;44(5):680-686

Colilla S, Crow A et al. Estimates of current and future incidence and prevalence of atrial fibrillation in the U.S. adult population. American Journal of Cardiology 2013;112(8): 1142-1147.

Comtois P, Kneller J. Od circles and spirals: bridging the gap between the leading circle and spiral wave concepts of cardiac re-entry. Europace 2005;7:10-20.

Coronel R, Wilms-Schopman FJ. Dispersion of repolarization and arrhythmogenesis. Heart Rhythm 2009;8;6(4): 537-543.

Coronel R, Wilms-Schopman FJ et al. Anti- or profibrillatory effects of Na(+) channel blockade depend on the site of application relative to gradients in repolarization. Frontiers in Physiology 2010;1: 10.

Cox JL, Canavan TE et al. The surgical treatment of atrial fibrillation. II. Intraoperative electrophysiologic mapping and description of the electrophysiologic basis of atrial flutter and atrial fibrillation. Journal of Thoracic Cardiovascular Surgery 1991;101:406-26.

Cuculich PS, Wang Y et al. Noninvasive characterization of epicardial activation in humans with diverse atrial fibrillation patterns. Circulation 2010;122(14): 1364-1372.

Dampney RA. Central neural control of the cardiovascular system: current perspectives. Advances in Physiology Education 2016;40(3): 283-296.

Daubert JP, Zareba W et al. Predictive value of ventricular arrhythmia inducibility for subsequent ventricular tachycardia or ventricular fibrillation in Multicenter Automatic Defibrillator Implantation Trial (MADIT) II patients. Journal of the American College of Cardiology 2006;47(1): 98-107.

De Bakker J, Coronel R et al. Ventricular tachycardia in the infarcted Langendorff-perfused human heart: role of the arrangement of surviving cardiac fibers. Journal of the American College of Cardiology 1990;15:1594-1607

De Groot NM, Houben RP et al. Electropathological substrate of longstanding persistent atrial fibrillation in patients with structural heart disease: epicardial breakthrough. Circulation 2010;122(17): 1674-1682.

De Ponti R, Marazzi M et al. Invasive electrophysiological evaluation and ablation in patients with asymptomatic ventricular pre-excitation persistent at exercise stress test. Europace 2015;17(6): 946-952.

Eckberg DL. Physiological basis for human autonomic rhythms. Annals of Medicine 2000;32(5): 341-349.

Ekman P, Levenson RW et al. Autonomic nervous system activity distinguishes among emotions. Science 1983;221(4616): 1208-1210.

Ezekowitz JA, Rowe BH et al. Systematic review: implantable cardioverter defibrillators for adults with left ventricular systolic dysfunction. Annals of Internal Medicine 147(4): 251-262.

Fallavollita JA, and Canty JM. Dysinnervated but viable myocardium in ischemic heart disease. Journal of Nuclear Cardiology 2010;17(6): 1107-1115.

Fallavollita JA, Heavey BM et al. Regional Myocardial Sympathetic Denervation Predicts the Risk of Sudden Cardiac Arrest in Ischemic Cardiomyopathy. Journal of the American College of Cardiology. 2014;63(2):141-149

Ferrie JE, Kivimaki M et al. Job insecurity and incident coronary heart disease: the Whitehall II prospective cohort study. Atherosclerosis 2013;227(1): 178-181.

Finlay M, Lambiase PD et al. Effect of mental stress on dynamic electrophysiological properties of the endocardium and epicardium in humans. Heart Rhythm 2016;13(1):175-182.

Ganesan AN (a), Shipp NJ et al. Long-term outcomes of catheter ablation of atrial fibrillation: a systematic review and meta-analysis. Journal of the American Heart Association 2013;2(2): e004549.

Ganesan AN (b), Kuklik P et al. Bipolar electrogram shannon entropy at sites of rotational activation: implications for ablation of atrial fibrillation. Circulation Arrhythmia and Electrophysiology 2013;6(1): 48-57.

Garcia-Calvo R, Chorro FJ et al. The effects of selective stellate ganglion manipulation on ventricular refractoriness and excitability. Pacing and Clinical Electrophysiology 1992;15:1492-1503.

Garfinkel A, Kim YH et al. Preventing ventricular fibrillation by flattening cardiac restitution. Proceedings of the National Academy of Science 2000;97:6061-6066.

Gasperin D, Netuveli G et al. Effect of psychological stress on blood pressure increase: a meta-analysis of cohort studies. Cadernos de Saude Publica 2009;25(4): 715-726.

Gomes JA, Cain MA et al. Prediction of long-term outcomes by signal-averaged electrocardiography in patients with unsustained ventricular tachycardia, coronary artery disease, and left ventricular dysfunction. Circulation 2001;104(4): 436-441.

Gomez P, Zimmermann P et al. Respiratory responses associated with affective processing of film stimuli. Biological Psychology 2005;68(3):223-35.

Gray RA, Pertsov AM et al. Spatial and temporal organization during cardiac fibrillation. Nature 1998;392(6671): 75-78.

Greenstein JL, Winslow RL. Integrative systems models of cardiac excitation-contraction coupling. Circulation Research 2011;108(1): 70-84.

Haissaguerre M, Marcus FI et al. Radiofrequency catheter ablation in unusual mechanisms of atrial fibrillation: report of three cases. Journal of Cardiovascular Electrophysiology 1994;5(9): 743-751.

Haissaguerre M, Jais P et al. Spontaneous initiation of atrial fibrillation by ectopic beats originating in the pulmonary veins. New England Journal of Medicine 1998:339(10): 659-666.

Haissaguerre M, Hocini MM et al. Driver domains in persistent atrial fibrillation. Circulation 2014;130(7): 530-538.

Hammill SC, Tchou PJ et al. Establishment of signal-averaged electrocardiographic criteria with Frank XYZ leads and spectral filter used alone and in combination with ejection fraction to predict inducible ventricular tachycardia in coronary artery disease. American Journal of Cardiology 1992;70(3): 316-320.

Hanson B, Sutton P et al. Interaction of activation-repolarization coupling and restitution properties in humans.” Circulation Arrhythmia and Electrophysiology 2009;2(2): 162-170.

Hanson B, Gill JS et al. Cyclical modulation of human ventricular repolarization by respiration. Frontiers in Physiology 2012;3: 379.

Hanson B, Child N et al. Oscillatory behavior of ventricular action potential duration in heart failure patients at respiratory rate and low frequency. Frontiers Physiology 2014 5:414.

Hartikainen J, Kuikka J et al. Sympathetic reinnervation after acute myocardial infarction. American Journal of Cardiology 1996;77(1): 5-9.

Haws CW, Burgess MJ. Effects of bilateral and unilateral stellate stimulation on canine ventricular refractory periods at sites overlapping innervation. Circulation Research 1978;42:195-198.

Haws CW, Lux RL. Correlation between in vivo transmembrane action potential durations and activation-recovery intervals from electrograms. Effects of interventions that alter repolarization time. Circulation 1990;81(1): 281-288.

Heijman J, Volders PG et al. Local control of beta-adrenergic stimulation: Effects on ventricular myocyte electrophysiology and ca(2+)-transient. Journal of Molecular and Cellular Cardiology 2011;50:863-871

Hill Y, Child N et al. Investigating a novel activation-repolarisation time metric to predict localised vulnerability to reentry using computational modelling. PLOS One 2016;11(3): e0149342

Homma I, Masaoka Y. Breathing rhythms and emotions. Experimental Physiology 2008;93(9):1011-21

Inoue H, Zipes DP. Results of sympathetic denervation in the canine heart: supersensitivity that may be arrhythmogenic. Circulation 1987;75(4): 877-887.

Jacobson AF, Senior R et al. Myocardial iodine-123 meta-iodobenzylguanidine imaging and cardiac events in heart failure. Results of the prospective ADMIRE-HF (AdreView Myocardial Imaging for Risk Evaluation in Heart Failure) study. Journal of the American College of Cardiology 2010;55(20): 2212-2221.

January CT, Wann LS et al. 2014 AHA/ACC/HRS guideline for the management of patients with atrial fibrillation: a report of the American College of Cardiology/American Heart Association Task Force on Practice Guidelines and the Heart Rhythm Society. Journal of the American College of Cardiology 2014;64(21): e1-76.

Jensen B, Wang T et al. Evolution and development of the building plan of the vertebrate heart. Biochimica et Biophysica Acta 2013;1833(4): 783-794.

John AS, Mongillo M et al. Pre- and post-synaptic sympathetic function in human hibernating myocardium. European Journal of Nuclear Medicine and Molecular Imaging 2007;34(12): 1973-1980.

Kalifa J, Tanaka K et al. Mechanisms of wave fractionation at boundaries of high-frequency excitation in the posterior left atrium of the isolated sheep heart during atrial fibrillation. Circulation 2006;113(5): 626-633.

Kammerling JJ, Green FJ et al. Denervation supersensitivity of refractoriness in noninfarcted areas apical to transmural myocardial infarction. Circulation 1987;76(2): 383-393.

Karamitsos TD, Francis JM et al. The role of cardiovascular magnetic resonance imaging in heart failure. Journal of the American College of Cardiology 2009;54(15): 1407-1424.

Katona PG, Poitras JW et al. Cardiac vagal efferent activity and heart period in the carotid sinus reflex. American Journal of Physiology 1970;218(4): 1030-1037.

Kaye DM, Lefkovits J et al. Adverse consequences of high sympathetic nervous activity in the failing human heart." Journal of the American College of Cardiology 1995;26(5): 1257-1263.

Khairy P, Van Hare GF et al. PACES/HRS Expert Consensus Statement on the Recognition and Management of Arrhythmias in Adult Congenital Heart Disease: developed in partnership between the Pediatric and Congenital Electrophysiology Society (PACES) and the Heart Rhythm Society (HRS). Endorsed by the governing bodies of PACES, HRS, the American College of Cardiology (ACC), the American Heart Association (AHA), the European Heart Rhythm Association (EHRA), the Canadian Heart Rhythm Society (CHRS), and the International Society for Adult Congenital Heart Disease (ISACHD)." Heart Rhythm 2014;11(10): e102-165.

Klem I, Weinsaft JW et al. Assessment of myocardial scarring improves risk stratification in patients evaluated for cardiac defibrillator implantation. Journal of the American College of Cardiology 2012;60(5): 408-420.

Kober L, Thune JJ et al. Defibrillator Implantation in Patients with Nonischemic Systolic Heart Failure. New England Journal of Medicine 2016;375(13): 1221-1230.

Konings KT, Kirchhof CJ et al. High-density mapping of electrically induced atrial fibrillation in humans. Circulation 1994;89(4): 1665-1680.

Kop WJ, Krantz DS et al. Effects of mental stress on coronary epicardial vasomotion and flow velocity in coronary artery disease: relationship with hemodynamic stress responses. Journal of the American College of Cardiology 2001;37(5): 1359-1366.

Kop W, Krantz DS et al. Effects of acute mental stress and exercise on T-wave alternans in patients with implantable cardioverter defibrillators and controls. Circulation 2004;109(15): 1864-1869.

Kossaify A, Refaat M. Programmed ventricular stimulation—indications and limitations: a comprehensive update and review. Hellenic Journal of Cardiology 2013;54(1): 39-46.

Koumi S, Backer CL et al. Beta-Adrenergic modulation of the inwardly rectifying potassium channel in isolated human ventricular myocytes. Alteration in channel response to beta-adrenergic stimulation in failing human hearts. Journal of Clinical Investigation 1995;96(6): 2870-2881.

Kreibig SD. Autonomic nervous system activity in emotion: a review. Biological Psychology 2010;84(3): 394-421.

Kruse I, Arnman K et al. A comparison of the acute and long-term hemodynamic effects of ventricular inhibited and atrial synchronous ventricular inhibited pacing. Circulation 1982;65(5): 846-855.

Kuklik P, Zeemering S et al. Reconstruction of instantaneous phase of unipolar atrial contact electrogram using a concept of sinusoidal recomposition and Hilbert transform. IEEE Transactions of Biomedical Engineering 2015;62(1):296-301

Kumana CR. Are blood pressure surges associated with sympathetic stimulation aggravated by beta-adrenoceptor antagonist treatment? Postgraduate Medical Journal 1986;62(730): 731-735.

Kuruvilla S, Adenaw N et al. Late gadolinium enhancement on cardiac magnetic resonance predicts adverse cardiovascular outcomes in nonischemic cardiomyopathy: a systematic review and meta-analysis. Circulation Cardiovascular Imaging 2014;7(2): 250-258.

Lackner H, Papousek K et al. Phase synchronization of haemodynamic variables and respiration during mental challenge. International Journal of Psychophysiology 2011;79(3):401-409.

Lampert R, Joska T et al. Emotional and physical precipitants of ventricular arrhythmia. Circulation 2002;106(14): 1800-1805.

Lampert R, Shusterman V et al. Anger-induced T-wave alternans predicts future ventricular arrhythmias in patients with implantable cardioverter-defibrillators. Journal of the American College of Cardiology 2009;53(9): 774-778.

Lampert R. Behavioral influences on cardiac arrhythmias. Trends in Cardiovascular Medicine 2016;26(1): 68-77.

Larochelle P, Tobe SW et al. Beta-Blockers in hypertension: studies and meta-analyses over the years. Canadian Journal of Cardiology 2014;30(5 Suppl): S16-22.

Laughner J, Shome S et al. Practical Considerations of Mapping Persistent Atrial Fibrillation with Whole-Chamber Basket Catheters. Journal of the American College of Cardiology: Clinical Electrophysiology 2016;2;1:55-65.

Law MP, Schafers K et al. Molecular imaging of cardiac sympathetic innervation by 11C-mHED and PET: from man to mouse? Journal of Nuclear Medicine 2010;51(8): 1269-1276.

Lee G, Sanders P et al. Catheter ablation of atrial arrhythmias: state of the art. Lancet 2012;380(9852): 1509-1519.

Lee G, Kumar S et al. Epicardial wave mapping in human long-lasting persistent atrial fibrillation: transient rotational circuits, complex wavefronts, and disorganized activity. European Heart Journal 2014;35(2): 86-97.

Levenson RW, Ekman P et al. Voluntary facial action generates emotion-specific autonomic nervous system activity. Psychophysiology 1990;27(4): 363-384.

Lin YJ, Lo MT et al. Prevalence, characteristics, mapping, and catheter ablation of potential rotors in nonparoxysmal atrial fibrillation. Circulation Arrhythmia and Electrophysiology 2013;6(5): 851-858.

Liu J, Laksman Z et al. The electrophysiological development of cardiomyocytes. Advanced Drug Delivery Reviews 2016;96: 253-273.

Luisi AJ, Fallavollita JA et al. Spatial inhomogeneity of sympathetic nerve function in hibernating myocardium. Circulation 2002;06(7): 779-781.

Luisi AJ, Suzuki G et al. Regional 11C-hydroxyephedrine retention in hibernating myocardium: chronic inhomogeneity of sympathetic innervation in the absence of infarction. Journal of Nuclear Medicine 2005;46(8): 1368-1374.

Makikallio TH, Barthel P et al. Prediction of sudden cardiac death after acute myocardial infarction: role of Holter monitoring in the modern treatment era. European Heart Journal 2005;26(8): 762-769.

Martinez C, Katholing A et al. Increasing incidence of non-valvular atrial fibrillation in the UK from 2001 to 2013. Heart 2015;101(21): 1748-1754.

Martins JB, Zipes DP. Effects of sympathetic and vagal nerves on recovery properties of the endocardium and epicardium of the canine left ventricle. Circulation Research 1980;46:100-110.

Matsunari I, Aoki H et al. Iodine-123 metaiodobenzylguanidine imaging and carbon-11 hydroxyephedrine positron emission tomography compared in patients with left ventricular dysfunction. Circulation Cardiovascular Imaging 2010;3(5): 595-603.

Meyer C, Rana OR et al. Augmentation of left ventricular contractility by cardiac sympathetic neural stimulation. Circulation 2010;121:1286-1294.

Middlekauff HR, Stevenson WG et al. Syncope in advanced heart failure: high risk of sudden death regardless of origin of syncope. Journal of the American College of Cardiology 1993;21(1): 110-116.

Millar CK, Kralios FA et al. Correlation between refractory periods and activation-recovery intervals from electrograms: effects of rate and adrenergic interventions. Circulation 1985;72(6): 1372-1379.

Mines GR. On dynamic equilibrium in the heart. Journal of Physiology 1913;46:349-383.

Mitchell MR, Powell T et al. Electrical properties and response to noradrenaline of individual heart cells isolated from human ventricular tissue. Cardiovascular Research 1986;20(12): 869-876.

Miyano H, Nakayama Y et al. Dynamic sympathetic regulation of left ventricular contractility studied in the isolated canine heart. American Journal of Physiology 1998;275(2 Pt 2): H400-408.

Moe GK, Rheinboldt WC et al. A Computer Model of Atrial Fibrillation. American Heart Journal 1964;67: 200-220.

Morimont P, Lambermont B et al. Arterial dP/dt max accurately reflects left ventricular contractility during shock when adequate vascular filling is achieved. BMC Cardiovascular Disorders 2012;12: 13.

Morrison SC, Kumana CR et al. Selective and nonselective beta-adrenoceptor blockade in hypertension: responses to changes in posture, cold and exercise. Circulation 1982;65(6): 1171-1177.

Moss AJ, Hall WJ et al. Improved survival with an implanted defibrillator in patients with coronary disease at high risk for ventricular arrhythmia. Multicenter Automatic Defibrillator Implantation Trial Investigators. New England Journal of Medicine 1996;335(26): 1933-1940.

Moss AJ (a), Zareba W et al. Prophylactic implantation of a defibrillator in patients with myocardial infarction and reduced ejection fraction. New England Journal of Medicine 2002;346(12): 877-883.

Moss AJ (b), Daubert J et al. MADIT-II: clinical implications. Cardiac Electrophysiology Review 2002;6(4): 463-465.

Mostofsky E, Maclure M et al. Risk of acute myocardial infarction after the death of a significant person in one's life: the Determinants of Myocardial Infarction Onset Study. Circulation 2012;125(3): 491-496.

Myers RW, Pearlman AS et al. Beneficial effects of vagal stimulation and bradycardia during experimental acute myocardial ischemia. Circulation 1974;49(5): 943-947.

Nademanee K, McKenzie J et al. A new approach for catheter ablation of atrial fibrillation: mapping of the electrophysiologic substrate. Journal of the American College of Cardiology 2004;43(11): 2044-2053.

Narayan SM (a), Krummen DE et al. Computational mapping identifies localized mechanisms for ablation of atrial fibrillation. PLoS One 2012;7(9): e46034.

Narayan SM (b), Krummen DE et al. Treatment of atrial fibrillation by the ablation of localized sources: CONFIRM (Conventional Ablation for Atrial Fibrillation With or Without Focal Impulse and Rotor Modulation) trial. Journal of the American College of Cardiology 2012;60(7): 628-636.

Narayan SM, Krummen D et al. Direct or coincidental elimination of stable rotors or focal sources may explain successful atrial fibrillation ablation: on-

treatment analysis of the CONFIRM trial (Conventional ablation for AF with or without focal impulse and rotor modulation). Journal of the American College of Cardiology 2013;62(2):138-147.

Narayan SM, Baykaner T et al. Ablation of rotor and focal sources reduces late recurrence of atrial fibrillation compared with trigger ablation alone: extended follow-up of the CONFIRM trial (Conventional Ablation for Atrial Fibrillation With or Without Focal Impulse and Rotor Modulation). Journal of the American College of Cardiology 2014;63(17): 1761-1768.

Nash MP, Mourad A et al. Evidence for multiple mechanisms in human ventricular fibrillation. Circulation 2006;114(6): 536-542.

Ng GA(a), Brack KE et al. Autonomic modulation of electrical restitution, alternans and ventricular fibrillation initiation in the isolated heart. Cardiovascular Research 2007;73(4): 750-760.

Ng J, Goldberger JJ. Understanding and interpreting dominant frequency analysis of AF electrograms. Journal of Cardiovascular Electrophysiology 2007;18(6): 680-685.

Niemeijer MN, Van den Berg ME et al. Declining incidence of sudden cardiac death from 1990-2010 in a general middle-aged and elderly population: The Rotterdam Study. Heart Rhythm 2015;12(1): 123-129.

Niizeki K, Saitoh T. Incoherent oscillations of respiratory sinus arrhythmia during acute mental stress in humans. American Journal of Physiology Heart and Circulatory Physiology 2012;302(1):H359-67.

Nogami A, Aonuma K et al. Usefulness of early versus late programmed ventricular stimulation in acute myocardial infarction. American Journal of Cardiology 1991;68(1): 13-20.

Nowak B, Voigtlander T et al. Cardiac output in single-lead VDD pacing versus rate-matched VVIR pacing. American Journal of Cardiology 1995;75(14):904-907.

Obeyesekere M, Gula LJ et al. Risk of sudden death in Wolff-Parkinson-White syndrome: how high is the risk? Circulation 2012;125(5): 659-660.

Oral H, Chugh A et al. Radiofrequency catheter ablation of chronic atrial fibrillation guided by complex electrograms. Circulation 2007;115(20): 2606-2612.

Oral H, Chugh A et al. A randomized assessment of the incremental role of ablation of complex fractionated atrial electrograms after antral pulmonary vein isolation for long-lasting persistent atrial fibrillation. Journal of the American College of Cardiology 2009;53(9): 782-789.

Orini M, Bailon R et al. Characterization of dynamic interactions between cardiovascular signals by time-frequency coherence. IEEE Transactions on biomedical engineering 2012;59:663-673.

Orth-Gomer K, Wamala SP et al. Marital stress worsens prognosis in women with coronary heart disease: The Stockholm Female Coronary Risk Study. Journal of the American Medical Association 2000;284(23): 3008-3014.

Lang PG, Bradley MM et al. International Affective Picture System (IAPS): *Instruction manual and affective ratings* - technical report A4. The center for research in psychophysiology, University of Florida: Gainsville; 1999.

Packer M, Bristow MR et al. The effect of carvedilol on morbidity and mortality in patients with chronic heart failure. U.S. Carvedilol Heart Failure Study Group. New England Journal of Medicine 1996;334(21): 1349-1355.

Parati G, Esler M. The human sympathetic nervous system: its relevance in hypertension and heart failure. European Heart Journal 2012; 33(9): 1058-1066.

Paul M, Gerss J et al. Role of programmed ventricular stimulation in patients with Brugada syndrome: a meta-analysis of worldwide published data. European Heart Journal 2007;28(17): 2126-2133.

Pedersen CT, Kay GN et al. EHRA/HRS/APHRS expert consensus on ventricular arrhythmias. Heart Rhythm 2014;11(10): e166-196.

Philips B, Madhavan S et al. Outcomes of catheter ablation of ventricular tachycardia in arrhythmogenic right ventricular dysplasia/cardiomyopathy. Circulation Arrhythmia and Electrophysiology 2012;5(3): 499-505.

Pohjola-Sintonen S, Siltanen P et al. Usefulness of QTc interval on the discharge electrocardiogram for predicting survival after acute myocardial infarction. American Journal of Cardiology 1986;57(13): 1066-1068.

Pokorny J, Stanek V et al. Sudden cardiac death thirty years ago and at present. The role of autonomic disturbances in acute myocardial infarction revisited. Physiological Research 2011;60(5): 715-728.

Priori SG, Gasparini M et al. Risk stratification in Brugada syndrome: results of the PRELUDE (PRogrammed ELectrical stimUlation preDictive valuE) registry. Journal of the American College of Cardiology 2012;59(1): 37-45.

Priori SG, Wilde AA et al. HRS/EHRA/APHRS expert consensus statement on the diagnosis and management of patients with inherited primary arrhythmia syndromes: document endorsed by HRS, EHRA, and APHRS. Heart Rhythm 2013;10(12): 1932-1963.

Priori SG, Blomstrom-Lundqvist C et al. 2015 ESC Guidelines for the management of patients with ventricular arrhythmias and the prevention of sudden cardiac death: The Task Force for the Management of Patients with Ventricular Arrhythmias and the Prevention of Sudden Cardiac Death of the European Society of Cardiology (ESC). European Heart Journal 2015;36(41): 2793-2867.

Rainville P, Bechara A et al. Basic emotions are associated with distinct patterns of cardiorespiratory activity. International Journal of Psychophysiology 2006;61(1): 5-18.

Riccio ML, Koller ML et al. Electrical restitution and spatiotemporal organization during ventricular fibrillation. Circulation Research 1999;84:955-963.

Rosenspire KC, Haka MS et al. Synthesis and preliminary evaluation of carbon-11-meta-hydroxyephedrine: a false transmitter agent for heart neuronal imaging. Journal of Nuclear Medicine 1990;31(8): 1328-1334.

Rubart M, Zipes DP. Mechanisms of sudden cardiac death. Journal of Clinical Investigation 2005;115(9): 2305-2315.

Sanders P, Berenfeld O et al. Spectral analysis identifies sites of high-frequency activity maintaining atrial fibrillation in humans. Circulation 2005;112(6): 789-797.

Sasano T, Abraham MR et al. Abnormal sympathetic innervation of viable myocardium and the substrate of ventricular tachycardia after myocardial infarction. Journal of the American College of Cardiology 2008;51(23): 2266-2275.

Saumarez RC, Camm AJ et al. Ventricular fibrillation in hypertrophic cardiomyopathy is associated with increased fractionation of paced right ventricular electrograms. Circulation 1992;86:467-474.

Schaefer A, Nils F, et al. Assessing the Effectiveness of a large database of emotion eliciting films: A new tool for emotion researchers. Cognition Emotion 2010;24: 1153-1172.

Schwartz PJ, Billman GE et al. Autonomic mechanisms in ventricular fibrillation induced by myocardial ischemia during exercise in dogs with healed myocardial infarction. An experimental preparation for sudden cardiac death. Circulation 1984;69(4): 790-800.

Schwartz PJ. QT prolongation, sudden death, and sympathetic imbalance: The pendulum swings. Journal of Cardiovascular Electrophysiology 2001;12:1074-1077.

Segal OR, Chow AW et al. Mechnisms that initiate ventricular tachycardia in the infarcted human heart. Heart Rhythm 2010;7:57-64

Sheikh A, Patel NJ et al. Trends in Hospitalization for Atrial Fibrillation: Epidemiology, Cost, and Implications for the Future. Progress in Cardiovascular Diseases 2015;58(2): 105-116.

Skanes AC, Mandapati R et al. Spatiotemporal periodicity during atrial fibrillation in the isolated sheep heart. Circulation 1998;98(12): 1236-1248.

Skinner JE, Reed JC. Blockade of frontocortical-brain stem pathway prevents ventricular fibrillation of ischemic heart. American Journal of Physiology 1981;240(2): H156-163.

Solomon SD, Anavekar N et al. Influence of ejection fraction on cardiovascular outcomes in a broad spectrum of heart failure patients. Circulation 2005;112(24): 3738-3744.

Sprengelmeyer R, Rausch M et al. Neural structures associated with recognition of facial expressions of basic emotions. Proceedings of the Royal Society of London Biological Sciences 1998;265:1927-1931.

Stevenson WG, Facc P et al. Exploring Postinfarction Reentrant Ventricular Tachycardia with Entrainment Mapping. Journal of the American College of Cardiology 1997;29(6):1180-9

Stevenson WG, Delacretaz E. Radiofrequency catheter ablation of ventricular tachycardia. Heart 2000;84:553-559.

Taggart P, Sutton P et al. Effect of adrenergic stimulation on action potential duration restitution in humans. Circulation 2003;107(2): 285-289.

Taggart P, Sutton P et al. The effect of mental stress on the non-dipolar components of the T wave: modulation by hypnosis. Psychosomatic Medicine 2005;67(3): 376-383.

Taggart P, Boyett MR et al. Anger, emotion, and arrhythmias: from brain to heart. Frontiers in Physiology 2011;2: 67.

Terrenoire C, Clancy CE et al. Autonomic control of cardiac action potentials: Role of potassium channel kinetics in response to sympathetic stimulation. Circulation Research 2005;96:e25-34.

Toivonen L, Helenius K et al. Electrocardiographic repolarization during stress from awakening on alarm call. Journal of the American College of Cardiology 1997;30(3): 774-779.

Tsukamoto T, Morita K et al. Decreased myocardial beta-adrenergic receptor density in relation to increased sympathetic tone in patients with nonischemic cardiomyopathy. Journal of Nuclear Medicine 2007;48(11): 1777-1782.

Umapathy K, Nair K et al. Phase mapping of cardiac fibrillation. Circulation Arrhythmia and Electrophysiology 2010;3(1): 105-114.

Van der Borne, Rahnama M et al. Contrasting effects of phentolamine and nitroprusside on neural and cardiovascular variability. American Journal of Physiology Heart and Circulatory Physiology 2001;281: H559-565.

Van Duijvenboden S, Hanson B et al. Effect of autonomic blocking agents on the respiratory-related oscillations of ventricular action potential duration in humans. . American Journal of Physiology Heart and Circulatory Physiology 2015;309(12):H2108-H2117.

Van Herwaarden CL, Binkhorst RA et al. Effects of propranolol and metoprolol on haemodynamic and respiratory indices and on perceived exertion during exercise in hypertensive patients. British Heart Journal 1979;41(1): 99-105.

Van Weerd JH, Christoffels VM. The formation and function of the cardiac conduction system. Development 2016;143(2): 197-210.

Vaquero M, Calvo D et al. Cardiac fibrillation: from ion channels to rotors in the human heart. Heart Rhythm 2008;5:872-9.

Vaseghi M, Shivkumar K. The role of the autonomic nervous system in sudden cardiac death. Progress in Cardiovascular Diseases 2008;50(6): 404-419.

Vaseghi M (a), Zhou W et al. Sympathetic innervation of the anterior left ventricular wall by the right and left stellate ganglia. Heart Rhythm 2012;9(8):1303-1309

Vaseghi M (b), Lux RL et al. Sympathetic Stimulation Increases Dispersion of Repolarization in Humans with Myocardial Infarction. American Journal of Physiology Heart and Circulatory Physiology 2012;302(9):H1838-1846

Verma A, Jiang CJ et al. Approaches to catheter ablation for persistent atrial fibrillation. New England Journal of Medicine 2015;372(19): 1812-1822.

Volders PG, Stengl M et al. Probing the contribution of IKs to canine ventricular repolarization: key role for beta-adrenergic receptor stimulation. Circulation 2003;107(21): 2753-2760.

Vracko R, Thorning D et al. Nerve fibers in human myocardial scars. Human Pathology 1991;22(2): 138-146.

Wellens HJ, Schuilenburg RM et al. Electrical stimulation of the heart in patients with ventricular tachycardia. Circulation 1972;46(2): 216-226.

Westermann RSK, Stahl G et al. Relative effectiveness and validity of mood induction procedures: a meta-analysis. European Journal of Social Psychology 1996;26: 557-580.

Western D, Taggart P et al. Real-time feedback of dynamic cardiac repolarization properties. Conference Proceedings IEEE Engineering in Medicine and Biology Society 2010;114-117.

Western D, Hanson B et al. Measurement bias in activation-recovery intervals from unipolar electrograms. American Journal of Physiology. Heart and Circulatory Physiology 2015;308(4): H331-338.

Workman AJ. Cardiac adrenergic control and atrial fibrillation. Naunyn-Schmiedebergs Archives of Pharmacology 2010;381(3): 235-249.

Wyatt RF, Evans AK. Estimation of ventricular transmembrane action potential durations and repolarization times from unipolar electrograms. American Journal of Cardiology 1981;47: 488.

Yang SG, Kittnar O. New insights into application of cardiac monophasic action potential. Physiological Research 2010;59(5): 645-650.

Yartz AR, Hawk LW. Addressing the specificity of affective startle modulation: fear versus disgust. Biological Psychology 2002;59:55-68.

Zareba W, Moss AJ et al. Dispersion of ventricular repolarization and arrhythmic cardiac death in coronary artery disease. American Journal of Cardiology 1994;74(6): 550-553.

Zimetbaum PJ, Buxton AE et al. Electrocardiographic predictors of arrhythmic death and total mortality in the multicenter unsustained tachycardia trial. Circulation 2004;110(7): 766-769.

Zipes DP. Influence of myocardial ischemia and infarction on autonomic innervation of heart. Circulation 1990;82(4): 1095-1105.

Zipes DP, Jalife J. Cardiac Electrophysiology From Cell to Bedside. Chapter 35 Autonomic Modulation of Cardiac Arrhythmias. 4th edition. Saunders Elsevier, 2004.